

This study of airborne observations of halogenated VOCs (HVOCs) represents a valuable addition to the knowledge of these compounds over the Southern Ocean, where few data exist. The study confirms the current view that the main sources of  $\text{CHBr}_3$  and  $\text{CH}_2\text{Br}_2$  are biological, and that  $\text{CH}_3\text{I}$  has both biological and non-biological sources. The authors have put forward a novel concept of using enrichment ratios of HVOCs to  $\text{O}_2$  to infer the contribution or otherwise of ocean biological sources, and propose a new function to estimate non-biological emission fluxes of  $\text{CH}_3\text{I}$ . The dataset has been used to evaluate the CAM-Chem HVOC emission scheme at high latitudes in the Southern Hemisphere. The take home message/s from this evaluation are rather opaque – they could do with being put in context. E.g., do they infer that fluxes from these regions are poorly known, or problems with the models mixing /convection schemes special to these latitudes, or issues with photo-oxidation rates?. In terms of presentation, the paper has a number of typographical and other errors, listed below, and needs a thorough reading (I doubt I captured all of them). However overall, I think this manuscript presents sufficiently novel results to be suitable for publication, once these matters have been attended to.

We appreciate the reviewer's time and comments. We have done our best to clarify the goals and findings of this study. We argue that emissions of HVOCs over the Southern Ocean are poorly known using mixing ratio comparisons with a global climate model and state of the art biogenic flux parameterizations based on chl *a* that show persistent model biases. Thereafter, we seek to address this problem by proposing new approaches to estimate regional HVOC fluxes using airborne observations. We demonstrate two additional approaches for deriving HVOC flux estimates using airborne observations, and model output. We hope that the reviewer finds our article suitable for publication following these revisions.

L34-38 The regional enrichment ratios should be put in context here - there is no explanation as their relevance.

We no longer report enrichment ratios in the abstract. We do however, attempt to explain the role of  $\text{O}_2$ -HVOC enrichment ratios in inferring a biological flux of HVOCs. This passage now reads, "The first approach takes advantage of the robust relationships that were found between airborne observations of  $\text{O}_2$  and  $\text{CHBr}_3$ ,  $\text{CH}_2\text{Br}_2$ , and  $\text{CHClBr}_2$ ; we use these linear regressions with  $\text{O}_2$  and modeled  $\text{O}_2$  distributions to infer a biological flux of HVOCs." L30-33.

L51- 52 "Indeed, HVOCs may be among the most important sources of inorganic bromine to the whole atmosphere ..... (Murphy et al., in review)." This is not conventional wisdom and thus quite a bold statement. Are the authors confident that the Murphy et al paper will be published soon?

Murphy et al. (2019) has now been published and the citation has been revised. We have also moderated the language to reflect that this statement challenges conventional wisdom. This passage L50-54 now reads, "In the marine boundary layer and lower troposphere, sea salt is the main source of reactive bromine (Finlayson-Pitts 1982, Simpson et al. 2019). Yet HVOCs may also be a more important source of inorganic bromine to the whole atmosphere than previously thought, according to a recent study, which indicates that sea salt is scarce and insufficient to control the bromine budget in the middle and upper troposphere (Murphy et al., 2019)."

L61-64 The anthropogenic sources of CH<sub>3</sub>Br have changed over time and now are dominated by quarantine and pre-shipment (QPS) applications (not controlled by the Montreal Protocol). Please stick to the most recent information from WMO 2018 (and update the reference).

Both the information and citation on anthropogenic sources of CH<sub>3</sub>Br have been revised in L65-68: “CH<sub>3</sub>I is also formed through non-biological reactions in surface seawater, and CH<sub>3</sub>Br is emitted as a result of quarantine and pre-shipment activities, which are not regulated by the Montreal Protocol (e.g., Moore and Zafiriou; 1994, [Engel and Rigby, 2018](#)).

Elizabeth Asher 9/3/2019 11:46 AM

Deleted: WMO

L119- 130 The last paragraph of the introduction would benefit from an introduction to the concept of enrichment ratios of HVOCs to O<sub>2</sub>, which feature prominently in the abstract.

We have revised this passage in L122-139 to read, “In Section 3.1 and 3.2, we report new airborne observations of CHBr<sub>3</sub>, CH<sub>2</sub>Br<sub>2</sub>, CH<sub>3</sub>I, CHClBr<sub>2</sub>, CHBrCl<sub>2</sub>, and CH<sub>3</sub>Br from high latitudes in the Southern Hemisphere, where data are scarce, and large-scale regional mixing ratio comparisons for HVOCs with the community earth system model (CESM) atmospheric component with chemistry (CAM-Chem). In section 3.4, we present two novel approaches to estimate regional fluxes of HVOCs for comparison with global climate models’ parameterizations or climatologies. One approach uses correlations of HVOCs to marine, oxygen (O<sub>2</sub>) of marine origin, as measured by deviations in the ratio of O<sub>2</sub> to nitrogen (N<sub>2</sub>) ( $\delta(O_2/N_2)$  see Sect. 2.1.2 and 3.1.2) to determine the importance of regional biological HVOC sources. The robust correlations of CHBr<sub>3</sub> and CH<sub>2</sub>Br<sub>2</sub> with  $\delta(O_2/N_2)$  are indicative of a strong biological source. Our first approach exploits the ratio of HVOCs to oxygen (O<sub>2</sub>) determined from linear regressions (i.e. the enrichment ratio), and the ocean flux of O<sub>2</sub> from CESM’s ocean component, to estimate the marine biogenic flux of several HVOCs. The second approach relies on observed HVOC mixing ratios, the Stochastic Time-Inverted Lagrangian Transport (STILT) particle dispersion model and geophysical datasets (see Sect. 2.3 and 3.3). We assess contributions from previously hypothesized regional sources for the Southern Ocean, and estimate HVOC fluxes based on regressions between upstream influences and observed mixing ratios and distributions of remotely sensed data.”

L235-245 The fact that the polyhalogenated bromocarbons are likely co-emitted is not new – there are numerous papers that show this, and the discussion could elaborate on those a bit more. What is also missing from this paragraph is a discussion of macroalgal sources of these compounds, although this is presumably not relevant for the Antarctic.

We have expanded the discussion of previous findings of co-emitted polyhalogenated bromocarbons and cited several additional studies. This passage L390 - 401 now reads, “Previous studies have documented co-located source regions of CHBr<sub>3</sub> and CH<sub>2</sub>Br<sub>2</sub> in the Southern Ocean (e.g. Hughes et al., 2009; Carpenter et al., 2000; Nightingale et al. 1995; Laturmus et al. 1996), and laboratory studies have demonstrated that phytoplankton and their associated bacteria cultures, including a cold water diatom isolated from coastal waters along the Antarctic Peninsula and common to the Southern Ocean, produce both CHBr<sub>3</sub> and CH<sub>2</sub>Br<sub>2</sub> (Hughes et al., 2013; Tokarczyk and Moore 1994, Sturges et al., 1993). The non-linearity observed in ratios of these two gases at low CHBr<sub>3</sub> may reflect the different rates of their production or loss in seawater, or possibly, the influence of air masses from distant, more productive low-latitude source regions. Several studies have documented bacterially mediated loss of CH<sub>2</sub>Br<sub>2</sub>, but not

CHBr<sub>3</sub>, and report distinct ratios of CH<sub>2</sub>Br<sub>2</sub> to CHBr<sub>3</sub> in seawater during the growth and senescent phases of a phytoplankton bloom (e.g. Carpenter et al. 2009, Hughes et al 2013). ”

L244-245 “For instance, Huges et al. (2013) also report distinct seawater slopes between CH<sub>2</sub>Br<sub>2</sub> to CHBr<sub>3</sub> , when chl a was increasing.” It is not clear what is meant by this. Please rephrase

This statement has been rephrased on L398, “Several studies have documented bacterially mediated loss of CH<sub>2</sub>Br<sub>2</sub>, but not CHBr<sub>3</sub>, and report distinct ratios of CH<sub>2</sub>Br<sub>2</sub> to CHBr<sub>3</sub> in seawater during the growth and senescent phases of a phytoplankton bloom (e.g. Carpenter et al. 2009, Hughes et al 2013).”

L361- 366 “In both regions, the model under predicts CH<sub>3</sub>I above the MBL, which may indicate slower observed photochemical loss than the model predicts.” Has this been found in other CAM-Chem studies – e.g. is it a general result? If not, could a different source emission distribution (i.e. more homogeneous source) explain these results?

We have revised the text to reflect that indeed this result has been found in other CAM-Chem studies, and that the observed difference at high latitudes in the SH at ~10 km altitude may be due to the zonal transport of air masses from lower latitudes, where differences in CH<sub>3</sub>I in the UTLS have also been observed. For instance, in Ordonez et al. (2012), Fig. 10 illustrates the consistent under prediction of the observed CH<sub>3</sub>I mixing ratios, and these authors attribute this discrepancy to the strength of convective cells rapidly transporting air masses to the UTLS. This section L494-499 now reads as follows: “In both regions, the model most likely under predicts CH<sub>3</sub>I in the upper troposphere and lower stratosphere (UTLS), likely stemming from the poleward transport of lower latitude air masses, where CAM-Chem also exhibits a negative bias. Mixing ratio comparisons with CAM-Chem over the tropics (see Ordonez et al. Figure 10) depict similar or larger discrepancies, and have been attributed to stronger than anticipated convective cells in the tropics.”

L555-L560 onwards. There is no mention in Moore and Zarifou 1994 nor Richter and Wallace 2004 as far as I can see on the influence of iron availability – do the authors mean iodide availability?!

We have both fixed a typo and clarified the discussion on proposed non-biological chemical mechanisms for CH<sub>3</sub>I production in the ocean, which include the radical recombination reaction proposed by Moore and Zarifou (1994), and the substitution reaction, requiring an oxidant such as iron III, proposed by Williams et al. (2007). This passage L563-569 now reads, “This non-biological source, though not fully understood, requires light, a humic like substance at the surface ocean supplying a carbon source and methyl group, and reactive iodine (Moore and Zarifou 1994; Richter and Wallace 2004). Thus far, two chemical mechanisms have been proposed for the non-biological production of methyl iodide, one – a radical recombination of a methyl group and iodine involving UV photolysis (e.g. Moore and Zarifou 1994), and the second, a substitution reaction involving the reduction of an oxidant, such as iron III (e.g. Williams et al. 2007).”

L1036 – Note that units should be pmol m<sup>-2</sup> hr<sup>-1</sup> (not m<sup>2</sup>). Please state whether the values given for the observations are means or medians. It would be also be good to include their ranges.

We have corrected this typo on L1068. The units on Table 1 now read “ $\mu\text{mol m}^{-2} \text{hr}^{-1}$ .”

Ln 82. atmospheric Ln 213. “oppose” should be “opposed” Ln 213. “Huges” should be “Hughes” Ln 242 : “HOVCs” Ln 469. “Zafarou” should be “Zafariou” Ln 980. “includind” LN 1015. “fluxed”

L81, L253, L391, L518, L1171- Typos have been corrected to read, “Atmospheric,” “opposed,” “HVOCs,” “Zafariou,” and “fluxes.” Other typos previously listed have been deleted from the text.

## Response to Reviewer #2

The paper presented by Asher et al., provides a valuable contribution to the understanding of the distribution and sources of halogenated organic substances from the Southern Ocean. The work publishes airborne observations of VHOC in an understudies region and applies new concepts for source determinations related to measurements of O<sub>2</sub> and CO<sub>2</sub> and geophysical datasets. It underlines current knowledge of the biological sources of CHBr<sub>3</sub> and CH<sub>2</sub>Br<sub>2</sub> by applying their ratio to oceanic oxygen emissions. CH<sub>3</sub>I appears to have a dominant biological source in the area of the Patagonian shelf, while closer to Antarctica a photochemical source appears to be dominant. The paper also compares the derived emissions of the novel concepts to the output of a global climate model. I agree that the presentation of data from several compounds and several campaigns is a difficult task. Also the loaded content of the paper: evaluation of model predictions, calculation of biogenic enrichment ratios, identification of regional sources, and novel means of parameterizing ocean fluxes, which was only summarized clearly in the conclusion section of the paper, makes the task of writing not easier. While the authors present their results and outcomes, which are not totally exciting and sometimes are also not very convincing due to poor correlations, their novel approaches and novel concepts are more exciting, but are poorly presented. They could do a much better job in explaining and presenting their concepts and the overall goal of the paper, which for me remains more a concept than a result paper. The results underline the novel approaches, as they do not contradict earlier studies and the novel approaches can be more useful and should be tested for and in future studies. The authors should think about a different setup of their paper, putting their concepts more into the focus, but clearly their approaches need to be described more clearly and in more detail throughout the text. Also they authors should think about the title. Also technically the paper needs improvement, as abbreviations are sometimes not introduced, sometimes edits are not clearly overworked, which led to typos and grammar mistakes and also I wonder if it would be possible to make some sentences less bulky and loaded. Some figures are too small, some legends appear odd and there appear to be misunderstandings with some references. Overall I think the work behind the paper is very valuable and should be published in ACP, but the presentation of the work needs prior strong improvement.

We appreciate the reviewer's constructive criticism. We have refocused our paper on the approaches and concepts outlined here, rather than our results. We also argue that emissions of HVOCs over the Southern ocean are poorly known and seek to address this problem by proposing new approaches to estimate regional HVOC fluxes using airborne observations. We have sought to better outline the two novel approaches to estimate HVOC fluxes and explain why these approaches represent an important step forward in the field. We have also done our best to improve the presentation by reorganizing the structure of the paper, simplified the language and corrected typos and grammar errors. We hope that the reviewer finds our article suitable for publication following these revisions.

L22- 25 We also use CH<sub>3</sub>Br from the University of Miami Advanced Whole Air Sampler(AWAS) on ORCAS and from the UC Irvine Whole Air Sampler (WAS) on ATom-2. In connection with the first and the third sentence, this is a strange sentence. I think there is too much detail in the first two sentences about the instrumentation, which could be abandoned for the abstract and only explained later in the text.

We agree with the reviewer and have revised the text to include less detail on instrumentation. This section on L22-25 now reads: "We present observations of CHBr<sub>3</sub>, CH<sub>2</sub>Br<sub>2</sub>, CH<sub>3</sub>I, CHClBr<sub>2</sub>, CHBrCl<sub>2</sub>,

and CH<sub>3</sub>Br during the O<sub>2</sub>/N<sub>2</sub> Ratio and CO<sub>2</sub> Airborne Southern Ocean (ORCAS) study and the 2<sup>nd</sup> Atmospheric Tomography mission (ATom-2), in January and February of 2016 and 2017.”

L32-38 Based on these relationships What does this refer to?... it is unclear

We have done our best to clarify how the regressions of HVOC mixing ratios with upwind influences and O<sub>2</sub> are used to estimate basin-wide fluxes on L30-33: “... we demonstrate two novel approaches to estimate HVOC fluxes; the first approach takes advantage of the robust relationships that were found between airborne observations of O<sub>2</sub> and CHBr<sub>3</sub>, CH<sub>2</sub>Br<sub>2</sub>, and CHClBr<sub>2</sub>; we use these linear regressions with O<sub>2</sub> and modeled O<sub>2</sub> distributions to infer a biological flux of HVOCs.”

L49-53 Indeed, HVOCs may be among the most important sources of inorganic bromine to the whole atmosphere, since recent evidence indicates that sea salt is scarce.. This is not true, as there is enough literature out to show how sea salt aerosol dominates the bromine in the lower troposphere. If the authors want to keep this sentence they have to provide more evidence, than just an upcoming paper. I suggest rewriting and specifying the statement to the known literature.

We have added a sentence to reflect that sea salt aerosol is critical to the bromine budget in the lower troposphere, and have moderated the language of the sentence regarding the contribution of bromocarbons to the middle and upper troposphere to reflect that this statement challenges conventional wisdom. This passage L50-54 now reads, “In the marine boundary layer and lower troposphere, sea salt is the main source of reactive bromine (Finlayson-Pitts 1982, Simpson et al. 2019). Yet HVOCs may also be a more important source of inorganic bromine to the whole atmosphere than previously thought, according to a recent study, which indicates that sea salt is scarce and insufficient to control the bromine budget in the middle and upper troposphere (Murphy et al., 2019).”

L75-80 There is an important observational paper missing which the authors need to relate to in the discussion of their results later on in the paper. It is: Regional sinks of bromoform in the Southern Ocean from 2013 from Mattsson et al. in GRL, where he shows the heterogeneity of the sources, which make the ocean a sink at times. Therefore also the next sentence needs to be revised: These studies indicate moderate ocean sources of CHBr<sub>3</sub> and CH<sub>2</sub>Br<sub>2</sub> at high latitudes in the Southern Hemisphere, and refer to Mattsson., possibly in line 79.

This passage has been revised on L79-84: “Mattsson et al. (2013) noted that the ocean also acts as a sink for HVOCs, when HVOC undersaturated surface waters equilibrate with air masses transported from source regions. The spatially heterogeneous ocean sources of CHBr<sub>3</sub> and CH<sub>2</sub>Br<sub>2</sub> at high latitudes in the Southern Hemisphere are often underestimated in global atmospheric models (Hossaini et al., 2013; Ordoñez et al., 2012; Ziska et al., 2013).”

L94-103 Here you need to relate to Salawitch (2011?).. –most trace gases in tropospheric air enter the stratosphere in the tropics, move poleward and descend to the troposphere at middle and high latitudes. Salawitch claims, that the polar bromine can be influenced by large scale subsidence from the lower latitudes. . .

This passage has been rewritten to reflect this on L99-103, “As a result of limited vertical transport in these regions, however, air-sea fluxes lead to strong vertical gradients. Zonal transport from lower latitudes has a large impact on the vertical gradients of trace gas mixing ratios over polar regions (Salawitch 2010). Given their extended photochemical lifetimes at high latitudes (see Sect. 2.3 for a brief discussion), many HVOC distributions are particularly sensitive to zonal transport at altitude.”

L105-106 [Few constraints on HVOC mixing ratios or emissions based on airborne data exist at high latitudes in the Southern Hemisphere. What does this mean?](#)

This sentence has been rewritten (L108-109) and is hopefully more clear: “Few airborne observations of HVOCs exist at high latitudes in the Southern Hemisphere.”

L117 [This is pmol . . . not nmol mol<sup>-1</sup>](#)

The correction has been made on 119, “ACE-1 measurements of CH<sub>3</sub>I in the MBL indicate a strong ocean source between 40° S and 50° S in austral summer, with mixing ratios above 1.2 pmol below ~1 km (Blake et al., 1999).”

L131 – 136 [Here you could \(you need to do it somewhere\) elaborate on the O<sub>2</sub>/N<sub>2</sub> concept and why you chose to relate the HVOHCs to those.](#)

We now discuss the concept and purpose of relating HVOCs to O<sub>2</sub>/N<sub>2</sub> in L126-L134: “In section 3.4, we present two novel approaches to estimate regional fluxes of HVOCs for comparison with global climate models’ parameterizations or climatologies. One approach uses correlations of HVOCs to marine, oxygen (O<sub>2</sub>) of marine origin, as measured by deviations in the ratio of O<sub>2</sub> to nitrogen (N<sub>2</sub>) ( $\delta(O_2/N_2)$  see Sect. 2.1.2 and 3.1.2) to determine the importance of regional biological HVOC sources. The robust correlations of CHBr<sub>3</sub> and CH<sub>2</sub>Br<sub>2</sub> with  $\delta(O_2/N_2)$  are indicative of a strong biological source. Our first approach exploits the ratio of HVOCs to oxygen (O<sub>2</sub>) determined from linear regressions (i.e. the enrichment ratio), and the ocean flux of O<sub>2</sub> from CESM’s ocean component, to estimate the marine biogenic flux of several HVOCs.”

L141-144 [Please include the regions into Figure 1.](#)

We now include the regions in Fig. 1.

L144-152 [If you only refer to two flights from ATom-2, the sentence could be easier to read.](#)

This sentence has been revised to read, “On Feb. 10 and 13, 2017 the sixth and seventh ATom-2 research flights passed over the eastern Pacific sector poleward of 60° S (defined here as Region 1) and over the Patagonian Shelf between 40° S and 55° S and between 70° W and 55° W (defined here as Region 2), respectively.”

L204 [Model is missing](#)

Although this passage has been revised, “Model” has been added when CESM is first introduced in the introduction on L126: “In Section 3.1 and 3.2, we report new airborne observations of  $\text{CHBr}_3$ ,  $\text{CH}_2\text{Br}_2$ ,  $\text{CH}_3\text{I}$ ,  $\text{CHClBr}_2$ ,  $\text{CHBrCl}_2$ , and  $\text{CH}_3\text{Br}$  from high latitudes in the Southern Hemisphere, where data are scarce, and large-scale regional mixing ratio comparisons for HVOCs with the community earth system model (CESM) atmospheric component with chemistry (CAM-Chem).”

L207 [You did not introduce CAM.](#)

CAM is now referred to here as “CESM’s atmosphere component. Please see above comment.

L1215 [What is a broadening effect?](#)

L217 We have specified “pressure broadening effect” on the  $\text{CO}_2$  and  $\text{CH}_4$  spectrum in cavity ring down instruments, which has been observed in several studies due to the influence of water vapor (e.g. Chen et al. 2013). This sentence now reads, “Dry-air mole fractions were calculated using empirical corrections to account for dilution and pressure broadening effects as determined in the laboratory before and after the campaign deployments, and in-flight calibrations were used to determine an offset correction for each flight.”

L243-L252 [We note that the non-linearity observed in ratios of these two gases at low  \$\text{CHBr}\_3\$  levels likely reflects the differences in emissions during strong phytoplankton blooms, as oppose to other periods. The ratio may simply \(and more likely\) reflect other air masses from more distant source regions, which is reflected in a ratio which favors the longer lived compound \( \$\text{CH}\_2\text{Br}\_2\$ \) over the shorter-lived compound \( \$\text{CHBr}\_3\$ \) which is emitted in larger quantities in a biological source region \(refer to Yokouchi, 20xx\) but more rapidly degraded during transport.](#)

Our analysis focuses on the bottom 2 km of the atmosphere, and as such largely reflects recent enhancements in HVOCs. Nevertheless, we have clarified this passage to reflect that contributions from zonal transport from low latitude regions cannot fully be ruled out, and have further expanded on the differences in  $\text{CH}_2\text{Br}_2$  and  $\text{CHBr}_3$  production and loss rates in surface waters. This passage L395-405 now reads, “The non-linearity observed in ratios of these two gases at low  $\text{CHBr}_3$  may reflect the different rates of their production or loss in seawater, or possibly, the influence of air masses from distant, more productive low-latitude source regions. Several studies have documented bacterially mediated loss of  $\text{CH}_2\text{Br}_2$ , but not  $\text{CHBr}_3$ , and report distinct ratios of  $\text{CH}_2\text{Br}_2$  to  $\text{CHBr}_3$  in seawater during the growth and senescent phases of a phytoplankton bloom (e.g. Carpenter et al. 2009, Hughes et al 2013). Although this analysis is restricted to the bottom 2 km of the atmosphere, zonal transport of air masses with lower ratios of  $\text{CH}_2\text{Br}_2$  to  $\text{CHBr}_3$  ratios, as have been observed in the MBL over productive, low-latitude regions, may also have influenced our observations (Yokouchi et al. 2005).”

L246-248 [For instance, Huges et al. \(2013\) also report distinct seawater slopes between  \$\text{CH}\_2\text{Br}\_2\$  to  \$\text{CHBr}\_3\$ , when chl a was increasing. This is a weak sentence; can you give it more meaning?](#)



This sentence has been rewritten on L398, “Several studies have documented bacterially mediated loss of  $\text{CH}_2\text{Br}_2$ , but not  $\text{CHBr}_3$ , and report distinct ratios of  $\text{CH}_2\text{Br}_2$  to  $\text{CHBr}_3$  in seawater during the growth and senescent phases of a phytoplankton bloom (e.g. Carpenter et al. 2009, Hughes et al 2013).”

L257-258 please explain the concept: What do you expect from the ratio of the HVOHCs and the marine oxygen.

L415-418 We have revised this passage, “We sought to test if the biologically mediated production of bromocarbons and oxygen result in similar atmospheric distributions. Conversely, we expected HVOHC atmospheric distributions and  $\text{CO}_2$  distributions to anticorrelate because  $\text{CO}_2$  fixation in surface waters is proportional to the production of oxygen.”

L288 238/241-242: Where did you get this equilibration times? Support them by reference or evidence. And also the air-sea fluxes of  $\text{O}_2$  and  $\text{CHBr}_3$  are not very similar. Revise. L444 This sentence now reads, “The bulk air-sea equilibration time for an excess of  $\text{CHBr}_3$  and other HVOHCs is less than two weeks, although the photochemical loss of HVOHCs will alter their ratio over time (see Supplement for details on calculations of bulk sea air equilibration times).” The section in the supplement (L1177-1185) reads as follows: “To support the interpretation of our results, we calculate nominal equilibration times. For estimates of bulk sea air equilibration times for HVOHCs,  $\text{O}_2$ , and  $\text{CO}_2$ , we assume a mixed layer depth of 30 m, a temperature of  $0^\circ\text{C}$ , a salinity of 35 PSU, and carbonate buffering according to eq. 8.3.10 in Sarmiento and Gruber (2006), and transfer velocities according to Nightingale et al., (2000). The Schmidt number (i.e. the ratio of the kinematic viscosity of a gas, divided by the molecular diffusivity) for  $\text{O}_2$ ,  $\text{CO}_2$  and  $\text{CH}_3\text{Br}$  were calculated according to Wanninkhof (2014), and the Schmidt numbers for  $\text{CHBr}_3$  and  $\text{CH}_3\text{I}$  were calculated according to Quack and Wallace (2003) and Moore and Groszko (1999), respectively. The results are provided in Sect. 3.1.2.”

L291-300 This paragraph is a little back and forth between compounds and regions; it can be sorted for easier reading.

We have done our best to clarify this paragraph in L455-465: “Our observations suggest a biological source for  $\text{CHBr}_3$  and  $\text{CH}_2\text{Br}_2$  in both Region 1 and Region 2 (Fig. 4). Interestingly, the slope of the regression between  $\text{CHBr}_3$  and  $\text{O}_2$  appears distinct in Region 1 and Region 2, but between  $\text{CH}_2\text{Br}_2$  is the same. Molar enrichment ratios are  $0.20 \pm 0.01$ , and  $0.07 \pm 0.004$  pmol : mol for  $\text{CHBr}_3$  and  $\text{CH}_2\text{Br}_2$  to  $\text{O}_2$  in Region 1, and  $0.32 \pm 0.02$ , and  $0.07 \pm 0.004$  pmol : mol in Region 2. We observe a weaker relationship between  $\text{CH}_3\text{I}$  and  $\text{CHClBr}_2$  and  $\text{O}_2$  in Region 1 (Fig. 4c, d), consistent with the existence of other, non-biological sources of  $\text{CH}_3\text{I}$  in this region. Figure 4f illustrates a strong relationship between  $\text{CH}_3\text{I}$  and  $\text{O}_2$ , as well as  $\text{CHClBr}_2$  and  $\text{O}_2$ , in Region 2, however, which implies that the dominant sources of  $\text{CH}_3\text{I}$  and  $\text{CHClBr}_2$  emissions over the Patagonian Shelf are biological. The corresponding molar enrichment ratios of  $\text{CH}_3\text{I}$  to  $\text{O}_2$  and  $\text{CHClBr}_2$  to  $\text{O}_2$  in Region 2 are  $0.38 \pm 0.03$  pmol : mol and  $0.19 \pm 0.04$  pmol: mol, respectively.”

263. This should have come earlier, when you start with the equilibria (238, 241). And do you also reference the atmospheric lifetimes?

L44 We now refer the reader to the supplement here for further reading on the calculation of equilibration times. Please see two responses up for details.

L336 – 337 [FINN and MEGAN 2.1 products. I guess the abbreviations need to be explained a bit as well as the products](#)

L247 “The model uses chemistry described by Tilmes et al. (2016), biomass burning and biogenic emissions from the Fire INventory of NCAR (FINN; Wiedinmyer et al. 2011) and MEGAN (Model of Emissions of Gasses and Aerosols from Nature) 2.1 products (Guenther et al., 2012) with additional tropospheric halogen chemistry described in Fernandez et al. (2014) and Saiz-Lopez et al. (2014), including ocean emissions of  $\text{CHBr}_3$ ,  $\text{CH}_2\text{Br}_2$ ,  $\text{CHBr}_2\text{Cl}$ , and  $\text{CHBrCl}_2$ , with parameterized emissions based on chlorophyll *a* (*chl a*) concentrations and scaled by a factor of 2.5 over coastal regions, as opposed to open ocean regions (Ordoñez et al. 2012).”

L341 [from this sentence it is not clear where the oceanic emissions are derived from. I guess its Ordonez, 2012?](#) Done. Ordonez et al. (2012) has been cited. Please see above.

L343 [Ordonez, 2012 does not include  \$\text{CH}\_3\text{Br}\$ . Revise](#)

We respectfully disagree with the reviewer. Indeed, Ordonez does prescribe a lower boundary condition for  $\text{CH}_3\text{Br}$  and show mixing ratio comparisons for this compound. There is not a biogenic flux prescribed for  $\text{CH}_3\text{Br}$ .

L393 [GDAS has to be introduced.](#)

L271 “STILT was run using 0.5° Global Data Assimilation System (GDAS) reanalysis winds to investigate the transport history of air sampled along the flight track (Stephens et al., 2018).”

416-418 [We consider the wind direction error to evaluate the possible size of spatial errors in footprint location. There appears to be something wrong with the grammar? The sentence is not understandable. Given median wind speeds in this domain, this corresponds to a possible error of 260 km/day possible error. Here is also something wrong.](#)

L287 We have revised this passage to read, “For wind speed, a small bias may be present, where we find a median difference between observations and reanalysis of 0.68 m/s, a 5% relative bias. The 1-sigma of the wind speed difference is 2.3 m/s, corresponding to a 19% 1-sigma uncertainty in wind speed. In its simplest approximation, the surface influence strength error is perfectly correlated with the wind speed error, and thus we take 19% as an approximation of the surface influence strength uncertainty. The uncertainty in surface influence location depends on the error in the wind direction. We find a 1-sigma error of 14 degrees in wind speed, which corresponds to a possible error of 260 km/day.”

L448- 449 OCI and GIOP have to be introduced. What does . . .and its uncertainty . . .mean? how do you obtain a  $0.25^\circ \times 0.25^\circ$  gridded uncertainty in the detrital material absorption? It is also not clear from section 5.2.

OCI and GIOP are introduced, and we have done our best to clarify the meaning of GIOP absorption uncertainty in L350-362: “Due to persistent cloud cover over the Southern Ocean, which often precludes the retrieval of remotely sensed ocean color data, we used 8-day mean composite Aqua MODIS L3 distributions of chl *a* from the Ocean Color Index (OCI) algorithm and absorption due to gelbstoff and detrital material at 443 nm from the Generalized Inherent Optical Properties (GIOP) model (NASA Goddard Space Flight Center, 2014). Absorption due to gelbstoff and detrital material at 443 nm is used as a proxy for colored dissolved organic matter (CDOM; <https://oceancolor.gsfc.nasa.gov/atbd/giop/>). CDOM is hypothesized to be an important source of carbon for the photochemical production of  $\text{CH}_3\text{I}$  (Moore et al., 1994). The GIOP model also publishes an uncertainty in the absorption due to gelbstoff and detrital material at 443 nm. Raw 4 km x 4 km data were geometrically averaged, based on lognormal probability density functions, to a spatial resolution of  $0.25^\circ \times 0.25^\circ$  for use with gridded surface influences. We used the ratio of the  $0.25^\circ \times 0.25^\circ$  gridded uncertainty in the detrital material absorption to the absorption as the relative uncertainty for flux calculations (see Sect. 3.4.2).”

L477 and elsewhere – Is the new terminology geophysical influence function something different than the surface influence function? Or why do you change the wording? Its unclear.

We do not mean to confuse the reader with superfluous terminology: “geophysical influence function” has been replaced everywhere with “surface influence function.”

403 to 404. Can you give an example for H and s. What is the potential geophysical source distribution s?

H is the surface influence based on a sample’s back trajectories in the boundary layer ( $\text{ppt m}^2 \text{ s pmol}^{-1}$ ). An example of s would be the distribution of chl. a at the ocean surface ( $\mu\text{g m}^{-3}$ ) or the distribution of fractional sea ice at the ocean surface, which is unitless.

412: here the potential source distributions is Hs1, Hs2. . .? And not s? Is HS1 the same as Hs1? 415-416: We used the standard deviation of the regression coefficients and the relative uncertainty in the source fields, added in quadrature, to estimate the uncertainty in these fluxes (see Fig. 7 and Sect. 5.2 for fractional uncertainties). 418: How did you calculate and do you report the relative uncertainty of the regression coefficients? There is no standard deviation of the regression coefficients in Fig 7 and sect 5.2 does not explain fractional uncertainties and no explanation is found about relative uncertainties in source fields. Or are you relating to surface influence strength uncertainty here. There needs to be more explanation about this added here.

L316-L333 Yes Hs1 is the same as HS2. This passage has been revised and two capitalization typos have been corrected to clarify the role of upstream influence functions and geophysical source distributions in these regressions with surface influence functions. Also an example of a geophysical source distribution s, was given, Chl. *a*, now L304. The relative uncertainty of regression coefficients for Figure 9 is reported, and used to calculate the flux shown in Figure 11 as described in Sect. 3.4.2. To clarify, in

those regressions where a flux was not calculated based on the relationship (e.g. Fig 7-8), the uncertainty in the regression coefficients is not reported.

L501 why did you include. . . such as CH<sub>3</sub>I in Region 1? The second half sentence does not add information?

The phrase “such as CH<sub>3</sub>I in Region 1” has been deleted.

L500-501 Note, sea ice did not include land ice; however, we also found a negative correlation between upstream land ice influence and mixing ratios of HVOCs. Why do you add the sentence starting with however? How did you get the correlations when it is not included and does it help the interpretation of the results? It appears misleading and redundant.

This statement on L521 has been revised to read, “We found no positive relationships between upstream sea-ice influence and any measured HVOC Region 1 (Fig. 7).”

L506 We note that over-turned first year sea-ice, which can expose under-ice algae colonies to the air, likely still present a local source of CHBr<sub>3</sub>, CH<sub>2</sub>Br<sub>2</sub>, or other VOHCs to the MBL. How does this speculation relate to your study and how does it help your interpretations? It stands a bit loose currently.

The statements regarding land ice and overturned first-year ice have been deleted.

Sect. 4.2 What was the temporal resolution of the input data shortwave and detrital material- add in section 4.2.

The temporal resolution of the input shortwave radiation data is every six hours and detrital data is every eight days, as specified elsewhere on L351 (a) and L365 (b).

a) “Due to persistent cloud cover over the Southern Ocean, which often precludes the retrieval of remotely sensed ocean color data, we used 8-day mean composite Aqua MODIS L3 distributions of chl *a* from the Ocean Color Index (OCI) algorithm and absorption due to gelbstoff and detrital material at 443 nm from the Generalized Inherent Optical Properties (GIOP) model (NASA Goddard Space Flight Center, 2014).”

b) “The National Center for Environmental Prediction (NCEP) provides Final Global Data Assimilation System (GDAS/FNL) global data of downward shortwave radiation at the surface at 0.25 degree and 6-hour resolution (NCEP, 2015).”

L557-562 This section is wrong. There is no study (at least not the referenced ones) which proves a relationship between iron availability and methyl iodide. The authors have misinterpreted the cited studies. Please check and revise.

L565-569 A typo has been corrected and this passage has been revised and clarified. The role of iron is briefly explicitly discussed as a possible oxidant for one of two proposed abiotic CH<sub>3</sub>I reactions: “This

non-biological source, though not fully understood, requires light, a humic like substance at the surface ocean supplying a carbon source and methyl group, and reactive iodine (Moore and Zarifou 1994; Richter and Wallace 2004). Thus far, two chemical mechanisms have been proposed for the non-biological production of methyl iodide, one – a radical recombination of a methyl group and iodine involving UV photolysis (e.g. Moore and Zarifou 1994), and the second, a substitution reaction involving the reduction of an oxidant, such as iron III (e.g. Williams et al. 2007).”

L564-565 [citing the link between temperature and PAR to the solar radiation..this wording is strange..also add which temperature is needed. . .water . may be its easier to just write revealing the link to solar radiation ..or similar](#)

L570 Done, this statement has been revised, “Several previous studies have correlated mixing ratios of CH<sub>3</sub>I to satellite retrievals of PAR and surface ocean temperature, revealing a link to solar radiation (e.g. Happell et al., 1996; Yokouchi et al., 2001).”

L424 [please introduce TUV. This section appears to beat the wrong place. I would expect this earlier in the description of the model, e.g. in 4.1., where you also talk about uncertainties due to meteorology.](#)

TUV is now introduced. Note, this section L419-429 has been moved up as suggested to the end of Sect. 2.3 L295-306: “Finally, we note that photochemical loss during transport is not accounted for in this analysis. Low OH mixing ratios, cold temperatures, and lower photolysis rates due to angled sunlight at high latitudes lead to longer than average HVOC lifetimes. For instance, assuming an average diurnal OH concentration of 0.03 pptv, and average photochemical loss according to the Tropospheric Ultraviolet and Visible (TUV) radiation model and the Mainz Spectral data site ([http://satellite.mpic.de/spectral\\_atlas](http://satellite.mpic.de/spectral_atlas)) for Jan. 29 under clear sky conditions at 60° S, CHBr<sub>3</sub> has a lifetime of 30 days, CH<sub>2</sub>Br<sub>2</sub> has a lifetime of 270 days, CH<sub>3</sub>I has a lifetime of 7 days, and CHClBr<sub>2</sub> has a lifetime of 63 days. As such, the photochemical lifetimes of these gases are greater than or equal to the time of our back-trajectory analysis. Moreover, OH concentrations in this region have large uncertainties, the inclusion of which would lead to more, not less, uncertainty in surface influence based regression coefficients and estimated fluxes.”

L571-576.

[as explained earlier the concept needs to be introduced more clearly earlier..e.g. why do you not take the VOHC directly but apply their relationship to oxygen?](#)

Our goal was not to suggest the “correct” regional flux of HVOCs based on data from two austral summers (and relatively few measurements from the Atom-2 campaign in 2017), but to demonstrate that airborne data can be used to develop other empirically based parameterizations, which could work better. We argue that despite the its inherent uncertainties in the parameterization of biogenic HVOC fluxes based on O<sub>2</sub>, the current CAM-Chem scheme based on chl. *a* leads to biases that exceed 50-100% for these compounds. Moreover, the uncertainties in remotely sensed chl.*a* are rarely considered in such parameterizations.

How can a model and an observation based flux-estimate be wrong by around 50%? And why do you think that a simple down scaling of the calculated oxygen fluxes leads to a robust flux estimate for VOHC, respectively why is this better, than taking just the VOHC fluxes? Can you explain this concept in the text please? Also it is unclear why you calculate all your influence functions to the VOHC mixing ratios directly, and not to their relation to oxygen and why for the flux calculation this now appears better?

O<sub>2</sub> and CO<sub>2</sub> fluxes are not well constrained at high latitudes in the southern hemispheres. In fact, the ORCAS campaign sought primarily to address this problem. Please see Stephens et al. (2018) for details. Although we agree with the reviewer that the simple downscaling is crude, this large discrepancy between observations and model or climatological mean values is due to inter-annual variability. The uncertainty discussed in L546-548 is meant to account for errors in the spatial variability in the fluxes, and does not include the mean absolute difference that is adjusted for in downscaling.

L632-634 I strongly believe that the calculation of the regression surface influence functions need to be shown in the text not in the legend of figure 9. Regression coefficients from the MLR with surface influence functions are now shown in here on L641-644 not in the legend of Fig. 9, “We used a multiple linear regression ( $\pm$  1 standard deviations; Equation 2), where Hs1 and Hs2 are the surface influence functions of downward shortwave radiation and detrital absorption, respectively, with an intercept  $b = 0.19 \pm 0.01$ , and influence coefficients  $a_1 = 3.7E-5 \pm 1.3E-5$ ,  $a_2 = 3.5 \pm 0.74$ , and an interaction term with the coefficient  $-5.2E-4 \pm 1.5E-4$  (c).”

Table 1. You need to indicate in table 1, which method you used in “This study” to derive the reported flux, as there are several methods here.

The approaches (O<sub>2</sub> vs. MLR using surface influence functions) has been clarified here.

L678-680 this also appears true for CHBr<sub>3</sub>, CHClBr<sub>2</sub> in region 1 ..and for the entire troposphere for CHBrCl<sub>2</sub>

We have rewritten this passage. L692-704: “Our flux estimates based on the relationship of HVOC mixing ratios to other airborne observations and remotely sensed parameters compared relatively well with those derived from global models and ship-based studies (Table 1). Our emission estimates of CHBr<sub>3</sub>, CH<sub>2</sub>Br<sub>2</sub>, and CHClBr<sub>2</sub> are significantly higher than CAM-Chem’s globally prescribed emissions in Region 1, where HVOC mixing ratios are under predicted (Table 1; Fig. 5). Similarly, our estimate of CHClBr<sub>2</sub> emissions is also significantly higher than CAM-Chem’s in Region 2, where CHClBr<sub>2</sub> mixing ratios remained under predicted. Nevertheless, our emission estimates of CHBr<sub>3</sub>, CH<sub>2</sub>Br<sub>2</sub>, CH<sub>3</sub>I, are lower than most prior estimates based on either other models or localized studies using seawater-side measurements from the Antarctic polar region in summer. In the case of CH<sub>3</sub>I, our estimated emissions suggest that the prescribed emissions in CAM-Chem may be too high in Region 1 and Region 2. Our parameterizations of the CH<sub>3</sub>I flux could be used to explore inter-annual variability in emissions, which is not captured by the Bell et al. (2002) CH<sub>3</sub>I climatology currently employed in CAM-Chem.”

L660-664 although they were significantly higher than CAM-Chem's prescribed emissions in Region 1, where VOHC mixing ratios are under predicted (Table 1; Fig. 5). Can you please add the comparison to CAM-Chem at the beginning. It would be better structured if you don't jump between comparisons.

We have clarified these two passages. Please see above.

L675 – 684 parameterizations..these are different ..and you need to add which compounds you are referring to in this sentence. Here it would be good to extend on the methods and why they appear so useful and how you would extend them to other species.

L705-711 We have done our best to clarify this passage: "To extend these relationships to year-round and global parameterizations for use in global climate models, they must be studied using airborne observations in other seasons and regions. These approaches may help parameterize emissions of new species that can be correlated with surface influence functions or the biological production of oxygen or may improve existing emissions, where persistent biases exist. Finally, future airborne observations of HVOCs have the potential to further improve our understanding of air-sea flux rates and their drivers for these chemically and climatically important gases over the Southern Ocean."

Figure 2. Are the data of the campaigns merged? Detection limits need to be added. The label of CH3I is odd.

Yes, the data are merged. Detection limits have been added to the legend.

Figure 3. Please specify one name for the campaigns and keep it. Here in one figure the authors switch between Atom-2, Atom and Atom. Line 937 to 939 in the legend : This sentence does not make sense.

All mentions of ATom are now listed as ATom-2.

Figure 4. There appears to be an old legend as d, g and h are missing as well as CHClBr2. The applied regressions appear to be the same, thus it would be good to elaborate in the text about the method to reduce the legend, e.g. what means. using variables scaled to their range? In the legend? Also here only regressions above 0.2 are shown.

The legend has been revised, and a statement has been added to say that only regressions with  $r^2 > 0.2$  are shown.

Figure 5,6. Switching between CESM in the figure and CAM-Chem1.2 does not help clarity. . . .multiplied by the percentage of data below detection.. . . was it used for calculating the mean? ..rephrase for clarity.

CESM in all the figure axes has been relabeled CAM-Chem. The sentence regarding data below the DL has been revised to read, "Again, the binned mean includes measurements below the detection limit (DL), which for this calculation are assigned a value equal to the DL multiplied by the percentage of data below detection."

Figure 7,8. Talking of statistical significance with  $r^2 \ll 0.2$  and looking at the plots with scattered values and no surface influence, is a bold exaggeration. And the p-values can be abandoned from the figure and just the threshold mentioned, as they do not help the statistics.

P-values listed on the plots have been replaced with p-value thresholds (e.g.  $p < 0.001$ ).

Figure 9. The labeling of the figures is too small, the p- value redundant and the legend for figure c.) too intricate. I strongly believe that the calculation of the regression surface influence functions need to be shown in the text not in the legend of figure 9.

The size of figure labels is larger. The calculation is now shown in the text as discussed above.

Figure 10. The figures and labeling of a to c are too small. ( I suggest single plots, resolution as Figure 1?. It must be  $\text{pmol m}^{-2} \text{hr}^{-1}$  also in the legend. Also clarify that these are model results. How do the mentioned CESM (CAM- Chem 1.2)  $\text{O}_2$  fluxes relate to the figure? And is this also 2016?

The labeling is now larger, and as now stated in the figure legend, represents the year 2016. CESM ocean component  $\text{O}_2$  fluxes (not shown here) were multiplied by the regression coefficients shown in Fig. 4 to infer a biological flux of HVOCs, as explained in Sect. 5.1.

Figure 11. fluxes not fluxed

Done, and now reads, "fluxes."



### Response to Reviewer #3

Anonymous Referee #3 The manuscript of Asher et al. describes airborne observations of halogenated volatile organic compounds over the Southern Ocean and improved emission flux estimates, based on modeling studies and correlative O<sub>2</sub> observations. This is an important and interesting study that should be published in *Atmos. Chem. Phys.* after consideration of the following points. The authors should consider improving the presentation by first presenting their data and methods and then discussing the results. This study contains important new methods and approaches compared to previous studies but the presentation is not always clear. As an example, a key result is the presentation of “regional enrichment ratios” for HVOCs, but it did not become sufficiently clear to me, how they are defined and how they were calculated.

We appreciate the reviewer’s comments and suggestions. We have done our best to reorganize the paper accordingly, by first discussing our methods and data sources and discussing our results second. We have paid particular attention to clarifying the discussion of regional enrichment ratios for HVOCs in the abstract as well as in sections 3.12 and 3.31.

#### Specific Comments:

Specific comments: L32-34: in the same sentence “halogenated hydrocarbon” and “halogenated volatile organic compounds (HVOCs)” are used. If the two mean the same, use only one name. If there is a distinction, please define.

Indeed- these are the same. The wording has been revised. Only the term “halogenated volatile organic compounds (HVOCs)” is now used.

L47-49: Is there a particular logic for the order of the citations given? They are neither sorted according to year, nor alphabetically.

This has been corrected and special attention has been paid to the order of citations throughout the paper.

L50: “recent evidence indicates that sea salt is scarce and insufficient”: this is a strong statement that should be backed up with more than a manuscript in review.

We appreciate the reviewer’s comment. Although this study is now published, this statement has been amended to better reflect current understanding on L50 – 54: “In the marine boundary layer and lower troposphere, sea salt is the main source of reactive bromine. Yet HVOCs may also be a more important source of inorganic bromine to the whole atmosphere than previously thought, according to a recent study, which indicates that sea salt is scarce and insufficient to control the bromine budget in the middle and upper troposphere (Murphy et al., 2019).”

L66: You may cite Abrahamsson et al. (2018) already at this stage.

Done. L670: “Over the Southern Ocean specifically, hypothesized sources of HVOCs include: coastal macroalgae, phytoplankton, sea ice algae, and photochemical or dust stimulated non-biological production at the sea surface (e.g., Abrahamsson et al. 2018, Manley and Dastoor 1998; Moore and Zafiriou 1994; Moore et al., 1996; Richter and Wallace 2004; Williams et al., 2007; Tokarczyk and Moore 1994; Sturges et al., 1992).”

L96: The point “support quantitative air-sea flux estimates” is less obvious than the other points so a reference may be helpful here.

Thank you, we have revised this sentence on L106 to read, “Aircraft observations can rapidly map basin-wide vertical distributions, support quantitative flux estimates, and provide spatial constraints to atmospheric models (e.g. Xiang et al. 2010x; Stephens et al 2018; Wofsy et al. 2011).”

L211: “We note that the non-linearity observed in ratios of these two gases at low  $\text{CHBr}_3$  levels likely reflects the differences in emissions during strong phytoplankton blooms, as oppose to other periods.” Could not the different lifetimes also effect this?

L395-409 Thank you, this passage has been amended to reflect this possibility, and we have done our best to clarify the wording: “The non-linearity observed in ratios of these two gases at low  $\text{CHBr}_3$  may reflect the different rates of their production or loss in seawater, or possibly, the influence of air masses from distant, more productive low-latitude source regions. Several studies have documented bacterially mediated loss of  $\text{CH}_2\text{Br}_2$ , but not  $\text{CHBr}_3$ , and report distinct ratios of  $\text{CH}_2\text{Br}_2$  to  $\text{CHBr}_3$  in seawater during the growth and senescent phases of a phytoplankton bloom (e.g. Carpenter et al. 2009, Hughes et al 2013). Although this analysis is restricted to the bottom 2 km of the atmosphere, zonal transport of air masses with lower ratios of  $\text{CH}_2\text{Br}_2$  to  $\text{CHBr}_3$  ratios, as have been observed in the MBL over productive, low-latitude regions, may also have influenced our observations (Yokouchi et al. 2005).”

Fig. 3. Units missing for the axes

This has been corrected- thank you for brining it to our attention.

Fig. 4. Why are some units given as nmol/mol and others as ppt ?

This too has now been corrected, the axes all read ppt. Again, thank you for brining this to our attention.

L222: Sorry, but I don't know what a type II major axis regression is. A few more words may help.

L426-L431 We have added a short passage to clarify the meaning and utility of the type II major axis regression in this analysis: “We used a type II major axis regression model (bivariate) to balance the influences of uncorrelated processes and measurement uncertainty in HVOCs (on the y-axis) and uncorrelated processes and measurement uncertainty in  $\text{O}_2$  and  $\text{CO}_2$  (on the x-axis) on the regression slope (Ayers et al. 2001; Glover et al., 2011). As noted by previous studies, simple least squares linear regressions fail to account for uncertainties in predictor variables (e.g. Cantrell et al. 2008).”

L250: Please explain how the molar enrichment ratios are defined and/or calculated. This seems to be critical, but not well explained. Is this just the slope of the regression between CHBr3 (or CH2Br2) and O2?

Yes, the molar enrichment ratios are equivalent to the slope of the regression, although the units of O<sub>2</sub> must be converted from O<sub>2</sub>/N<sub>2</sub> (per meg) to equivalent ppm (multiplying O<sub>2</sub>/N<sub>2</sub> by the X<sub>O<sub>2</sub></sub>, in dry air = 0.2093).

L351: “In its simplest approximation, the wind speed error will correlate with surface influence error” I understand that this is in general may be a reasonable assumption, but it is not obvious to me why the error in the influence function (in ppt m<sup>2</sup> s pmol<sup>-1</sup>) should be proportional to the error in wind speed. More justification of this argument would be needed here.

As explained in Xiang et al. 2010, now cited here, the STILT model error (E) represents a combination of source and model transport error. Although model transport error is difficult to quantify precisely, it is influenced first and foremost by differences in simulated and actual wind speed, wind direction, and boundary layer height. This passage L280-294 now reads, “Uncertainty in the surface influence value is strongly influenced by the accuracy of the underlying meteorological transport, as discussed in Xiang et al. (2010). We evaluated the GDAS reanalysis winds by comparing model winds interpolated in space and averaged between corresponding time points and pressure levels to match aircraft observations. By evaluating observed winds compared with modeled winds along the flight tracks we can estimate uncertainty in the surface influence values. We consider the observation-model differences in both wind speed and direction to approximate errors in surface influence strength and location. For wind speed, a small bias may be present, where we find a median difference between observations and reanalysis of 0.68 m/s, a 5% relative bias. The 1-sigma of the wind speed difference is 2.3 m/s, corresponding to a 19% 1-sigma uncertainty in wind speed. In its simplest approximation, the surface influence strength error is perfectly correlated with the wind speed error, and thus we take 19% as an approximation of the surface influence strength uncertainty. The uncertainty in surface influence location depends on the error in the wind direction. We find a 1-sigma error of 14 degrees in wind speed, which corresponds to a possible error of 260 km/day.”

L389: PAR: please spell out (as far as I can see first defined in L476)

L369 Thank you. This is now done.

L431: “We note that over-turned first year sea-ice, which can expose under-ice algae colonies to the air, likely still present a local source of CHBr3, CH2Br2, or other HVOCs to the MBL.” What is this statement based on?

As it is irrelevant to the main objective of the paper, this statement has been removed.

L499: Reference to Fig.9 in L499 was not clear to me. Was really Fig.9 meant here?

594 Fig. 10 is now referenced here, “For  $\text{CHBr}_3$ ,  $\text{CH}_2\text{Br}_2$ , and  $\text{CHClBr}_2$  we construct ocean emission inventories for January and February using a scaled version of gridded modeled air-sea  $\text{O}_2$  fluxes and the slopes (i.e. molar ratios) of linear correlations between  $\delta(\text{O}_2/\text{N}_2)$  and HVOC mixing ratios (Fig. 10).”

Fig. 9c: Caption not very clear, would be helpful if the description in the caption can be improved.

The wording of this caption has been rewritten. As now discussed elsewhere in the text (Sect. 2.3.1) the surface influence function (e.g.  $\text{HS}_1$ ) is the product of the surface influence and a relevant surface source field.

5.2 Why are STILT based emission estimates presented only for  $\text{CH}_3\text{I}$ ? Why is it not possible to perform this for other HVOCs as well?

Indeed, it is possible to estimate STILT emissions for other gases such as  $\text{CHBr}_3$  and  $\text{CH}_2\text{Br}_2$ . At present, we have not done this, as the correlations with STILT surface influence functions were less strong than those with  $\text{O}_2/\text{N}_2$ , as now stated in the text L653-656.

Figure S4: “Consecutive samples in and out of dips into the MBL”: Sorry, I don’t really understand what is meant here, please re-word.

This has been reworded as requested to read, “Consecutive TOGA VOC sample locations, their back-trajectories and surface influences in the lower troposphere on two different flights (a-c; Jan. 21, 2016, and d-f; Jan. 30, 2016).”

Technical corrections: L134: “low attitude” -> “low altitude”

Done.

L183: citation should be part of the sentence

Done.

1 **Novel approaches to improve estimates of short-lived halocarbon emissions during summer**  
2 **from the Southern Ocean [using airborne observations](#)**

3 **Elizabeth Asher<sup>1</sup>, Rebecca S. Hornbrook<sup>1</sup>, Britton B. Stephens<sup>1</sup>, Doug Kinnison<sup>1</sup>, Eric J. Morgan<sup>5</sup>, Ralph F.**  
4 **Keeling<sup>5</sup>, Elliot L. Atlas<sup>6</sup>, Sue M. Schauffler<sup>1</sup>, Simone Tilmes<sup>1</sup>, Eric A. Kort<sup>2</sup>, Martin S. Hoecker-Martínez<sup>3</sup>,**  
5 **Matt C. Long<sup>1</sup>, Jean-François Lamarque<sup>1</sup>, Alfonso Saiz-Lopez<sup>4,1</sup>, Kathryn McKain<sup>7,8</sup>, Colm Sweeney<sup>8</sup>, Alan J.**  
6 **Hills<sup>1</sup>, and Eric C. Apel<sup>1</sup>**

7 <sup>1</sup>National Center for Atmospheric Research, Boulder, Colorado, USA

8 <sup>2</sup>University of Michigan, Climate and Space Sciences and Engineering, Ann Arbor, Michigan, USA

9 <sup>3</sup>University of Redlands, Physics Department, Redlands, California, USA

10 <sup>4</sup>Department of Atmospheric Chemistry and Climate, Institute of Physical Chemistry Rocasolano, CSIC,  
11 Madrid, Spain

12 <sup>5</sup>Scripps Institution of Oceanography, University of California, San Diego, California, USA

13 <sup>6</sup>University of Miami, Department of Atmospheric Sciences, Miami, Florida, USA

14 <sup>7</sup>Cooperative Institute for Research in Environmental Sciences, University of Colorado, Boulder,  
15 Colorado, USA

16 <sup>8</sup>National Oceanic and Atmospheric Administration, Boulder, Colorado, USA

17

18

## 19 Abstract.

20 Fluxes of halogenated volatile organic compounds (VOCs) over the Southern Ocean remain  
21 poorly understood, and few atmospheric measurements exist to constrain modeled emissions of  
22 these compounds. We present observations of  $\text{CHBr}_3$ ,  $\text{CH}_2\text{Br}_2$ ,  $\text{CH}_3\text{I}$ ,  $\text{CHClBr}_2$ ,  $\text{CHBrCl}_2$ , and  
23  $\text{CH}_3\text{Br}$  during the  $\text{O}_2/\text{N}_2$  Ratio and  $\text{CO}_2$  Airborne Southern Ocean (ORCAS) study and the 2<sup>nd</sup>  
24 Atmospheric Tomography mission (ATom-2), in January and February of 2016 and 2017. Good  
25 model-measurement correlations were obtained between these observations and simulations from  
26 the Community Earth System Model (CESM) atmospheric component with chemistry (CAM-  
27 Chem) for  $\text{CHBr}_3$ ,  $\text{CH}_2\text{Br}_2$ ,  $\text{CH}_3\text{I}$ , and  $\text{CHClBr}_2$  but all showed significant differences in  
28 model:measurement ratios. The model:measurement comparison for  $\text{CH}_3\text{Br}$  was satisfactory and  
29 for  $\text{CHBrCl}_2$  the low levels present precluded us from making a complete assessment.  
30 Thereafter, we demonstrate two novel approaches to estimate halogenated VOC fluxes; the first  
31 approach takes advantage of the robust relationships that were found between airborne  
32 observations of  $\text{O}_2$  and  $\text{CHBr}_3$ ,  $\text{CH}_2\text{Br}_2$ , and  $\text{CHClBr}_2$ ; we use these linear regressions with  $\text{O}_2$   
33 and modeled  $\text{O}_2$  distributions to infer a biological flux of halogenated VOCs. The second  
34 approach uses the Stochastic Time-Inverted Lagrangian Transport (STILT) particle dispersion  
35 model to explore the relationships between observed mixing ratios and the product of the  
36 upstream surface influence and sea ice, chl *a*, absorption due to detritus, and downward  
37 shortwave radiation at the surface, which in turn relate to various regional hypothesized sources  
38 of halogenated VOCs such as marine phytoplankton, phytoplankton in sea ice brines, and  
39 decomposing organic matter in surface seawater. These relationships can help evaluate the  
40 likelihood of particular halogenated VOC sources, and in the case of statistically significant  
41 correlations, such as was found for  $\text{CH}_3\text{I}$ , may be used to derive an estimated flux field. Our  
42 results are consistent with a biogenic regional source of  $\text{CHBr}_3$ , and both non-biological and  
43 biological sources of  $\text{CH}_3\text{I}$  over these regions.

44

## 45 1 Introduction

46 Emissions of halogenated volatile organic compounds (VOCs) influence regional atmospheric  
47 chemistry and global climate. Through the production of reactive halogen radicals at high  
48 latitudes, halogenated VOCs contribute to tropospheric and stratospheric ozone destruction, and  
49 alter the sulfur, mercury, nitrogen oxide and hydrogen oxide cycles (e.g. Schroeder et al., 1998;  
50 Boucher et al., 2003; Bloss et al., 2005; von Glasow and Crutzen; 2007; Saiz-Lopez et al., 2007;  
51 Obrist et al., 2011; Engel and Rigby, 2018). In the marine boundary layer and lower  
52 troposphere, sea salt is the main source of reactive bromine (Finlayson-Pitts 1982, Simpson et  
53 al., 2015). Yet halogenated VOCs may also be a more important source of inorganic bromine to  
54 the whole atmosphere than previously thought, according to a recent study, which indicates that  
55 sea salt is scarce and insufficient to control the bromine budget in the middle and upper  
56 troposphere (Murphy et al., 2019).

57 Phytoplankton and macroalgae in the ocean are the main sources to the atmosphere of several  
58 very short-lived bromocarbons, including bromoform ( $\text{CHBr}_3$ ), dibromomethane ( $\text{CH}_2\text{Br}_2$ ),

Elizabeth Asher 9/3/2019 11:07 AM

Deleted: H

Elizabeth Asher 7/5/2019 2:01 PM

Deleted: -side

Elizabeth Asher 7/5/2019 2:05 PM

Deleted: We show mixing ratio comparisons

Elizabeth Asher 7/6/2019 2:51 PM

Deleted: Thereafter, we

Elizabeth Asher 9/3/2019 11:07 AM

Deleted: H

Elizabeth Asher 9/3/2019 11:08 AM

Deleted: H

Elizabeth Asher 9/3/2019 11:08 AM

Deleted: H

Elizabeth Asher 9/3/2019 11:08 AM

Deleted: H

68 dibromochloromethane (CHClBr<sub>2</sub>), and bromodichloromethane (CHBrCl<sub>2</sub>) (Moore et al., 1996;  
69 Carpenter et al. 2003; Butler et al., 2007; Raimund et al., 2011). Other [halogenated](#) VOCs, such  
70 as methyl iodide (CH<sub>3</sub>I), and methyl bromide (CH<sub>3</sub>Br) have many natural sources, such as  
71 coastal macroalgae, phytoplankton, temperate forest soil and litter, and biomass burning (e.g.,  
72 Bell et al., 2002; Sive et al., 2007; Colomb et al. 2008; Drewer et al., 2008). CH<sub>3</sub>I is also formed  
73 through non-biological reactions in surface seawater, and CH<sub>3</sub>Br is emitted as a result of  
74 quarantine and pre-shipment activities, which are not regulated by the Montreal Protocol (e.g.,  
75 Moore and Zafirou, 1994, [Engel and Rigby, 2018](#)). Over the Southern Ocean specifically,  
76 hypothesized sources of [halogenated](#) VOCs include: coastal macroalgae, phytoplankton, sea ice  
77 algae, and photochemical or dust stimulated non-biological production at the sea surface (e.g.,  
78 [Abrahamsson et al. 2018](#), Manley and Dastoor 1998; Moore and Zafirou 1994; [Moore et al.,](#)  
79 [1996](#); Richter and Wallace 2004; Williams et al., 2007; Tokarczyk and Moore 1994; Sturges et  
80 al., 1992).

Elizabeth Asher 9/3/2019 11:08 AM  
Deleted: H

Elizabeth Asher 7/7/2019 9:48 AM  
Deleted: the

Elizabeth Asher 9/3/2019 11:46 AM  
Deleted: WMO

Elizabeth Asher 9/3/2019 11:08 AM  
Deleted: H

81 We largely owe our current understanding of marine [halogenated](#) VOC emissions over the  
82 Southern Ocean to ship-based field campaigns and laboratory process studies (e.g., Abrahamsson  
83 et al. 2004a,b; Atkinson et al., 2012; Carpenter et al., 2007; Moore et al., 1996; Chuck et al.,  
84 2005; Butler et al., 2007; Raimund et al., 2011; Hughes et al., 2009; [Mattsson et al. 2013](#);  
85 Hughes et al., 2013). These studies have reported surface water and sea-ice [halogenated VOC](#)  
86 [supersaturation](#) and corresponding elevated levels of [halogenated VOCs](#) in the marine boundary  
87 layer (MBL) [in summer](#), and have identified numerous biological and non-biological [ocean](#)  
88 sources for these compounds. [Mattsson et al. \(2013\)](#) noted that the ocean also acts as a sink for  
89 [halogenated VOCs, when undersaturated surface waters equilibrate with air masses transported](#)  
90 [from halogenated VOC source regions. The spatially heterogeneous](#) ocean sources of CHBr<sub>3</sub> and  
91 CH<sub>2</sub>Br<sub>2</sub> at high latitudes in the Southern Hemisphere are often underestimated in global  
92 atmospheric models (Hossaini et al., 2013; Ordoñez et al., 2012; Ziska et al., 2013). Ship-based  
93 and Lagrangian float observations provide invaluable information on the sources and temporal  
94 variability of compounds in the surface ocean. These methods offer the advantage of  
95 simultaneous measurements of both air and seawater to evaluate the gases' saturation state in the  
96 surface ocean and calculate fluxes. Yet ship-based measurements onboard these slow moving  
97 platforms also have drawbacks: they under sample the spatial variability of [halogenated](#) VOCs  
98 (e.g., Butler et al., 2007) and require assumptions about gas-exchange rates to estimate fluxes.

Elizabeth Asher 9/3/2019 11:08 AM  
Deleted: H

Elizabeth Asher 7/7/2019 9:49 AM  
Deleted: ,

Elizabeth Asher 9/3/2019 11:09 AM  
Deleted: H

99 To disentangle the roles of atmospheric transport and spatial variability of emissions on  
100 [halogenated](#) VOC distributions requires large-scale atmospheric observations. At low latitudes,  
101 large-scale convection at the intertropical convergence zone carries bromocarbons and other  
102 [halogenated](#) VOCs into the free troposphere and lower stratosphere (e.g., Liang et al., 2014;  
103 Navarro et al., 2015). [Polar regions](#) are characterized by stable boundary layers in summer.  
104 [Wind shear, frontal systems, and internal gravity waves](#) create turbulence [and control](#) vertical  
105 mixing within and across a stable [polar](#) boundary layer (e.g. Anderson et al., 2008), [and small,](#)  
106 [convective plumes may form over the marginal sea ice zone, related to sea ice leads as well as](#)  
107 [winds from ice-covered to open-ocean waters \(e.g. Schnell et al., 1989\). As a result of limited](#)  
108 [vertical transport in these regions, however, air-sea fluxes lead to strong vertical gradients.](#)  
109 [Zonal transport from lower latitudes has a large impact on the vertical gradients of trace gas](#)

Elizabeth Asher 9/3/2019 11:09 AM  
Deleted: H

Elizabeth Asher 9/3/2019 11:09 AM  
Deleted: H

119 [mixing ratios over polar regions \(Salawitch 2010\)](#). Given their extended photochemical lifetimes  
120 at high latitudes (see Sect. 2.3 for a brief discussion), [many halogenated VOC distributions](#) are  
121 [particularly sensitive to zonal transport at altitude](#).

Elizabeth Asher 9/3/2019 11:09 AM

Deleted: H

122 Aircraft observations can rapidly map basin-wide vertical distributions, support quantitative flux  
123 estimates, and provide spatial constraints to atmospheric models (e.g. [Xiang et al., 2010](#);  
124 [Stephens et al., 2018](#); [Wofsy et al., 2011](#)). Few airborne observations of halogenated VOCs exist  
125 at high latitudes in the Southern Hemisphere. Two earlier aircraft campaigns that have measured  
126 summertime halogenated VOCs in this region are the first Aerosol Characterization Experiment  
127 (ACE-1; Bates et al., 1999) and the first High-performance Instrumented Airborne Platform for  
128 Environmental Research (HIAPER) Pole-to-Pole Observations (HIPPO; Wofsy, 2011)  
129 campaign. For these two aircraft campaigns, whole air samples were collected onboard the  
130 NSF/NCAR C-130 and the NSF/NCAR Gulfstream V (GV) during latitudinal transects over the  
131 Pacific Ocean as far south as 60° S and 67° S, respectively. However, the ACE-1 and HIPPO  
132 campaigns obtained relatively few whole air samples in this region, with  $\leq 100$  samples poleward  
133 of 60° S combined (e.g., Blake et al., 1999; Hossaini et al., 2013). ACE-1 measurements of CH<sub>3</sub>I  
134 in the MBL indicate a strong ocean source between 40° S and 50° S in austral summer, with  
135 mixing ratios above 1.2 pmol below ~1 km (Blake et al., 1999).

Elizabeth Asher 6/16/2019 4:20 PM

Deleted: air-sea

Elizabeth Asher 9/3/2019 11:09 AM

Deleted: H

136 [Halogenated](#) VOC emissions are frequently incorporated into earth system models, using either  
137 climatologies or parameterizations based on satellite observations of chlorophyll and  
138 geographical region and evaluated using mixing ratio comparisons with airborne observations. In  
139 [Section 3.1 and 3.2](#), we report new airborne observations of CHBr<sub>3</sub>, CH<sub>2</sub>Br<sub>2</sub>, CH<sub>3</sub>I, CHClBr<sub>2</sub>,  
140 CHBrCl<sub>2</sub>, and CH<sub>3</sub>Br from high latitudes in the Southern Hemisphere, where data are scarce, and  
141 large-scale regional mixing ratio comparisons for halogenated VOCs with the community earth  
142 system model (CESM) atmospheric component with chemistry (CAM-Chem). In section 3.4, we  
143 present two novel approaches to estimate regional fluxes of halogenated VOCs for comparison  
144 with global climate models' parameterizations or climatologies. One approach uses correlations  
145 of halogenated VOCs to marine oxygen (O<sub>2</sub>) of marine origin, as measured by deviations in the  
146 ratio of O<sub>2</sub> to nitrogen (N<sub>2</sub>) ( $\delta(O_2/N_2)$  see Sect. 2.1.2 and 3.1.2). We exploit robust ratios of  
147 halogenated VOCs to oxygen (O<sub>2</sub>) determined from linear regressions (i.e. the enrichment ratio),  
148 and the ocean flux of O<sub>2</sub> from CESM's ocean component, to estimate the marine biogenic flux of  
149 several halogenated VOCs. The second approach relies on observed halogenated VOC mixing  
150 ratios, the Stochastic Time-Inverted Lagrangian Transport (STILT) particle dispersion model and  
151 geophysical datasets (see Sect. 2.3 and 3.3). We assess contributions from previously  
152 hypothesized regional sources for the Southern Ocean, and estimate halogenated VOC fluxes  
153 based on regressions between upstream influences and observed mixing ratios and distributions  
154 of remotely sensed data.

Elizabeth Asher 9/3/2019 11:10 AM

Deleted: H

Elizabeth Asher 7/7/2019 10:08 AM

Deleted: climate

## 156 [2 Methods](#)

### 157 [2.1 Measurements](#)

158 Atmospheric measurements for this study were collected at high latitudes in the Southern  
159 Hemisphere as part of the O<sub>2</sub>/N<sub>2</sub> Ratio and CO<sub>2</sub> Airborne Southern Ocean (ORCAS) study

Elizabeth Asher 7/5/2019 2:13 PM

Deleted: Observations

Elizabeth Asher 7/5/2019 2:13 PM

Deleted: Overview



167 (Stephens et al., 2018), and the second NASA Atmospheric Tomography Mission (ATom-2),  
168 near Punta Arenas, Chile (Fig. 1). The ORCAS field campaign took place from Jan. 15 – Feb.  
169 29, 2016 onboard the NSF/NCAR GV. On Feb. 10 and 13, 2017 the [sixth and seventh ATom-2](#)  
170 [research flights](#) passed over the eastern Pacific sector poleward of 60° S (defined here as Region  
171 1) and over the Patagonian Shelf between 40° S and 55° S and between 70° W and 50° W  
172 (defined here as Region 2), [respectively](#). The two regions for this study are defined based  
173 loosely on dynamic biogeochemical provinces identified using bathymetry, algal biomass, sea  
174 surface temperature and salinity (Reygondeau et al., 2013).

175 Both projects featured en route vertical profiling from near the ocean surface (~ 150 m) to the  
176 upper-troposphere, with 74 ORCAS and seven ATom-2 (during the sixth and seventh flights)  
177 low-altitude level legs in the MBL. These campaigns shared a number of instruments, including  
178 the NCAR Trace Gas Organic Analyzer (TOGA), the NCAR Atmospheric Oxygen (AO2)  
179 instrument, a Picarro cavity ringdown spectrometer operated by NOAA, discussed below. More  
180 information about individual instruments may be found in Stephens et al., 2018 and at  
181 [https://www.eol.ucar.edu/field\\_projects/orcas](https://www.eol.ucar.edu/field_projects/orcas) and <https://espo.nasa.gov/atom/content/ATom>.

182

### 183 2.1.1 Halogenated VOCs

184 During ORCAS and ATom-2 TOGA provided mixing ratios of over 60 organic compounds,  
185 including [halogenated VOCs](#). [The instrument, described in Apel et al. \(2015\), continuously](#)  
186 [collects and analyzes samples for CHBr<sub>3</sub>, CH<sub>2</sub>Br<sub>2</sub>, CHClBr<sub>2</sub>, CHBrCl<sub>2</sub>, and CH<sub>3</sub>I among other](#)  
187 [compounds, with a 35-second sampling period and repeats the cycle every two-minutes using](#)  
188 [online fast gas chromatography and mass spectrometry. This study also leverages measurements](#)  
189 [of CH<sub>3</sub>Br from whole air samples from the U. Miami / NCAR Advanced Whole Air Sampler](#)  
190 [\(AWAS; Schauffler et al., 1999\) onboard the GV during the ORCAS campaign and the UC](#)  
191 [Irvine Whole Air Sampler \(WAS; Blake et al., 2001\) onboard the DC-8 during the ATom-2](#)  
192 [campaign. Halogenated VOCs reported here have an overall ±15% accuracy and ±3% relative](#)  
193 [precision, and detection limits of 0.03 ppt for CH<sub>3</sub>I, 0.2 ppt for CHBr<sub>3</sub>, 0.03 ppt for CH<sub>2</sub>Br<sub>2</sub>, 0.03](#)  
194 [ppt for CHClBr<sub>2</sub>, 0.05 ppt for CHBrCl<sub>2</sub>, and 0.2 ppt for CH<sub>3</sub>Br – 0.2 ppt. In addition,](#)  
195 comparisons between onboard collected whole air samples and in-flight TOGA measurements,  
196 when sharing over half of their sampling period with TOGA measurements, showed good  
197 correlations for CHBr<sub>3</sub>, CH<sub>2</sub>Br<sub>2</sub>, CH<sub>3</sub>I, and CHClBr<sub>2</sub>, although there were some calibration  
198 differences (Fig. S1 and Fig. S2). In addition to the comparison between co-located atmospheric  
199 measurements, we also conducted a lab inter-comparison following the campaign between  
200 NOAA’s programmable flask package (PFP) and TOGA (Table S1; see supplement for details).

201

### 202 2.1.2 δ(O<sub>2</sub>/N<sub>2</sub>) and CO<sub>2</sub>

203 The AO2 instrument measures variations in atmospheric O<sub>2</sub>, which are reported as relative  
204 deviations in the oxygen to nitrogen ratio (δ(O<sub>2</sub>/N<sub>2</sub>)), following a dilution correction for CO<sub>2</sub>  
205 (Keeling et al., 1998; Stephens et al., 2018). The instrument’s precision is ±2 per meg units (one

Elizabeth Asher 6/16/2019 1:28 PM

Deleted: t

Elizabeth Asher 7/7/2019 10:48 AM

Deleted: 2

Elizabeth Asher 9/3/2019 11:10 AM

Deleted: H

Elizabeth Asher 7/5/2019 2:14 PM

Deleted: , at background levels

Elizabeth Asher 7/8/2019 5:29 PM

Deleted: The instrument, described in  
Apel et al. (2015), continuously collects and  
analyzes samples

Elizabeth Asher 7/8/2019 5:29 PM

Deleted:

214 in one million relative) for a 5 second measurement (Stephens et al., 2003; Stephens et al.,  
 215 manuscript in preparation, 2019). Anthropogenic, biogenic, and oceanic processes introduce O<sub>2</sub>  
 216 perturbations that are superimposed on the background concentrations of O<sub>2</sub> in air (XO<sub>2</sub>, in dry  
 217 air = 0.2095). [Air-sea O<sub>2</sub> fluxes are driven by both biological production and consumption of O<sub>2</sub>](#)  
 218 [and by heating and cooling of surface waters.](#) O<sub>2</sub> is consumed when fossil fuels are burned and  
 219 produced [and consumed](#) during terrestrial photosynthesis [and respiration](#). Seasonal changes in  
 220 the ocean heat content lead to small changes in atmospheric N<sub>2</sub>. As others have done, we  
 221 isolated the air-sea O<sub>2</sub> signal by subtracting model estimates of the terrestrial O<sub>2</sub>, fossil-fuel O<sub>2</sub>,  
 222 and air-sea N<sub>2</sub> flux influences from the δ(O<sub>2</sub>/N<sub>2</sub>) measurements (Equation 1; [Keeling et al., 1998;](#)  
 223 [Garcia and Keeling, 2001; Stephens et al., 2018](#)). The difference of the δ(O<sub>2</sub>/N<sub>2</sub>) measurement  
 224 and these modeled [components](#) is multiplied by XO<sub>2</sub> to convert to ppm equivalents as needed  
 225 (ppm eq; Keeling et al., 1998; Equation 1).

$$226 \text{O}_{2\text{-ppm-equiv}} = [\delta(\text{O}_2/\text{N}_2) - \delta(\text{O}_2/\text{N}_2)_{\text{Land}} - \delta(\text{O}_2/\text{N}_2)_{\text{Fossil Fuel}} - \delta(\text{O}_2/\text{N}_2)_{\text{N}_2}] \times \text{XO}_2 \quad (1)$$

227 We obtained the modeled δ(O<sub>2</sub>/N<sub>2</sub>) signal [terrestrial](#) influences from the land model component  
 228 of the [CESM](#), the fossil fuel combustion influences from the Carbon Dioxide Information  
 229 Analysis Center (CDIAC; Boden et al. 2017), and the air-sea N<sub>2</sub> influences from the oceanic  
 230 component of CESM. These fluxes were all advected through the specified dynamics version of  
 231 [CESM's atmosphere component](#), as described below in Sect. [2.2](#) and in Stephens et al. (2018).

232 CO<sub>2</sub> measurements were provided by NOAA's Picarro G2401-m cavity ring down spectrometer  
 233 modified to have a ~1.2 sec measurement interval and a lower cell pressure of 80 Torr, which  
 234 enabled the instrument to function at the full range of GV altitudes. (McKain et al. [manuscript in](#)  
 235 [preparation, 2019](#)). Dry-air mole fractions were calculated using empirical corrections to account  
 236 for dilution and [pressure](#) broadening effects [as determined](#) in the laboratory before and after the  
 237 campaign deployments, and in-flight calibrations were used to determine an offset correction for  
 238 each flight. Corrected CO<sub>2</sub> data have a total average uncertainty of 0.07 ppm (McKain et al.  
 239 [manuscript in preparation](#), 2019). To merge them with the TOGA data, these faster O<sub>2</sub> and CO<sub>2</sub>  
 240 measurements were arithmetically averaged over TOGA's 35-s sampling periods (Stephens et  
 241 al., 2017 and <https://espo.nasa.gov/atom/content/ATom>).

## 244 2.2 CAM-Chem model configuration

245 [The CESM version 1, atmospheric component with chemistry \(CAM-Chem\) is a global three-](#)  
 246 [dimensional chemistry climate model that extends from the Earth's surface to the stratopause.](#)  
 247 [CAM-Chem version 1.2 includes all the physical parameterizations of Neale et al. \(2013\) and a](#)  
 248 [finite volume dynamical core \(Lin, 2004\) for tracer advection. The model has a horizontal](#)  
 249 [resolution of 0.9° latitude × 1.25° longitude, with 56 vertical hybrid levels and a time-step of 30](#)  
 250 [minutes. Meteorology is specified using the NASA Global Modeling and Assimilation Office](#)  
 251 [\(GMAO\) Goddard Earth Observing System Model, version 5 \(GEOS-5; Rienecker et al., 2008\)](#)  
 252 [\(GEOS-5\), following the specified dynamic procedure described by Lamarque et al. \(2012\).](#)  
 253 [Winds, temperatures, surface pressure, surface stress, and latent and sensible heat fluxes are](#)

- Elizabeth Asher 7/7/2019 11:02 AM  
Formatted: Font:Italic
- Elizabeth Asher 8/4/2019 2:03 PM  
Deleted: 3
- Elizabeth Asher 7/7/2019 11:03 AM  
Formatted: Subscript
- Elizabeth Asher 6/16/2019 1:28 PM  
Deleted: (Keeling et al., 1998; Garcia and Keeling, 2001; Stephens et al., 2018)
- Elizabeth Asher 7/7/2019 11:04 AM  
Deleted: photosynthesis
- Elizabeth Asher 7/7/2019 11:04 AM  
Formatted: Subscript
- Elizabeth Asher 7/7/2019 11:04 AM  
Deleted: combustion
- Elizabeth Asher 7/7/2019 11:04 AM  
Formatted: Subscript
- Elizabeth Asher 7/7/2019 11:05 AM  
Deleted: values
- Elizabeth Asher 7/8/2019 5:30 PM  
Deleted: .
- Elizabeth Asher 7/7/2019 11:05 AM  
Deleted: land
- Elizabeth Asher 7/7/2019 11:09 AM  
Deleted: Community Earth System (
- Elizabeth Asher 7/7/2019 11:09 AM  
Deleted: )
- Elizabeth Asher 7/7/2019 11:11 AM  
Deleted: 3.1
- Elizabeth Asher 8/4/2019 2:04 PM  
Deleted: The XO<sub>2</sub> in 2016 is the Tohjima et al. (2005) value from the year 2000 adjusted for the 4 ppm yr<sup>-1</sup> or ~20 per meg yr<sup>-1</sup> decrease in O<sub>2</sub> between 2000 and 2016.
- Elizabeth Asher 7/7/2019 11:11 AM  
Deleted: .. in prep., 2019
- Elizabeth Asher 7/8/2019 5:30 PM  
Deleted: in prep.

271 nudged using a 5-hour relaxation timescale to GEOS-5  $1^\circ \times 1^\circ$  meteorology. The sea surface  
272 temperature boundary condition is derived from the Merged Hadley-NOAA Optimal  
273 Interpolation Sea Surface Temperature and Sea-Ice Concentration product (Hurrell et al., 2008).  
274 The model uses chemistry described by Tilmes et al. (2016), biomass burning and biogenic  
275 emissions from the Fire INventory of NCAR (FINN; Wiedinmyer et al., 2011) and MEGAN  
276 (Model of Emissions of Gasses and Aerosols from Nature) 2.1 products (Guenther et al., 2012)  
277 and additional tropospheric halogen chemistry described in Fernandez et al. (2014) and Saiz-  
278 Lopez et al. (2014). These include ocean emissions of  $\text{CHBr}_3$ ,  $\text{CH}_2\text{Br}_2$ ,  $\text{CHBr}_2\text{Cl}$ , and  $\text{CHBrCl}_2$ ,  
279 with parameterized emissions based on chlorophyll *a* (chl *a*) concentrations and scaled by a  
280 factor of 2.5 over coastal regions, as opposed to open ocean regions (Ordoñez et al., 2012). The  
281 model used an existing  $\text{CH}_3\text{I}$  flux climatology (Bell et al., 2002), and  $\text{CH}_3\text{Br}$  was constrained to a  
282 surface lower boundary condition, also described by Ordoñez et al. (2012). This version of the  
283 model was run for the period of the ORCAS field campaign (January and February 2016),  
284 following a 24-month spin-up. To facilitate comparisons to ORCAS observations, output  
285 included vertical profiles of modeled constituents from the two nearest latitude and two nearest  
286 longitude model grid-points (four profiles in total) to the airborne observations at every 30-min  
287 model time-step. Following the run, simulated constituent distributions were linearly interpolated  
288 to the altitude, latitude and longitude along the flight track, yielding co-located modeled  
289 constituents and airborne observations. This version of the model has not yet been run for the  
290 ATom-2 period.

291

### 292 **2.3 STILT model configuration**

293 The Stochastic Time-Inverted Lagrangian Transport (STILT; Lin et al., 2003) particle dispersion  
294 model uses a receptor oriented framework to infer surface sources or sinks of trace gases from  
295 atmospheric observations collected downstream, thus simulating the upstream influences that are  
296 ultimately measured at the receptor site. The model tracks ensembles of particle trajectories  
297 backward in time and the resulting distributions of these particles can be used to define surface  
298 influence maps for each observation. STILT was run using 0.5° Global Data Assimilation System  
299 (GDAS) reanalysis winds to investigate the transport history of air sampled along the flight track  
300 (Stephens et al., 2018). For each TOGA observation, an ensemble of 4,096 particles was  
301 released from the sampling location and followed over a backwards simulation period of seven  
302 days. Particles in the lower half of the simulated MBL are assigned a surface influence value,  
303 which quantitatively links observed mixing ratios to surface sources (Lin et al., 2003). The  
304 average surface influence of all 4,096 particles per sampling location yields an hourly and  
305 spatially gridded surface influence value ( $\text{ppt m}^2 \text{ s pmol}^{-1}$ ) at a spatial resolution of  $0.25^\circ \times 0.25^\circ$   
306 for each sample point.

307 Uncertainty in the surface influence value is strongly influenced by the accuracy of the  
308 underlying meteorological transport, as discussed in Xiang et al. (2010). We evaluated the  
309 GDAS reanalysis winds by comparing model winds interpolated in space and averaged between  
310 corresponding time points and pressure levels to match aircraft observations. By evaluating  
311 observed winds compared with modeled winds along the flight tracks we can estimate

312 uncertainty in the surface influence values. We consider the observation-model differences in  
313 both wind speed and direction to approximate errors in surface influence strength and location.  
314 For wind speed, a small bias may be present, where we find a median difference between  
315 observations and reanalysis of 0.68 m/s, a 5% relative bias. The 1-sigma of the wind speed  
316 difference is 2.3 m/s, corresponding to a 19% 1-sigma uncertainty in wind speed. In its simplest  
317 approximation, the surface influence strength error is perfectly correlated with the wind speed  
318 error, and thus we take 19% as an approximation of the surface influence strength uncertainty.  
319 The uncertainty in surface influence location depends on the error in the wind direction. We find  
320 a 1-sigma error of 14 degrees in wind speed, which corresponds to a possible error of 260  
321 km/day.

322 Finally, we note that photochemical loss during transport is not accounted for in this analysis.  
323 Low OH mixing ratios, cold temperatures, and lower photolysis rates due to angled sunlight at  
324 high latitudes lead to longer than average halogenated VOC lifetimes. For instance, assuming an  
325 average diurnal OH concentration of 0.03 ppt, and average photochemical loss according to the  
326 Tropospheric Ultraviolet and Visible (TUV) radiation model and the Mainz Spectral data site  
327 ([http://satellite.mpic.de/spectral\\_atlas](http://satellite.mpic.de/spectral_atlas)) for Jan. 29 under clear sky conditions at 60° S, CHBr<sub>3</sub> has  
328 a lifetime of 30 days, CH<sub>2</sub>Br<sub>2</sub> has a lifetime of 270 days, CH<sub>3</sub>I has a lifetime of 7 days, and  
329 CHClBr<sub>2</sub> has a lifetime of 63 days. As such, the photochemical lifetimes of these gases are  
330 greater than or equal to the time of our back-trajectory analysis. Moreover, OH concentrations in  
331 this region have large uncertainties, the inclusion of which would lead to more, not less,  
332 uncertainty in surface influence based regression coefficients and estimated fluxes (see Sect. 2.3  
333 and 3.3 for details).

334

### 335 **2.3.1 STILT surface influence functions**

336 For this study, we used STILT surface influence distributions with remotely sensed ocean  
337 surface and reanalysis data (i.e. surface source fields) in linear and multi-linear regressions to  
338 generate empirical STILT influence functions. Surface influence functions can help explain  
339 observed mixing ratios of CHBr<sub>3</sub>, CH<sub>2</sub>Br<sub>2</sub>, CH<sub>3</sub>Br and CH<sub>3</sub>I, evaluate the likelihood of particular  
340 halogenated VOC sources, and in the case of statistically significant correlations, may be used to  
341 derive an estimated flux field (See Sect. 3.3 and 3.4.2 for details).

342

343 We tested whether observed mixing ratios ( $Z$ ) could be explained by a linear relationship in  
344 which the predictor variable is a surface influence function, equal to the product of the surface  
345 influence ( $H$ ) and a potential geophysical surface source field(s), such as chl  $a$ , as well as an  
346 intercept ( $b$ ), a slope ( $a$ ), and error term  $\xi$  (Equation 2; Fig. S5). This relationship can be  
347 generalized as a multiple linear regression with multiple surface influence functions ( $Hs_1, Hs_2, \dots$ )  
348 and slope coefficients ( $a_1, a_2$ ; Equation 3), when multiple sources contribute to observed  
349 halogenated VOC mixing ratios. The multiple linear regression may also include an interaction  
350 term ( $Hs_2$ ) between predictor variables (e.g.  $Hs_1$  and  $Hs_2$ ) with a slope coefficient ( $a_3$ ) to improve  
351 the fit. Statistical correlations between mixing ratios and surface influence functions may be

352 used to support or reject hypothesized sources. A flux ( $\mu\text{mol m}^{-2} \text{s}^{-1}$ ) may then be estimated for  
353 each grid cell based on the product of the slopes ( $a_1, a_2, \dots$ ) and the potential source fields ( $s_1, s_2, \dots$ ).  
354 Grid cell fluxes are averaged over a geographical region to yield the average regional flux. We  
355 used the standard deviation of the regression coefficients and the relative uncertainty in the  
356 surface source, added in quadrature, to estimate the uncertainty in the flux (see Sect. 3.4.2 for  
357 fractional uncertainties). We note that the uncertainty in STILT transport (see Sect. 2.3 for  
358 details) is inherently reflected in the relative uncertainty of the regression coefficients ( $a_1, a_2, \dots$ ).

$$359 \quad Z = aHs + b + \xi \quad (2)$$

$$360 \quad Z = a_1Hs_1 + a_2Hs_2 + (a_3Hs_1Hs_2) \dots + b + \xi \quad (3)$$

361

### 362 **2.3.2 Surface Source Fields**

363 Geophysical surface source fields of remotely sensed and reanalysis data included a combination  
364 of sea ice concentration, chl  $a$ , absorption due to ocean detrital material, and downward  
365 shortwave radiation at the ocean surface.

366 We used daily sea ice concentration data (<https://nsidc.org/data/nsidc-0081>) at a 25 km x 25 km  
367 spatial resolution between 39.23° S and 90° S, 180° W – 180° E from the NASA National Snow  
368 and Ice Data Center Distributed Active Archive Center (NSIDC; Maslanik et al., 1999). This  
369 data reports the fraction of sea-ice cover, land-ice cover, and open water. Unfortunately, these  
370 data do not provide any information on sea ice thickness, or the presence of brine channels or  
371 melt ponds, which may modulate emissions from sea-ice covered regions. Sea ice concentration  
372 data were calculated using measurements of near-real-time passive microwave brightness  
373 temperature from the Special Sensor Microwave Image/Sounder (SSMIS) on the Defense  
374 Meteorological Satellite Program (DMSP) satellites. NSIDC sea ice concentration data were  
375 arithmetically averaged to yield 0.25° x 0.25° binned sea ice fraction for use with gridded surface  
376 influences.

377 Due to persistent cloud cover over the Southern Ocean, which often precludes the retrieval of  
378 remotely sensed ocean color data, we used 8-day mean composite Aqua MODIS L3 distributions  
379 of chl  $a$  from the Ocean Color Index (OCI) algorithm and absorption due to gelbstoff and detrital  
380 material at 443 nm from the Generalized Inherent Optical Properties (GIOP) model (NASA  
381 Goddard Space Flight Center, 2014). Absorption due to gelbstoff and detrital material at 443 nm  
382 is used as a proxy for colored dissolved organic matter (CDOM;  
383 <https://oceancolor.gsfc.nasa.gov/atbd/giop/>). CDOM is hypothesized to be an important source of  
384 carbon for the photochemical production of  $\text{CH}_2\text{I}$  (Moore et al., 1994). The GIOP model also  
385 publishes an uncertainty in the absorption due to gelbstoff and detrital material at 443 nm. Raw  
386 4 km x 4 km data were geometrically averaged, based on lognormal probability density  
387 functions, to a spatial resolution of 0.25° x 0.25° for use with gridded surface influences. We  
388 used the ratio of the 0.25° x 0.25° gridded uncertainty in the detrital material absorption to the  
389 absorption as the relative uncertainty for flux calculations (see Sect. 3.4.2).

Elizabeth Asher 7/5/2019 2:55 PM

Formatted: Font:

390 [The National Center for Environmental Prediction \(NCEP\) provides Final Global Data](#)  
391 [Assimilation System \(GDAS/FNL\) global data of downward shortwave radiation at the surface](#)  
392 [at 0.25 degree and 6-hour resolution \(NCEP, 2015\). We chose downward shortwave radiation](#)  
393 [for use with gridded surface influences because the photo-production of CH<sub>3</sub>I has been observed](#)  
394 [at all visible wavelengths \(Moore et al., 1994\). This reanalysis data is available at a higher](#)  
395 [temporal resolution and better spatial coverage than satellite retrievals of photosynthetically](#)  
396 [active radiation \(PAR\) or temperature.](#)

397

### 398 [3 Results and discussion](#)

#### 399 [3.1 Observed halogenated VOC patterns and relationships](#)

400 Zonal cross-sections of [halogenated](#) VOC data collected on ORCAS and ATom-2 illustrate  
401 unprecedented spatial sampling across our study area between the surface and 12 km (Fig. 2).  
402 Above average mixing ratios of CH<sub>3</sub>I, CHBr<sub>3</sub>, and CHClBr<sub>2</sub> typically remain confined to the  
403 lower ~2-4 km of the atmosphere (Fig. 2a, b, d). These compounds have lifetimes of  
404 approximately two months or less. Conversely, weak sources and longer lifetimes (≥ 3 months)  
405 may have contributed to similar concentrations of CH<sub>2</sub>Br<sub>2</sub> and CHBrCl<sub>2</sub> throughout the  
406 troposphere and above average mixing ratios as high as 8 km (Fig. 2c, e). Unfortunately, the  
407 availability of data above the detection limit and absence of BL enhancements for CHBrCl<sub>2</sub>  
408 preclude the identification of strong regional sources at this time. Meridional distributions also  
409 indicate lower latitude sources of CH<sub>3</sub>I and CH<sub>3</sub>Br ( $\leq 50^\circ$  S), potentially resulting from terrestrial  
410 and anthropogenic contributions, and higher latitude sources ( $> 60^\circ$  S) of CHBr<sub>3</sub>, CH<sub>2</sub>Br<sub>2</sub>, and  
411 CHClBr<sub>2</sub> (Fig. 2a-d,f).

412

##### 413 [3.1.1 Observed halogenated VOC interrelationships](#)

414 Across our study area in both 2016 and 2017, we found that CHBr<sub>3</sub> and CH<sub>2</sub>Br<sub>2</sub> exhibit a  
415 consistent enhancement ratio with each other in the bottom 2 km of the atmosphere both in  
416 Region 1 and Region 2, which suggests that these bromocarbon fluxes are closely coupled.  
417 Previous studies have documented co-located source regions of CHBr<sub>3</sub> and CH<sub>2</sub>Br<sub>2</sub> in the  
418 Southern Ocean (e.g. Hughes et al., 2009; [Carpenter et al., 2000](#); [Nightingale et al., 1995](#);  
419 [Laternus et al., 1996](#)), and laboratory studies [have demonstrated](#) that phytoplankton and their  
420 associated bacteria [cultures](#), including a [cold water](#) diatom isolated from coastal waters along the  
421 Antarctic Peninsula and common to the Southern Ocean, [produce](#) both CHBr<sub>3</sub> and CH<sub>2</sub>Br<sub>2</sub>  
422 (Hughes et al., 2013; Tokarczyk and Moore 1994, [Sturges et al., 1993](#)). [The non-linearity](#)  
423 [observed in ratios of these two gases at low CHBr<sub>3</sub> may reflect the different rates of their](#)  
424 [production or loss in seawater, or possibly, the influence of air masses from distant, more](#)  
425 [productive low-latitude source regions. Several studies have documented bacterially mediated](#)  
426 [loss of CH<sub>2</sub>Br<sub>2</sub>, but not CHBr<sub>3</sub>, and report distinct ratios of CH<sub>2</sub>Br<sub>2</sub> to CHBr<sub>3</sub> in seawater during](#)  
427 [the growth and senescent phases of a phytoplankton bloom \(e.g. Carpenter et al., 2009, Hughes](#)  
428 [et al., 2013\). Although this analysis is restricted to the bottom 2 km of the atmosphere, zonal](#)

Elizabeth Asher 9/3/2019 11:11 AM

Deleted: H

Elizabeth Asher 7/7/2019 11:15 AM

Deleted: ,

Elizabeth Asher 7/7/2019 11:16 AM

Deleted: and d

Elizabeth Asher 7/7/2019 11:16 AM

Deleted: (≥

Elizabeth Asher 7/7/2019 11:16 AM

Deleted: -

Elizabeth Asher 7/7/2019 11:16 AM

Deleted: ≤ -

Elizabeth Asher 9/3/2019 11:11 AM

Formatted: Font:Bold

Elizabeth Asher 7/7/2019 2:46 PM

Formatted: Font:Bold

Elizabeth Asher 7/8/2019 5:34 PM

Deleted: (Fig. 3a, c)

436 transport of air masses with lower ratios of  $\text{CH}_2\text{Br}_2$  to  $\text{CHBr}_3$  ratios, as have been observed in the  
437 MBL over productive, low-latitude regions, may also have influenced our observations  
438 (Yokouchi et al. 2005). Mixing ratios of  $\text{CHBr}_3$  and  $\text{CHClBr}_2$  were also correlated (Fig. 3d) in  
439 Region 2, and, a similar, weaker relationship was observed in Region 1 (Fig. 3b).  $\text{CHClBr}_2$  is a  
440 less well-studied compound than  $\text{CH}_2\text{Br}_2$ . Yet these consistent relationships suggest that  $\text{CHBr}_3$   
441 and  $\text{CHClBr}_2$  may either share some of the same sources or have sources that co-vary.

442

### 443 3.1.2 Observed halogenated VOC relationships to $\delta(\text{O}_2/\text{N}_2)$ and $\text{CO}_2$

444 We sought to test if the biologically mediated production of bromocarbons and oxygen result in  
445 similar atmospheric distributions. Conversely, we expected halogenated VOC atmospheric  
446 distributions and  $\text{CO}_2$  distributions to anticorrelate because  $\text{CO}_2$  fixation in surface waters is  
447 proportional to the production of oxygen.

448 For these comparisons, both  $\text{O}_2$  and  $\text{CO}_2$  mixing ratios from the upper troposphere (5-7 km) were  
449 subtracted from the data to detrend for seasonal and inter-annual variability (Fig. 4; Fig. S3). To  
450 isolate the contribution of ocean  $\text{O}_2$  fluxes, the ORCAS  $\delta(\text{O}_2/\text{N}_2)$  values reported here represent  
451 the  $\Delta\delta(\text{O}_2/\text{N}_2)$  to observed values between 5-7 km adjusted for CESM  $\text{O}_2$  land and fossil fuel  
452 contributions and the influence of air-sea  $\text{N}_2$  fluxes. In Fig. 4 we present type II major axis  
453 regression fits to data (fits were calculated using data scaled to their full range) between the  
454 ocean surface and the lowest 7 km for bromocarbons with photochemical lifetimes of  $\geq 1$  month  
455 and from the lowest 2 km for  $\text{CH}_3\text{I}$  with a photochemical lifetime of  $\sim 1$  week. We used a type II  
456 major axis regression model to balance the influences of uncorrelated processes and  
457 measurement uncertainty in halogenated VOCs (on the y-axis) and uncorrelated processes and  
458 measurement uncertainty in  $\text{O}_2$  and  $\text{CO}_2$  (on the x-axis) on the regression slope (Ayers et al.,  
459 2001; Glover et al., 2011). As noted by previous studies, simple least squares linear regressions  
460 fail to account for uncertainties in predictor variables (e.g. Cantrell et al., 2008).

461 The robust correlations of  $\text{CHBr}_3$  and  $\text{CH}_2\text{Br}_2$  with  $\delta(\text{O}_2/\text{N}_2)$ , in both 2016 and 2017 and in  
462 Region 1 and Region 2, provides support for a regional biogenic source of these two halogenated  
463 VOCs (Fig. 4a, b and Fig. 4d, e). The air-sea exchange of  $\text{O}_2$  during summer in the Southern  
464 Ocean is driven by net community production (the excess of photosynthesis over respiration) in  
465 the surface mixed layer, surface warming, and to a lesser extent ocean advection and mixing (e.g.  
466 Stephens et al., 1998; Tortell and Long 2009; Tortell et al., 2014). Note that we adjust for  
467 influences on the  $\delta(\text{O}_2/\text{N}_2)$  from thermal  $\text{N}_2$  fluxes (see Equation 1, Sect. 2.1.2 for details).  
468 Biological  $\text{O}_2$  supersaturation in the surface mixed layer develops quickly in the first several  
469 days of a phytoplankton bloom and diminishes as community respiration increases and air-sea  
470 gas exchange equilibrates the surface layer with the atmosphere on a timescale of  $\sim 1$  week.  
471  $\text{CHBr}_3$  and  $\text{CH}_2\text{Br}_2$  are emitted from phytoplankton during the exponential growth phase  
472 (Hughes et al., 2013), which often coincides with high net community production and the  
473 accumulation of  $\text{O}_2$  in surface waters. The bulk air-sea equilibration time for an excess of  $\text{CHBr}_3$   
474 and other halogenated VOCs is less than two weeks, although the photochemical loss of

Elizabeth Asher 7/5/2019 2:24 PM

Deleted: 2.5

Elizabeth Asher 7/7/2019 11:17 AM

Deleted:

Elizabeth Asher 9/3/2019 11:12 AM

Deleted: H

Elizabeth Asher 9/3/2019 11:12 AM

Formatted: Font:Bold

Elizabeth Asher 7/8/2019 5:43 PM

Deleted: (bivariate)

Elizabeth Asher 9/3/2019 11:12 AM

Deleted: H

Elizabeth Asher 7/7/2019 11:28 AM

Deleted: the

Elizabeth Asher 9/3/2019 11:12 AM

Deleted: H

Elizabeth Asher 7/7/2019 11:28 AM

Deleted: oxygen

Elizabeth Asher 7/7/2019 11:28 AM

Formatted: Subscript

Elizabeth Asher 7/7/2019 11:29 AM

Deleted: 3

Elizabeth Asher 7/7/2019 11:29 AM

Deleted: (

Elizabeth Asher 7/7/2019 11:29 AM

Deleted: ) is

Elizabeth Asher 9/3/2019 11:12 AM

Deleted: H

487 [halogenated VOCs](#) will alter their ratio over time (see Supplement for details on calculations of  
488 [bulk sea air equilibration times](#)).

489 Our observations suggest a biological source for  $\text{CHBr}_3$  and  $\text{CH}_2\text{Br}_2$  in [both Region 1 and Region](#)  
490 [2](#) (Fig. 4). [Interestingly, the slope of the regression between  \$\text{CHBr}\_3\$  and  \$\text{O}\_2\$  appears distinct in](#)  
491 [Region 1 and Region 2, but between  \$\text{CH}\_2\text{Br}\_2\$  is the same.](#) Molar enrichment ratios are  $0.20 \pm$   
492  $0.01$ , and  $0.07 \pm 0.004$  pmol : mol for  $\text{CHBr}_3$  and  $\text{CH}_2\text{Br}_2$  to  $\text{O}_2$  in Region 1, and  $0.32 \pm 0.02$ , and  
493  $0.07 \pm 0.004$  pmol : mol in Region 2. [We observe a weaker relationship between  \$\text{CH}\_3\text{I}\$  and](#)  
494  [\$\text{CHClBr}\_2\$  and  \$\text{O}\_2\$  in Region 1 \(Fig. 4c, d\), consistent with the existence of other, non-biological](#)  
495 [sources of  \$\text{CH}\_3\text{I}\$  in this region. Figure 4f illustrates a strong relationship between  \$\text{CH}\_3\text{I}\$  and  \$\text{O}\_2\$ ,](#)  
496 [as well as  \$\text{CHClBr}\_2\$  and  \$\text{O}\_2\$ , in Region 2, however, which implies that the dominant sources of](#)  
497  [\$\text{CH}\_3\text{I}\$  and  \$\text{CHClBr}\_2\$  emissions over the Patagonian Shelf are biological. The corresponding molar](#)  
498 [enrichment ratios of  \$\text{CH}\_3\text{I}\$  to  \$\text{O}\_2\$  and  \$\text{CHClBr}\_2\$  to  \$\text{O}\_2\$  in Region 2 are  \$0.38 \pm 0.03\$  pmol : mol and](#)  
499  [\$0.19 \pm 0.04\$  pmol: mol, respectively.](#)

Elizabeth Asher 7/7/2019 11:31 AM

Deleted: s

500 In contrast to  $\text{O}_2$ , air-sea fluxes of  $\text{CO}_2$  over the Southern Ocean during summer reflect the  
501 balance of opposing thermal and biological drivers (e.g. Stephens et al., 1998; 2018). Ocean  
502 buffering chemistry results in  $\text{CO}_2$  equilibration across the air-sea interface on a timescale of  
503 several months. ORCAS observations showed a depletion of  $\text{CO}_2$  in the MBL, indicating that  
504 uptake driven by net photosynthesis dominated over thermally driven outgassing during the  
505 several months preceding the campaign (Stephens et al., 2018).  $\text{CHBr}_3$  and  $\text{CH}_2\text{Br}_2$  in the  
506 lowest 7 km were negatively correlated with  $\text{CO}_2$  in both years in Region 1 and Region 2 (Fig.  
507 S3a, b, d, e). Interestingly,  $\text{CH}_3\text{I}$  was not correlated with  $\text{CO}_2$  in Region 1, likely due to the long  
508 air-sea equilibration timescale of  $\text{CO}_2$  compared with a 9-day air-sea equilibration time and a ~7-  
509 day photochemical lifetime for  $\text{CH}_3\text{I}$ . For longer lived species, correlations for [halogenated](#)  
510 [VOCs to  \$\text{CO}\_2\$  have similar  \$r^2\$ -values as those for \[halogenated\]\(#\) VOCs to  \$\delta\(\text{O}\_2/\text{N}\_2\)\$ , but model and](#)  
511 [climatological estimates of Southern Ocean  \$\text{CO}\_2\$  fluxes are much less certain than for  \$\text{O}\_2\$  \(Anav](#)  
512 [et al., 2015; Nevison et al., 2016\). As a result, we use modeled  \$\text{O}\_2\$  fluxes as the basis for our](#)  
513 [halogenated VOC flux estimates \(see Sect. 3.4.1 for details\).](#)

Elizabeth Asher 9/3/2019 11:12 AM

Deleted: H

Elizabeth Asher 9/3/2019 11:12 AM

Deleted: H

Elizabeth Asher 9/3/2019 11:12 AM

Deleted: H

514

### 515 **3.2 Model-observation comparisons**

516 The ORCAS dataset provides an exceptional opportunity to evaluate the CAM-Chem  
517 [halogenated](#) VOC emission scheme (Ordoñez et al., 2012) at high latitudes in the Southern  
518 Hemisphere. We compared modeled [halogenated](#) VOC constituents to corresponding  
519 observations along the ORCAS flight track (Fig. 5; Fig. 6). In these figures, we used type II  
520 major axis regression models to balance the measurement uncertainty (on the y-axis) and the  
521 inherent, yet difficult to quantify representativeness and errors in a global atmospheric chemistry  
522 model (on the x-axis). We note that this comparison may favor constituents with longer  
523 photochemical lifetimes, when transport and mixing dominate over source heterogeneity.

Elizabeth Asher 9/3/2019 11:15 AM

Deleted: H

Elizabeth Asher 9/3/2019 11:15 AM

Deleted: H

524 In Region 1 and Region 2, both the model and observations indicate that elevated mixing ratios  
525 of  $\text{CH}_3\text{I}$  remain confined to the MBL (Fig. 5a and Fig. 6a), presumably due to its relatively short



532 photochemical lifetime. Modeled and observed CH<sub>3</sub>I are poorly correlated in Region 1 ( $r^2 =$   
533 0.20; Fig. 5b) and better correlated in Region 2 ( $r^2 = 0.70$ ; Fig. 6b). In both regions, the model  
534 most likely under predicts CH<sub>3</sub>I in the upper troposphere and lower stratosphere (UTLS), likely  
535 stemming from the poleward transport of lower latitude air masses, where CAM-Chem also  
536 exhibits a negative bias. Mixing ratio comparisons with CAM-Chem over the tropics (see Figure  
537 10 in Ordoñez et al., 2012) depict similar or larger discrepancies, and have been attributed to  
538 stronger than anticipated convective cells in the tropics. We found strong correlations and  
539 agreement to within a factor of ~2 between modeled and observed CHBr<sub>3</sub> and CH<sub>2</sub>Br<sub>2</sub> (Fig. 5c-f  
540 and Fig. 6c-f). Relatively long lifetimes ( $\geq 1$  month) in Region 1 likely enable vertical and zonal  
541 transport of CHBr<sub>3</sub> and CH<sub>2</sub>Br<sub>2</sub> to the mid and upper troposphere (Fig. 5c and e). The model was  
542 biased low with respect to measurements of CH<sub>2</sub>Br by ~25% in Region 1 and Region 2 (Fig. 5g-  
543 h and Fig. 6g-h), potentially as a result of an incorrect surface lower boundary condition. The  
544 model underpredicted the mean vertical gradient in CHClBr<sub>2</sub>, although it did a reasonable job of  
545 representing the mean vertical gradient in CHBrCl<sub>2</sub>, in both Region 1 and Region 2. In both  
546 cases, however, the model failed to capture the spatial variability in both CHClBr<sub>2</sub> and CHBrCl<sub>2</sub>  
547 observations (Fig. 5i-l and Fig. 6i-l). Region 2 contains stronger sources of halogenated VOCs  
548 than Region 1, which has been documented in numerous ship-based campaigns and archived in  
549 the Halocarbons in the Ocean and Atmosphere database (HalOcAt; <https://halocat.geomar.de/>).  
550 Region 2 also has much higher chl *a* (Fig. S4), supporting biogenic sources for these gases.

551

### 552 **3.3 Relationships between STILT surface influence functions and observations**

553 We used the STILT model to explore the relationships between observed mixing ratios and the  
554 upstream surface influence functions (Equations 2-3) of sea ice, chl *a*, absorption due to detritus,  
555 and downward shortwave radiation at the surface, which relate to various regional hypothesized  
556 sources of halogenated VOCs such as marine phytoplankton, phytoplankton in sea ice brines,  
557 and decomposing organic matter in surface seawater (e.g. Moore and Zafiriou 1994; Moore et  
558 al., 1996; Tokarczyk and Moore 1994; Sturges et al., 1992).

559

560 We found no positive relationships between upstream sea-ice influence and any measured  
561 halogenated VOC Region 1 (Fig. 7). We interpret this result to mean that increased summertime  
562 sea ice acts either to reduce the production of halogenated VOCs by blocking sunlight or as a  
563 physical barrier to oceanic emissions of halogenated VOCs from under-ice algae. Both of these  
564 mechanisms are also consistent with a link between enhanced CHBr<sub>3</sub> and CH<sub>2</sub>Br<sub>2</sub> emissions due  
565 to sea-ice retreat and surface sea-ice melt water (Carpenter et al., 2007).

566 In other studies, it has also been proposed that sea ice could be an important source for CHBr<sub>3</sub>  
567 and other halogenated VOCs, since high mixing ratios of CHBr<sub>3</sub> have been observed at the sea-  
568 ice and ice-snow interface in the austral winter (Abrahamsson et al., 2018) and in under-ice algae  
569 in the austral spring (Sturges et al., 1993). At present, CAM-Chem v1.2 with very short-lived  
570 halogen chemistry does not include a regional flux of halogenated VOCs over sea-ice covered  
571 waters in summer, and our results do not indicate a need to include one. Our data, which were

Elizabeth Asher 7/7/2019 11:37 AM  
Deleted:

Elizabeth Asher 9/3/2019 11:15 AM  
Deleted: H

Elizabeth Asher 9/3/2019 11:15 AM  
Deleted: H

Elizabeth Asher 9/3/2019 11:15 AM  
Deleted: H

Elizabeth Asher 9/3/2019 11:15 AM  
Deleted: H

Elizabeth Asher 9/3/2019 11:15 AM  
Deleted: H

Elizabeth Asher 7/7/2019 11:44 AM  
Deleted: . High concentrations of CHBr<sub>3</sub>  
have been linked to sea ice retreat

Elizabeth Asher 9/3/2019 11:15 AM  
Deleted: H

Elizabeth Asher 9/3/2019 11:16 AM  
Deleted: H

582 collected in January and February, however, cannot assess the importance of sea ice as a source  
583 of [halogenated VOCs](#) in other seasons, such as winter or spring (Abrahamsson et al., 2018;  
584 Sturges et al., 1993). More field campaigns are needed to further study the seasonality and  
585 regional strength of sea ice related [halogenated VOC](#) emissions.

586 We observed a statistically significant positive correlation between the [surface influence function](#)  
587 of 8-day satellite composites of chl *a* concentration, which is widely used as a proxy for near-  
588 surface phytoplankton biomass, and mixing ratios of CHBr<sub>3</sub> and CH<sub>2</sub>Br<sub>2</sub> in Region 1 (Fig. 8a, b).  
589 This finding corroborates previous findings from ship-borne field campaigns and laboratory  
590 studies that have suggested a biogenic source for these two bromocarbons (e.g., Moore et al.,  
591 1996; Hughes et al., 2013), and further substantiates the current CAM-Chem parameterization of  
592 regional bromocarbon emissions using satellite retrievals of chl *a* in polar regions. CH<sub>3</sub>Br  
593 mixing ratios were not significantly correlated with chl *a* [surface influence functions](#) (Fig. 8c).  
594 Although potentially suggesting that marine phytoplankton and microalgae were not a strong  
595 regional source of CH<sub>3</sub>Br during ORCAS, it is also possible that the relatively long lifetime of  
596 CH<sub>3</sub>Br precludes a definitive analysis of its origin based on chl *a* using 7-day back-trajectories.  
597 Neither CHClBr<sub>2</sub> nor CHBrCl<sub>2</sub> were significantly correlated with chl *a* composite [surface](#)  
598 [influence functions](#) (data not shown); however, more observations of these short-lived species in  
599 the remote MBL are needed to substantiate this result.

600 Similar to Lai et al. (2011), we observed a significant correlation between mixing ratios of CH<sub>3</sub>I  
601 and total weekly upstream influence functions of 8-day chl *a* composites (Fig. 8d). Weaker  
602 correlations were observed with upstream influence functions on shorter timescales than seven  
603 days. We found that CH<sub>3</sub>I, particularly in Region 1, was better explained by a multi-linear  
604 regression with two predictors: 1) the influence function of downward shortwave radiation at the  
605 surface (Fig. 9a) and 2) the absorption of light due to detrital material (Fig. 9b), yielding  
606 improved agreement between predicted and observed CH<sub>3</sub>I (Fig. 9c). [Several previous studies](#)  
607 [have correlated mixing ratios of CH<sub>3</sub>I to satellite retrievals of PAR and surface ocean](#)  
608 [temperature, revealing a link to solar radiation \(e.g. Happell et al., 1996; Yokouchi et al., 2001\).](#)

609 Although certain species of phytoplankton are capable of producing CH<sub>3</sub>I (e.g. Manley and de la  
610 Cuesta 1997; Hughes et al., 2011), several studies also indicate a non-biological source for CH<sub>3</sub>I  
611 in the surface ocean. This non-biological source, though not fully understood, requires light, a  
612 humic like substance at the surface ocean [supplying a carbon source and methyl group](#), and  
613 [reactive iodine](#) (Moore and Zarifou 1994; Richter and Wallace 2004). [Thus far, two chemical](#)  
614 [mechanisms have been proposed for the non-biological production of methyl iodide, one – a](#)  
615 [radical recombination of a methyl group and iodine involving UV photolysis \(e.g. Moore and](#)  
616 [Zarifou 1994\), and two, a substitution reaction involving the reduction of an oxidant, such as iron](#)  
617 [III \(e.g. Williams et al. 2007\).](#)

### 619 [3.4 Flux estimation](#)

#### 620 [3.4.1 O<sub>2</sub>-based emission estimates](#)

Elizabeth Asher 9/3/2019 11:16 AM

Deleted: H

Elizabeth Asher 9/3/2019 11:16 AM

Deleted: H

Elizabeth Asher 7/8/2019 3:54 PM

Deleted: footprints

Elizabeth Asher 7/7/2019 11:44 AM

Deleted: the

Elizabeth Asher 7/7/2019 11:44 AM

Deleted: and Fig. 8

Elizabeth Asher 7/8/2019 3:54 PM

Deleted: footprints

Elizabeth Asher 7/7/2019 11:44 AM

Deleted:

Elizabeth Asher 7/8/2019 3:55 PM

Deleted: footprints

Elizabeth Asher 8/4/2019 4:08 PM

Deleted:

Elizabeth Asher 8/4/2019 4:08 PM

Deleted: Several previous studies have correlated mixing ratios of CH<sub>3</sub>I to satellite retrievals of PAR and temperature (e.g. Happell et al., 1996; Yokouchi et al., 2001). We note that chl *a*, which is a proxy for living algal biomass, was correlated with CDOM in Region 1 and Region 2, ( $r^2 = 0.24$ ; data not shown).

638 We present a novel approach that facilitates a basin-wide halogenated VOC flux estimate using  
639 the robust relationship between airborne observations of O<sub>2</sub> and halogenated VOCs combined  
640 with modeled O<sub>2</sub> fluxes. Unlike the existing CAM-Chem halogenated VOC biogenic flux  
641 parameterization, this method does not rely on weekly retrievals of chl *a* at high latitudes, which  
642 are often patchy. In addition, our study indicates that CHBr<sub>3</sub>, CH<sub>2</sub>Br<sub>2</sub>, and CHClBr<sub>2</sub> and CH<sub>3</sub>I are  
643 better correlated with marine derived O<sub>2</sub> than the upstream influence of chl *a*.

Elizabeth Asher 9/3/2019 11:16 AM  
Deleted: H

644 For CHBr<sub>3</sub>, CH<sub>2</sub>Br<sub>2</sub>, and CHClBr<sub>2</sub> we construct ocean emission inventories for January and  
645 February using a scaled version of gridded modeled air-sea O<sub>2</sub> fluxes and the slopes (i.e. molar  
646 ratios) of linear correlations between δ(O<sub>2</sub>/N<sub>2</sub>) and halogenated VOC mixing ratios (Fig. 10). O<sub>2</sub>  
647 fluxes were obtained from simulations using a configuration of the CESM model nudged to  
648 reanalysis temperatures and winds as described in Stephens et al. (2018). An earlier free running  
649 version of CESM was one of the best evaluated for reproducing the seasonal cycle of δ(O<sub>2</sub>/N<sub>2</sub>)  
650 over the Southern Ocean (Nevinson et al., 2015; 2016). To date, the north-south gradient in  
651 atmospheric O<sub>2</sub> has not been well reproduced by any models (Resplandy et al., 2016). Vertical  
652 gradients in O<sub>2</sub> on ORCAS indicate that CESM overestimated gradients by 47% on average;  
653 accordingly, O<sub>2</sub> fluxes were adjusted downward by 47% to better match the observations. This is  
654 obviously a very simple adjustment to the modeled fluxes, and the actual air-sea O<sub>2</sub> flux biases in  
655 CESM likely have a great deal of spatial and temporal heterogeneity. We calculated an  
656 uncertainty for the CESM flux using a second, independent estimate of O<sub>2</sub> fluxes based on  
657 dissolved O<sub>2</sub> measurements in surface seawater. The Garcia and Keeling (2001) climatology has  
658 much smoother temporal and spatial patterns than CESM flux estimates but also results in  
659 overestimated atmospheric O<sub>2</sub> spatial gradients. We calculate the relative uncertainty in O<sub>2</sub> flux  
660 as the ratio of the mean absolute difference between gridded Garcia and Keeling values (2001;  
661 also adjusted down by 51 % everywhere to better match ORCAS observations) to the CESM  
662 model flux estimates in Regions 1 and 2 (adjusted down by 47% everywhere). These  
663 disagreements were 7.3 % and 3.4 % for Regions 1 and 2, respectively. Based on the ratios of  
664 halogenated VOC to O<sub>2</sub> mixing ratios in bivariate least squares regressions and these adjusted O<sub>2</sub>  
665 fluxes, we estimate mean emissions of CHBr<sub>3</sub> and CH<sub>2</sub>Br<sub>2</sub> in Region 1 and Region 2. Relative  
666 uncertainty in the slopes (i.e., the standard deviation of the slopes) from these regressions and the  
667 mean relative uncertainties in regional O<sub>2</sub> fluxes were added in quadrature to yield uncertainties  
668 in calculated halogenated VOC emission rates.

Elizabeth Asher 7/8/2019 5:45 PM  
Deleted: to facilitate comparisons across regions and atmospheric models

Elizabeth Asher 7/7/2019 11:47 AM  
Deleted: O<sub>2</sub>/N<sub>2</sub>

669  
670 Figure 10 shows the mean emissions for Jan. and Feb. of CHBr<sub>3</sub>, CH<sub>2</sub>Br<sub>2</sub>, and CHClBr<sub>2</sub> in  
671 Region 1 and Region 2. Mean regional emissions of CHBr<sub>3</sub> and CH<sub>2</sub>Br<sub>2</sub> and CHClBr<sub>2</sub> are 91 ± 8,  
672 31 ± 17, and 11 ± 4 pmol m<sup>-2</sup> hr<sup>-1</sup> in Region 1 and 329 ± 23, 69 ± 5, and 24 ± 5 pmol m<sup>-2</sup> hr<sup>-1</sup> in  
673 Region 2 (Table 1). The mean flux of CH<sub>3</sub>I in Region 2 is 392 ± 32 (Table 1). Table 1 also lists  
674 the mean Jan. and Feb. CAM-Chem emissions from Region 1 and Region 2, as well as emissions  
675 from several other observational and modeling Antarctic polar studies. Our estimates fall within  
676 the range of these other studies, which span every month of the year and whose estimated fluxes  
677 range from negative (i.e. from the atmosphere into the ocean) to 3500 pmol m<sup>-2</sup> hr<sup>-1</sup> CHBr<sub>3</sub> in a  
678 coastal bay during its peak in primary production. CAM-Chem emissions for all species are

Elizabeth Asher 7/7/2019 11:49 AM  
Deleted: Region

Elizabeth Asher 9/3/2019 11:16 AM  
Deleted: H

Elizabeth Asher 7/7/2019 11:49 AM  
Deleted: (7.3% in Region 1 and 3.4 % in Region 2)

Elizabeth Asher 9/3/2019 11:16 AM  
Deleted: H

Elizabeth Asher 7/7/2019 11:50 AM  
Deleted: Antarctic polar

689 significantly lower than our observationally derived values in Region 1, with the exception of  
690 CH<sub>3</sub>I. Conversely, CAM-Chem emissions are significantly higher than our estimated emissions  
691 in Region 2, with the exception of CHClBr<sub>2</sub> in Region 1, which remains underpredicted by the  
692 model (Table 1). We note that in Region 2, CAM-Chem fluxes of CHBr<sub>3</sub> and CH<sub>2</sub>Br<sub>2</sub>, although  
693 still significantly different, are more similar to our estimated fluxes.

694

### 695 3.4.2 STILT-based emission estimates

696 Similar to our O<sub>2</sub>-based emission estimates, we used the relationship between surface influence  
697 functions and CH<sub>3</sub>I mixing ratios (Fig. 9) to predict a flux field in Region 1 (Fig. 11). We used a  
698 multiple linear regression ( $\pm 1$  standard deviations; Equation 2), where  $H_{s1}$  and  $H_{s2}$  are the  
699 downward shortwave radiation and detrital absorption surface influence functions, respectively,  
700 with an intercept  $b = 0.19 \pm 0.01$ , and influence coefficients  $a_1 = 3.7E-5 \pm 1.3E-5$ ,  $a_2 = 3.5 \pm 0.74$ ,  
701 and an interaction term with the coefficient  $a_3 = -5.2E-4 \pm 1.5E-4$  (Fig. 9c). These regression  
702 coefficients and interaction term were used to estimate an average non-biological flux of CH<sub>3</sub>I  
703 (Fig. 11; Table 1). This method could be used in place of the current Bell et al. (2002)  
704 climatology to update near weekly (~8 day) emissions of CH<sub>3</sub>I in future versions of CAM-Chem.  
705 Our estimated mean CH<sub>3</sub>I flux in Region 1 ( $35 \pm 29$  pmol m<sup>-2</sup> hr<sup>-1</sup>) is significantly lower than the  
706 current CAM-Chem estimated emissions (Table 1). As noted in Sect. 3.2, our observations of  
707 CH<sub>3</sub>I are also much lower than the modeled mixing ratios. As discussed above, the strong  
708 correlations between CH<sub>3</sub>I and O<sub>2</sub> in Region 2 also suggest a dominant biological source for this  
709 compound in this region. As a result, we have not used this relationship to parameterize a flux  
710 for CH<sub>3</sub>I in Region 2 (see Sect. 3.1.2 and 3.4.1 for details). We note that although it would be  
711 possible to provide STILT-based emission estimates for other halogenated VOCs (e.g. CHBr<sub>3</sub>  
712 and CH<sub>2</sub>Br<sub>2</sub>), the correlations these compounds were less strong with surface influence functions  
713 than those with O<sub>2</sub>/N<sub>2</sub>.

714

## 715 4 Conclusions

716 Our work combined TOGA and AWAS halogenated VOC airborne observations from the  
717 ORCAS and ATom-2 campaigns, with coincident measurements of O<sub>2</sub> and CO<sub>2</sub>, geophysical  
718 datasets and numerical models, including the global atmospheric chemistry model CAM-Chem,  
719 and the Lagrangian transport model, STILT. We evaluated model predictions, calculated molar  
720 enrichment ratios, inferred regional sources, and provided novel means of parameterizing ocean  
721 fluxes. We found that the Southern Ocean MBL is enriched in halogenated VOCs, but that these  
722 MBL enhancements are less pronounced at higher latitudes, i.e., poleward of 60° S (Region 1)  
723 than over the productive Patagonian shelf (Region 2). Overall, our results indicated that the  
724 Southern Ocean is a moderate regional sources of CHBr<sub>3</sub>, CH<sub>2</sub>Br<sub>2</sub>, and CH<sub>3</sub>I, and a weak source  
725 of CHClBr<sub>2</sub> and CHBrCl<sub>2</sub> in January and February. Good model-measurement correlations were  
726 obtained between our observations and simulations from the Community Earth System Model  
727 (CESM) atmospheric component with chemistry (CAM-Chem) for CHBr<sub>3</sub>, CH<sub>2</sub>Br<sub>2</sub>, CH<sub>3</sub>I, and  
728 CHClBr<sub>2</sub> but all showed significant differences in model:measurement ratios. The

Elizabeth Asher 7/7/2019 11:50 AM

Deleted: biological

Elizabeth Asher 7/8/2019 5:46 PM

Deleted:

Elizabeth Asher 7/7/2019 11:53 AM

Deleted: The shortwave radiation and detrital material influence function

Elizabeth Asher 7/7/2019 11:52 AM

Formatted: Subscript

Elizabeth Asher 7/7/2019 11:53 AM

Deleted: an

Elizabeth Asher 7/7/2019 11:53 AM

Deleted: from a multi-linear regression (Fig. 9)

Elizabeth Asher 7/7/2019 11:53 AM

Deleted: regional

Elizabeth Asher 7/7/2019 11:54 AM

Deleted: .

Elizabeth Asher 7/7/2019 11:55 AM

Formatted: Subscript

Elizabeth Asher 7/7/2019 11:55 AM

Formatted: Subscript

Elizabeth Asher 7/7/2019 11:55 AM

Formatted: Subscript

Elizabeth Asher 7/7/2019 11:55 AM

Formatted: Subscript

Elizabeth Asher 7/7/2019 11:55 AM

Deleted: 6

Elizabeth Asher 9/3/2019 11:16 AM

Deleted: H

Elizabeth Asher 7/7/2019 11:56 AM

Deleted: climate model

Elizabeth Asher 9/3/2019 11:16 AM

Deleted: H

Elizabeth Asher 7/8/2019 5:49 PM

Deleted: and

Elizabeth Asher 7/8/2019 5:49 PM

Deleted:

Elizabeth Asher 7/8/2019 5:49 PM

Deleted: in Region 1 (at higher latitudes) than in Region 2 over the productive Patagonian shelf

Elizabeth Asher 7/8/2019 5:50 PM

Deleted: poleward of 60° S (Region 1) and Patagonian Shelf (Region 2) are

Elizabeth Asher 7/8/2019 5:50 PM

Deleted: s

Elizabeth Asher 7/8/2019 5:53 PM

Deleted:

751 [model:measurement comparison for CH<sub>3</sub>Br](#) was satisfactory and for CHBrCl<sub>2</sub>, the low levels  
752 [present](#) precluded us from making a complete assessment.

753 [CHBr<sub>3</sub> and CH<sub>2</sub>Br<sub>2</sub>](#), exhibited strong and robust correlations with each other and with O<sub>2</sub> and  
754 [weaker but statistically significant correlations with the influence of chl \*a\*, which is a proxy for](#)  
755 [phytoplankton biomass. CHClBr<sub>2</sub> and CHBr<sub>3</sub> were well correlated with one another, particularly](#)  
756 [in Region 2. Together, these correlations suggested a biological source for these gases over the](#)  
757 [Southern Ocean. We found that CH<sub>3</sub>I mixing ratios in Region 1 were best correlated with a non-](#)  
758 [biological surface influence function, although biogenic CH<sub>3</sub>I emissions appear important in](#)  
759 [Region 2.](#)

760  
761 Our flux estimates based on the relationship of [halogenated](#) VOC mixing ratios to O<sub>2</sub> and  
762 remotely sensed parameters (for CH<sub>3</sub>I) were compared with those derived from global models  
763 and ship-based studies (Table 1). [Our emission estimates of CHBr<sub>3</sub>, CH<sub>2</sub>Br<sub>2</sub>, and CHClBr<sub>2</sub>](#) are  
764 significantly higher than CAM-Chem's [globally](#) prescribed emissions in Region 1, where  
765 [halogenated](#) VOC mixing ratios are under predicted (Table 1; Fig. 5). [Similarly, our estimate of](#)  
766 [CHClBr<sub>2</sub> emissions is also significantly higher than CAM-Chem's in Region 2, where CHClBr<sub>2</sub>](#)  
767 [mixing ratios remained underpredicted. Yet, to the best of our knowledge, CAM-Chem's global](#)  
768 [parameterization of halogenated VOC fluxes has not been compared with data at high latitudes.](#)  
769 [Indeed, our emission estimates of CHBr<sub>3</sub>, CH<sub>2</sub>Br<sub>2</sub>, CH<sub>3</sub>I fall within a range of CAM-Chem's](#)  
770 [esimates \(on the low end\) and most prior estimates based on either other models or localized](#)  
771 [studies using seawater-side measurements from the Antarctic polar region in summer \(on the](#)  
772 [high end\). In the case of CH<sub>3</sub>I, our estimated emissions suggest that the prescribed emissions in](#)  
773 [CAM-Chem may be too high in Region 1 and Region 2. Our parameterizations of the CH<sub>3</sub>I flux](#)  
774 [could be used to explore inter-annual variability in emissions, which is not captured by the Bell](#)  
775 [et al. \(2002\) CH<sub>3</sub>I climatology currently employed in CAM-Chem.](#)

776 To extend these relationships to year-round and global parameterizations for use in global  
777 climate models, they must be studied using airborne observations in other seasons and regions.  
778 [These approaches may help parameterize](#) emissions of new species [that can be correlated with](#)  
779 [surface influence functions or the biological production of oxygen or may improve existing](#)  
780 [emissions, where persistent biases exist. Finally, future airborne observations of halogenated](#)  
781 [VOCs have the potential to further improve our understanding of air-sea flux rates and their](#)  
782 [drivers for these chemically and climatically important gases over the Southern Ocean.](#)

783 *Data Availability.* The ORCAS and ATom-2 datasets are publically available at  
784 <https://doi.org/10.5065/D6SB445X> ; ([www.eol.ucar.edu/field\\_projects/orcas](http://www.eol.ucar.edu/field_projects/orcas)) and  
785 <https://doi.org/10.3334/ORNLDAAC/1581>.

786 *Author Contributions.* EA is responsible for the bulk of the conceptualization, formal analysis,  
787 writing, review, and editing with contributions from all authors. BBS and ECA were  
788 instrumental in the investigation and supervision related to this manuscript. RSH contributed to  
789 the conceptualization, as well as the investigation and [halogenated](#) VOC data curation for this  
790 project. BBS, EJM, and RFK were responsible for the data curation of  $\delta(O_2/N_2)$  data and  
791 contributed to formal analysis involving these data. MSHM along with EAK were responsible  
792 for STILT data curation and formal analysis, and the conceptualization and formal analysis of

- Elizabeth Asher 7/8/2019 5:53 PM  
**Deleted:** CAM-Chem provided a good foundation for HVOC, particularly for CHBr<sub>3</sub> and CH<sub>2</sub>Br<sub>2</sub> in Region 1 and Region 2. Conversely, CHClBr<sub>2</sub> and CHBrCl<sub>2</sub> were underestimated by a factor of two or three in the model, while CH<sub>3</sub>I were overestimated by a factor of more than three, and airborne observations indicated that the CAM-Chem CH<sub>3</sub>Br surface boundary condition may be too low by ~25%. ... 11
- Elizabeth Asher 9/3/2019 11:16 AM  
**Deleted:** H
- Elizabeth Asher 7/8/2019 5:53 PM  
**Deleted:** other airborne observations
- Elizabeth Asher 7/8/2019 5:53 PM  
**Formatted:** Subscript
- Elizabeth Asher 7/8/2019 5:54 PM  
**Deleted:** relatively well
- Elizabeth Asher 7/7/2019 12:02 PM  
**Deleted:** emission estimates of CHBr<sub>3</sub>, CH<sub>2</sub>Br<sub>2</sub>, CH<sub>3</sub>I, lower than most prior estimates from the Antarctic polar region in summer
- Elizabeth Asher 9/3/2019 11:16 AM  
**Deleted:** H
- Elizabeth Asher 7/7/2019 12:10 PM  
**Deleted:** Nevertheless,
- Elizabeth Asher 7/7/2019 12:10 PM  
**Deleted:** t
- Elizabeth Asher 7/7/2019 12:29 PM  
**Deleted:**
- Elizabeth Asher 7/7/2019 12:30 PM  
**Deleted:**
- Elizabeth Asher 9/3/2019 11:17 AM  
**Deleted:** H
- Elizabeth Asher 7/7/2019 12:30 PM  
**Deleted:** (
- Elizabeth Asher 7/7/2019 12:31 PM  
**Deleted:** )
- Elizabeth Asher 7/7/2019 12:31 PM  
**Deleted:** (
- Elizabeth Asher 7/7/2019 12:31 PM  
**Deleted:** )
- Elizabeth Asher 9/3/2019 11:17 AM  
**Deleted:** H
- Elizabeth Asher 7/7/2019 12:33 PM  
**Deleted:** O<sub>2</sub>/N<sub>2</sub>

822 SITLT-based geostatistical influence functions and flux estimates were also informed by these  
823 two. DK, along with ST, JFL and ASL were responsible for constructing CAM [halogenated](#)  
824 [VOC](#) emissions and conducting CAM runs. MCL was responsible [for](#) CESM simulations  
825 yielding O<sub>2</sub> fluxes and comparing this product alongside the Garcia and Keeling O<sub>2</sub> climatology  
826 in CAM. KMC and CM were responsible for the data curation of CO<sub>2</sub> observations. AJH  
827 contributed to the investigation for [halogenated](#) [VOC](#) data.

828

829 *Acknowledgements.* We would like to thank the ORCAS and ATom-2 science teams and the  
830 NCAR Research Aviation Facility and NASA DC-8 pilots, technicians and mechanics for their  
831 support during the field campaigns. In addition, we appreciate the NCAR EOL staff who have  
832 facilitated computing and data archival. In particular, we thank Tim Newberger for his help in  
833 supporting the NOAA Picarro CO<sub>2</sub> observations and Andrew Watt for his help in supporting the  
834 AO<sub>2</sub> O<sub>2</sub> observations. This work was made possible by grants from NSF Polar Programs  
835 (1501993, 1501997, 1501292, 1502301, 1543457), NSF Atmospheric Chemistry Grants  
836 1535364, 1623745, and 1623748 and NASA funding of the EVS2 Atmospheric Tomography  
837 (ATom) project, as well as the support of the NCAR Advanced Study Program (ASP)  
838 Postdoctoral Fellowship Program and computing support from Yellowstone, provided by  
839 NCAR's Computational and Information Systems Laboratory. The National Center for  
840 Atmospheric Research is sponsored by the National Science Foundation.

841

Elizabeth Asher 9/3/2019 11:17 AM

Deleted: H

Elizabeth Asher 9/3/2019 11:17 AM

Deleted: H

844 **References**

- 845 Abrahamsson, K., Lorén, A., Wulff, A. and Wängberg, S.-Å.: Air–sea exchange of halocarbons: the influence of  
846 diurnal and regional variations and distribution of pigments, *Deep Sea Research Part II: Topical Studies in*  
847 *Oceanography*, 51(22–24), 2789–2805, doi:10.1016/j.dsr2.2004.09.005, 2004a.
- 848 Abrahamsson, K., Bertilsson, S., Chierici, M., Fransson, A., Froneman, P. W., Lorén, A. and Pakhomov, E. A.:  
849 Variations of biochemical parameters along a transect in the Southern Ocean, with special emphasis on volatile  
850 halogenated organic compounds, *Deep Sea Research Part II: Topical Studies in Oceanography*, 51(22–24), 2745–  
851 2756, doi:10.1016/j.dsr2.2004.09.004, 2004b.
- 852 Abrahamsson, K., Granfors, A., Ahnoff, M., Cuevas, C. A. and Saiz-Lopez, A.: Organic bromine compounds  
853 produced in sea ice in Antarctic winter, *Nature Communications*, 9(1), doi:10.1038/s41467-018-07062-8, 2018.
- 854 Anav, A., Friedlingstein, P., Beer, C., Ciais, P., Harper, A., Jones, C., Murray-Tortarolo, G., Papale, D., Parazoo, N.  
855 C., Peylin, P., Piao, S., Sitch, S., Viovy, N., Wiltshire, A. and Zhao, M.: Spatiotemporal patterns of terrestrial gross  
856 primary production: A review: GPP Spatiotemporal Patterns, *Reviews of Geophysics*, 53(3), 785–818,  
857 doi:10.1002/2015RG000483, 2015.
- 858 Apel, E.: ORCAS Trace Organic Gas Analyzer (TOGA) VOC Data. Version 1.0, [online] Available from:  
859 <https://data.eol.ucar.edu/dataset/490.018> (Accessed 29 January 2019), 2017.
- 860 Apel, E. C., Hornbrook, R. S., Hills, A. J., Blake, N. J., Barth, M. C., Weinheimer, A., Cantrell, C., Rutledge, S. A.,  
861 Basarab, B., Crawford, J., Diskin, G., Homeyer, C. R., Campos, T., Flocke, F., Fried, A., Blake, D. R., Brune, W.,  
862 Pollack, I., Peischl, J., Ryerson, T., Wennberg, P. O., Crouse, J. D., Wisthaler, A., Mikoviny, T., Huey, G., Heikes,  
863 B., O’Sullivan, D. and Riemer, D. D.: Upper tropospheric ozone production from lightning NO<sub>x</sub>-impacted  
864 convection: Smoke ingestion case study from the DC3 campaign, *Journal of Geophysical Research: Atmospheres*,  
865 120(6), 2505–2523, doi:10.1002/2014JD022121, 2015.
- 866 Atkinson, H. M., Huang, R.-J., Chance, R., Roscoe, H. K., Hughes, C., Davison, B., Schönhardt, A., Mahajan, A. S.,  
867 Saiz-Lopez, A., Hoffmann, T. and Liss, P. S.: Iodine emissions from the sea ice of the Weddell Sea, *Atmospheric*  
868 *Chemistry and Physics*, 12(22), 11229–11244, doi:10.5194/acp-12-11229-2012, 2012.
- 869 Atlas, E.: ORCAS Advanced Whole Air Sampler (AWAS) Data. Version 1.0, [online] Available from:  
870 <https://data.eol.ucar.edu/dataset/490.027> (Accessed 29 January 2019), 2017.
- 871 Ayers, G. P.: Comment on regression analysis of air quality data, *Atmospheric Environment*, 35(13), 2423–2425,  
872 doi:10.1016/S1352-2310(00)00527-6, 2001.
- 873 Bates, T. S.: Preface [to special section on First Aerosol Characterization Experiment (AGE 1)], *Journal of*  
874 *Geophysical Research: Atmospheres*, 104(D17), 21645–21647, doi:10.1029/1999JD900365, 1999.
- 875 Bell, N., Hsu, L., Jacob, D. J., Schultz, M. G., Blake, D. R., Butler, J. H., King, D. B., Lobert, J. M. and Maier-  
876 Reimer, E.: Methyl iodide: Atmospheric budget and use as a tracer of marine convection in global models:  
877 GLOBAL ATMOSPHERIC METHYL IODIDE, *Journal of Geophysical Research: Atmospheres*, 107(D17), ACH  
878 8–1–ACH 8–12, doi:10.1029/2001JD001151, 2002.
- 879 Blake, N. J., Blake, D. R., Wingenter, O. W., Sive, B. C., Kang, C. H., Thornton, D. C., Bandy, A. R., Atlas, E.,  
880 Flocke, F., Harris, J. M. and Rowland, F. S.: Aircraft measurements of the latitudinal, vertical, and seasonal  
881 variations of NMHCs, methyl nitrate, methyl halides, and DMS during the First Aerosol Characterization  
882 Experiment (ACE 1), *Journal of Geophysical Research: Atmospheres*, 104(D17), 21803–21817,  
883 doi:10.1029/1999JD900238, 1999.
- 884 Blei, E. and Heal, M. R.: Methyl bromide and methyl chloride fluxes from temperate forest litter, *Atmospheric*  
885 *Environment*, 45(8), 1543–1547, doi:10.1016/j.atmosenv.2010.12.044, 2011.
- 886 [Bloss, W. J., J. D. Lee, G. P. Johnson, R. Sommariva, D. E. Heard, A. Saiz-Lopez, J. M. C. Plane, G. McFiggans,](#)  
887 [M. Flynn, P. Williams, A. R. Rickard and Z. L. Fleming: Impact of halogen monoxide chemistry upon boundary](#)  
888 [layer OH and HO<sub>2</sub> concentrations at a coastal site, \*Geophysical Research Letters\*, 32\(6\),](#)  
889 [doi:10.1029/2004GL022084, 2005.](https://doi.org/10.1029/2004GL022084)

890

- 891 Boden, T., Andres, R. and Marland, G.: Global, Regional, and National Fossil-Fuel CO<sub>2</sub> Emissions (1751 - 2014)  
892 (V. 2017), [online] Available from: <https://www.osti.gov/servlets/purl/1389331/> (Accessed 25 November 2018),  
893 2017.
- 894 Boucher, O., Moulin, C., Belviso, S., Aumont, O., Bopp, L., Cosme, E., von Kuhlmann, R., Lawrence, M. G., Pham,  
895 M., Reddy, M. S., Sciare, J. and Venkataraman, C.: DMS atmospheric concentrations and sulphate aerosol indirect  
896 radiative forcing: a sensitivity study to the DMS source representation and oxidation, *Atmospheric Chemistry and  
897 Physics*, 3(1), 49–65, doi:10.5194/acp-3-49-2003, 2003.
- 898 Butler, J. H., King, D. B., Lobert, J. M., Montzka, S. A., Yvon-Lewis, S. A., Hall, B. D., Warwick, N. J., Mondeel,  
899 D. J., Aydin, M. and Elkins, J. W.: Oceanic distributions and emissions of short-lived halocarbons: OCEANIC  
900 EMISSIONS OF SHORT-LIVED HALOCARBONS, *Global Biogeochemical Cycles*, 21(1),  
901 doi:10.1029/2006GB002732, 2007.
- 902 Cantrell, C. A.: Technical Note: Review of methods for linear least-squares fitting of data and application to  
903 atmospheric chemistry problems, *Atmospheric Chemistry and Physics*, 8(17), 5477–5487, doi:10.5194/acp-8-5477-  
904 2008, 2008.
- 905 Carpenter, L. J., Liss, P. S. and Penkett, S. A.: Marine organohalogens in the atmosphere over the Atlantic and  
906 Southern Oceans: MARINE ORGANOHALOGENS IN THE ATMOSPHERE, *Journal of Geophysical Research:*  
907 *Atmospheres*, 108(D9), n/a–n/a, doi:10.1029/2002JD002769, 2003.
- 908 Carpenter, L. J., Wevill, D. J., Palmer, C. J. and Michels, J.: Depth profiles of volatile iodine and bromine-  
909 containing halocarbons in coastal Antarctic waters, *Marine Chemistry*, 103(3-4), 227–236,  
910 doi:10.1016/j.marchem.2006.08.003, 2007.
- 911 Carpenter, L. J., Jones, C. E., Dunk, R. M., Hornsby, K. E. and Woeltjen, J.: Air-sea fluxes of biogenic bromine  
912 from the tropical and North Atlantic Ocean, *Atmospheric Chemistry and Physics*, 9(5), 1805–1816,  
913 doi:10.5194/acp-9-1805-2009, 2009.
- 914 Chuck, A. L.: Oceanic distributions and air-sea fluxes of biogenic halocarbons in the open ocean, *Journal of  
915 Geophysical Research*, 110(C10), doi:10.1029/2004JC002741, 2005.
- 916 Colomb, A., Yassaa, N., Williams, J., Peeken, I. and Lochte, K.: Screening volatile organic compounds (VOCs)  
917 emissions from five marine phytoplankton species by head space gas chromatography/mass spectrometry (HS-  
918 GC/MS), *Journal of Environmental Monitoring*, 10(3), 325, doi:10.1039/b715312k, 2008.
- 919 Drewer, J., Heal, K. V., Smith, K. A. and Heal, M. R.: Methyl bromide emissions to the atmosphere from temperate  
920 woodland ecosystems, *Global Change Biology*, doi:10.1111/j.1365-2486.2008.01676.x, 2008.
- 921 Emmons, L. K., Walters, S., Hess, P. G., Lamarque, J.-F., Pfister, G. G., Fillmore, D., Granier, C., Guenther, A.,  
922 Kinnison, D., Laepple, T., Orlando, J., Tie, X., Tyndall, G., Wiedinmyer, C., Baughcum, S. L. and Kloster, S.:  
923 Description and evaluation of the Model for Ozone and Related chemical Tracers, version 4 (MOZART-4),  
924 *Geoscientific Model Development*, 3(1), 43–67, doi:10.5194/gmd-3-43-2010, 2010.
- 925 Fernandez, R. P., Salawitch, R. J., Kinnison, D. E., Lamarque, J.-F. and Saiz-Lopez, A.: Bromine partitioning in the  
926 tropical tropopause layer: implications for stratospheric injection, *Atmospheric Chemistry and Physics*, 14(24),  
927 13391–13410, doi:10.5194/acp-14-13391-2014, 2014.
- 928 Finlayson-Pitts, B. J.: The Tropospheric Chemistry of Sea Salt: A Molecular-Level View of the Chemistry of NaCl  
929 and NaBr, *Chemical Reviews*, 103(12), 4801–4822, doi:10.1021/cr020653t, 2003.
- 930 Garcia, H. E. and Keeling, R. F.: On the global oxygen anomaly and air-sea flux, *Journal of Geophysical Research:*  
931 *Oceans*, 106(C12), 31155–31166, doi:10.1029/1999JC000200, 2001.
- 932 Gent, P. R., Danabasoglu, G., Donner, L. J., Holland, M. M., Hunke, E. C., Jayne, S. R., Lawrence, D. M., Neale, R.  
933 B., Rasch, P. J., Vertenstein, M., Worley, P. H., Yang, Z.-L. and Zhang, M.: The Community Climate System Model  
934 Version 4, *Journal of Climate*, 24(19), 4973–4991, doi:10.1175/2011JCLI4083.1, 2011.

Elizabeth Asher 8/4/2019 2:02 PM

**Deleted:** Bloss, W. J.: Impact of halogen monoxide chemistry upon boundary layer OH and HO<sub>2</sub> concentrations at a coastal site, *Geophysical Research Letters*, 32(6), doi:10.1029/2004GL022084, 2005.



940 von Glasow, R. and Crutzen, P. J.: Model study of multiphase DMS oxidation with a focus on halogens,  
941 Atmospheric Chemistry and Physics, 4(3), 589–608, doi:10.5194/acp-4-589-2004, 2004.

942 von Glasow, R., von Kuhlmann, R., Lawrence, M. G., Platt, U. and Crutzen, P. J.: Impact of reactive bromine  
943 chemistry in the troposphere, Atmospheric Chemistry and Physics, 4(11/12), 2481–2497, doi:10.5194/acp-4-2481-  
944 2004, 2004.

945 Glover, D. M., Jenkins, W. J. and Doney, S. C.: Modeling Methods for Marine Science, Cambridge University  
946 Press., 2011.

947 Guenther, A. B., Jiang, X., Heald, C. L., Sakulyanontvittaya, T., Duhl, T., Emmons, L. K. and Wang, X.: The Model  
948 of Emissions of Gases and Aerosols from Nature version 2.1 (MEGAN2.1): an extended and updated framework for  
949 modeling biogenic emissions, Geoscientific Model Development, 5(6), 1471–1492, doi:10.5194/gmd-5-1471-2012,  
950 2012.

951 Happell, J. D., Wallace, D. W. R., Wills, K. D., Wilke, R. J. and Neill, C. C.: A purge-and-trap capillary column gas  
952 chromatographic method for the measurement of halocarbons in water and air. [online] Available from:  
953 <http://www.osti.gov/servlets/purl/366493-84sOfy/webviewable/> (Accessed 26 July 2018), 1996.

954 Hossaini, R., Mantle, H., Chipperfield, M. P., Montzka, S. A., Hamer, P., Ziska, F., Quack, B., Krüger, K.,  
955 Tegtmeier, S., Atlas, E., Sala, S., Engel, A., Bönisch, H., Keber, T., Oram, D., Mills, G., Ordóñez, C., Saiz-Lopez,  
956 A., Warwick, N., Liang, Q., Feng, W., Moore, F., Miller, B. R., Marécal, V., Richards, N. A. D., Dorf, M. and  
957 Pfeilsticker, K.: Evaluating global emission inventories of biogenic bromocarbons, Atmospheric Chemistry and  
958 Physics, 13(23), 11819–11838, doi:10.5194/acp-13-11819-2013, 2013.

959 Hughes, C., Chuck, A. L., Rossetti, H., Mann, P. J., Turner, S. M., Clarke, A., Chance, R. and Liss, P. S.: Seasonal  
960 cycle of seawater bromoform and dibromomethane concentrations in a coastal bay on the western Antarctic  
961 Peninsula: BROMOCARBON SEASONALITY ANTARCTICA, Global Biogeochemical Cycles, 23(2), n/a–n/a,  
962 doi:10.1029/2008GB003268, 2009.

963 Hughes, C., Johnson, M., Utting, R., Turner, S., Malin, G., Clarke, A. and Liss, P. S.: Microbial control of  
964 bromocarbon concentrations in coastal waters of the western Antarctic Peninsula, Marine Chemistry, 151, 35–46,  
965 doi:10.1016/j.marchem.2013.01.007, 2013.

966 Hurrell, J. W., Hack, J. J., Shea, D., Caron, J. M. and Rosinski, J.: A New Sea Surface Temperature and Sea Ice  
967 Boundary Dataset for the Community Atmosphere Model, Journal of Climate, 21(19), 5145–5153,  
968 doi:10.1175/2008JCLI2292.1, 2008.

969 Keeling, R. F., Manning, A. C., McEvoy, E. M. and Shertz, S. R.: Methods for measuring changes in atmospheric O  
970 <sub>2</sub> concentration and their application in southern hemisphere air, Journal of Geophysical Research: Atmospheres,  
971 103(D3), 3381–3397, doi:10.1029/97JD02537, 1998.

972 Lai, S. C., Williams, J., Arnold, S. R., Atlas, E. L., Gebhardt, S. and Hoffmann, T.: Iodine containing species in the  
973 remote marine boundary layer: A link to oceanic phytoplankton: IODINE SPECIES AND PHYTOPLANKTON,  
974 Geophysical Research Letters, 38(20), n/a–n/a, doi:10.1029/2011GL049035, 2011.

975 Lamarque, J.-F.: Response of a coupled chemistry-climate model to changes in aerosol emissions: Global impact on  
976 the hydrological cycle and the tropospheric burdens of OH, ozone, and NO<sub>x</sub>, Geophysical Research Letters, 32(16),  
977 doi:10.1029/2005GL023419, 2005.

978 Lamarque, J.-F., Emmons, L. K., Hess, P. G., Kinnison, D. E., Tilmes, S., Vitt, F., Heald, C. L., Holland, E. A.,  
979 Lauritzen, P. H., Neu, J., Orlando, J. J., Rasch, P. J. and Tyndall, G. K.: CAM-chem: description and evaluation of  
980 interactive atmospheric chemistry in the Community Earth System Model, Geoscientific Model Development, 5(2),  
981 369–411, doi:10.5194/gmd-5-369-2012, 2012.

982 Laturnus, F.: Volatile halocarbons released from Arctic macroalgae, Marine Chemistry, 55(3-4), 359–366,  
983 doi:10.1016/S0304-4203(97)89401-7, 1996.

984 Liang, Q., Atlas, E., Blake, D., Dorf, M., Pfeilsticker, K. and Schauffler, S.: Convective transport of very short lived  
985 bromocarbons to the stratosphere, *Atmospheric Chemistry and Physics*, 14(11), 5781–5792, doi:10.5194/acp-14-  
986 5781-2014, 2014.

987 Lin, J. C.: A near-field tool for simulating the upstream influence of atmospheric observations: The Stochastic Time-  
988 Inverted Lagrangian Transport (STILT) model, *Journal of Geophysical Research*, 108(D16), ACH 2–1–ACH 2–17,  
989 doi:10.1029/2002JD003161, 2003.

990 Liu, X., Easter, R. C., Ghan, S. J., Zaveri, R., Rasch, P., Shi, X., Lamarque, J.-F., Gettelman, A., Morrison, H., Vitt,  
991 F., Conley, A., Park, S., Neale, R., Hannay, C., Ekman, A. M. L., Hess, P., Mahowald, N., Collins, W., Iacono, M.  
992 J., Bretherton, C. S., Flanner, M. G. and Mitchell, D.: Toward a minimal representation of aerosols in climate  
993 models: description and evaluation in the Community Atmosphere Model CAM5, *Geoscientific Model  
994 Development*, 5(3), 709–739, doi:10.5194/gmd-5-709-2012, 2012.

995 Manley, S. L. and Dastoor, M. N.: Methyl iodide (CH<sub>3</sub>I) production by kelp and associated microbes, *Marine  
996 Biology*, 98(4), 477–482, doi:10.1007/BF00391538, 1988.

997 Maslanik, J.: Near-Real-Time DMSP SSM/I-SSMIS Daily Polar Gridded Sea Ice Concentrations, Version 1, 1999.

998 Mattson, E., Karlsson, A., Smith, W. O. and Abrahamsson, K.: The relationship between biophysical variables and  
999 halocarbon distributions in the waters of the Amundsen and Ross Seas, Antarctica, *Marine Chemistry*, 140-141, 1–9,  
1000 doi:10.1016/j.marchem.2012.07.002, 2012.

1001 Mattsson, E., Karlsson, A. and Abrahamsson, K.: Regional sinks of bromoform in the Southern Ocean: REGIONAL  
1002 SINKS OF CHBR<sub>3</sub> IN THE ANTARCTIC, *Geophysical Research Letters*, 40(15), 3991–3996,  
1003 doi:10.1002/grl.50783, 2013.

1004 Moore, R. M. and Groszko, W.: Methyl iodide distribution in the ocean and fluxes to the atmosphere, *Journal of  
1005 Geophysical Research: Oceans*, 104(C5), 11163–11171, doi:10.1029/1998JC900073, 1999.

1006 Moore, R. M. and Zafiriou, O. C.: Photochemical production of methyl iodide in seawater, *Journal of Geophysical  
1007 Research*, 99(D8), 16415, doi:10.1029/94JD00786, 1994.

1008 Moore, R. M., Webb, M., Tokarczyk, R. and Wever, R.: Bromoperoxidase and iodoperoxidase enzymes and  
1009 production of halogenated methanes in marine diatom cultures, *Journal of Geophysical Research: Oceans*, 101(C9),  
1010 20899–20908, doi:10.1029/96JC01248, 1996.

1011 Murphy, D. M., Froyd, K. D., Bian, H., Brock, C. A., Dibb, J. E., DiGangi, J. P., Diskin, G., Dollner, M., Kupc, A.,  
1012 Scheuer, E. M., Schill, G. P., Weinzierl, B., Williamson, C. J. and Yu, P.: The distribution of sea-salt aerosol in the  
1013 global troposphere, *Atmospheric Chemistry and Physics Discussions*, 1–27, doi:10.5194/acp-2018-1013, 2018.

1014 NASA Goddard Space Flight Center, O. E. L.: SeaWiFS Ocean Color Data, 2014.

1015 National Centers For Environmental Prediction/National Weather Service/NOAA/U.S. Department Of Commerce:  
1016 NCEP GDAS/FNL 0.25 Degree Global Tropospheric Analyses and Forecast Grids, 2015.

1017 Navarro, M. A., Atlas, E. L., Saiz-Lopez, A., Rodriguez-Lloveras, X., Kinnison, D. E., Lamarque, J.-F., Tilmes, S.,  
1018 Filus, M., Harris, N. R. P., Meneguz, E., Ashfold, M. J., Manning, A. J., Cuevas, C. A., Schauffler, S. M. and  
1019 Donets, V.: Airborne measurements of organic bromine compounds in the Pacific tropical tropopause layer,  
1020 *Proceedings of the National Academy of Sciences*, 112(45), 13789–13793, doi:10.1073/pnas.1511463112, 2015.

1021 Neale, R. B., Richter, J., Park, S., Lauritzen, P. H., Vavrus, S. J., Rasch, P. J. and Zhang, M.: The Mean Climate of  
1022 the Community Atmosphere Model (CAM4) in Forced SST and Fully Coupled Experiments, *Journal of Climate*,  
1023 26(14), 5150–5168, doi:10.1175/JCLI-D-12-00236.1, 2013.

1024 Nevison, C. D., Manizza, M., Keeling, R. F., Kahru, M., Bopp, L., Dunne, J., Tiputra, J., Ilyina, T. and Mitchell, B.  
1025 G.: Evaluating the ocean biogeochemical components of Earth system models using atmospheric potential oxygen  
1026 and ocean color data, *Biogeosciences*, 12(1), 193–208, doi:10.5194/bg-12-193-2015, 2015.

1027 Nevison, C. D., Manizza, M., Keeling, R. F., Stephens, B. B., Bent, J. D., Dunne, J., Ilyina, T., Long, M.,  
1028 Resplandy, L., Tjiputra, J. and Yukimoto, S.: Evaluating CMIP5 ocean biogeochemistry and Southern Ocean carbon

1029 uptake using atmospheric potential oxygen: Present-day performance and future projection: CMIP5 APO AND  
1030 SOUTHERN OCEAN CARBON FLUX, *Geophysical Research Letters*, 43(5), 2077–2085,  
1031 doi:10.1002/2015GL067584, 2016.

1032 Nightingale, P. D., Malin, G. and Liss, P. S.: Production of chloroform and other low molecular-weight halocarbons  
1033 by some species of macroalgae, *Limnology and Oceanography*, 40(4), 680–689, doi:10.4319/lo.1995.40.4.0680,  
1034 1995.

1035 Nightingale, P. D., Malin, G., Law, C. S., Watson, A. J., Liss, P. S., Liddicoat, M. I., Boutin, J. and Upstill-Goddard,  
1036 R. C.: In situ evaluation of air-sea gas exchange parameterizations using novel conservative and volatile tracers,  
1037 *Global Biogeochemical Cycles*, 14(1), 373–387, 2000.

1038 Obrist, D., Tas, E., Peleg, M., Matveev, V., Faïn, X., Asaf, D. and Luria, M.: Bromine-induced oxidation of mercury  
1039 in the mid-latitude atmosphere, *Nature Geoscience*, 4, 22, 2010.

1040 Ordóñez, C., Lamarque, J.-F., Tilmes, S., Kinnison, D. E., Atlas, E. L., Blake, D. R., Sousa Santos, G., Brasseur, G.  
1041 and Saiz-Lopez, A.: Bromine and iodine chemistry in a global chemistry-climate model: description and evaluation  
1042 of very short-lived oceanic sources, *Atmospheric Chemistry and Physics*, 12(3), 1423–1447, doi:10.5194/acp-12-  
1043 1423-2012, 2012.

1044 Quack, B. and Wallace, D. W. R.: Air-sea flux of bromoform: Controls, rates, and implications: AIR-SEA FLUX  
1045 OF BROMOFORM, *Global Biogeochemical Cycles*, 17(1), doi:10.1029/2002GB001890, 2003.

1046 Raimund, S., Quack, B., Bozec, Y., Vernet, M., Rossi, V., Garçon, V., Morel, Y. and Morin, P.: Sources of short-  
1047 lived bromocarbons in the Iberian upwelling system, *Biogeosciences*, 8(6), 1551–1564, doi:10.5194/bg-8-1551-  
1048 2011, 2011.

1049 Read, K. A., Mahajan, A. S., Carpenter, L. J., Evans, M. J., Faria, B. V. E., Heard, D. E., Hopkins, J. R., Lee, J. D.,  
1050 Moller, S. J., Lewis, A. C., Mendes, L., McQuaid, J. B., Oetjen, H., Saiz-Lopez, A., Pilling, M. J. and Plane, J. M.  
1051 C.: Extensive halogen-mediated ozone destruction over the tropical Atlantic Ocean, *Nature*, 453(7199), 1232–1235,  
1052 doi:10.1038/nature07035, 2008.

1053 Resplandy, L., Keeling, R. F., Stephens, B. B., Bent, J. D., Jacobson, A., Rödenbeck, C. and Khatiwala, S.:  
1054 Constraints on oceanic meridional heat transport from combined measurements of oxygen and carbon, *Climate*  
1055 *Dynamics*, 47(9–10), 3335–3357, doi:10.1007/s00382-016-3029-3, 2016.

1056 Reygondeau, G., Longhurst, A., Martinez, E., Beaugrand, G., Antoine, D. and Maury, O.: Dynamic biogeochemical  
1057 provinces in the global ocean: DYNAMIC BIOGEOCHEMICAL PROVINCES, *Global Biogeochemical Cycles*,  
1058 27(4), 1046–1058, doi:10.1002/gbc.20089, 2013.

1059 Richter, U. and Wallace, D. W. R.: Production of methyl iodide in the tropical Atlantic Ocean: PRODUCTION OF  
1060 METHYL IODIDE, *Geophysical Research Letters*, 31(23), doi:10.1029/2004GL020779, 2004.

1061 Rienecker, M. M., Suarez, M. J., Todling, R., Bacmeister, J., Takacs, L., Liu, H. C., Gu, W., Sienkiewicz, M.,  
1062 Koster, R. D., Gelaro, R., Stajner, I. and Nielsen, J. E.: The GEOS-5 Data Assimilation System – Documentation of  
1063 Versions 5.0.1, 5.1.0, and 5.2.0, NASA/TM-2008-104606., 2008.

1064 Saiz-Lopez, A., Mahajan, A. S., Salmon, R. A., Bauguitte, S. J.-B., Jones, A. E., Roscoe, H. K. and Plane, J. M. C.:  
1065 Boundary Layer Halogens in Coastal Antarctica, *Science*, 317(5836), 348–351, doi:10.1126/science.1141408, 2007.

1066 Saiz-Lopez, A., Lamarque, J.-F., Kinnison, D. E., Tilmes, S., Ordóñez, C., Orlando, J. J., Conley, A. J., Plane, J. M.  
1067 C., Mahajan, A. S., Sousa Santos, G., Atlas, E. L., Blake, D. R., Sander, S. P., Schauffler, S., Thompson, A. M. and  
1068 Brasseur, G.: Estimating the climate significance of halogen-driven ozone loss in the tropical marine troposphere,  
1069 *Atmospheric Chemistry and Physics*, 12(9), 3939–3949, doi:10.5194/acp-12-3939-2012, 2012.

1070 Saiz-Lopez, A., Fernandez, R. P., Ordóñez, C., Kinnison, D. E., Gómez Martín, J. C., Lamarque, J.-F. and Tilmes,  
1071 S.: Iodine chemistry in the troposphere and its effect on ozone, *Atmospheric Chemistry and Physics*, 14(23), 13119–  
1072 13143, doi:10.5194/acp-14-13119-2014, 2014.

1073 Salawitch, R. J., Canty, T., Kurosu, T., Chance, K., Liang, Q., da Silva, A., Pawson, S., Nielsen, J. E., Rodriguez, J.  
1074 M., Bhartia, P. K., Liu, X., Huey, L. G., Liao, J., Stickel, R. E., Tanner, D. J., Dobb, J. E., Simpson, W. R.,  
1075 Donohoue, D., Weinheimer, A., Flocke, F., Knapp, D., Montzka, D., Neuman, J. A., Nowak, J. B., Ryerson, T. B.,  
1076 Oltmans, S., Blake, D. R., Atlas, E. L., Kinnison, D. E., Tilmes, S., Pan, L. L., Hendrick, F., Van Roozendaal, M.,  
1077 Kreher, K., Johnston, P. V., Gao, R. S., Johnson, B., Bui, T. P., Chen, G., Pierce, R. B., Crawford, J. H. and Jacob,  
1078 D. J.: A new interpretation of total column BrO during Arctic spring: FRONTIER, Geophysical Research Letters,  
1079 37(21), n/a–n/a, doi:10.1029/2010GL043798, 2010.

1080 Schauffler, S. M., Atlas, E. L., Blake, D. R., Flocke, F., Lueb, R. A., Lee-Taylor, J. M., Stroud, V. and Travnicek,  
1081 W.: Distributions of brominated organic compounds in the troposphere and lower stratosphere, Journal of  
1082 Geophysical Research: Atmospheres, 104(D17), 21513–21535, doi:10.1029/1999JD900197, 1999.

1083 Schroeder, W. H., Anlauf, K. G., Barrie, L. A., Lu, J. Y., Steffen, A., Schneeberger, D. R. and Berg, T.: Arctic  
1084 springtime depletion of mercury, Nature, 394, 331, 1998.

1085 Simpson, W. R., Brown, S. S., Saiz-Lopez, A., Thornton, J. A. and von Glasow, R.: Tropospheric Halogen  
1086 Chemistry: Sources, Cycling, and Impacts, Chemical Reviews, 115(10), 4035–4062, doi:10.1021/cr5006638, 2015.

1087 Sive, B. C., Varner, R. K., Mao, H., Blake, D. R., Wingenter, O. W. and Talbot, R.: A large terrestrial source of  
1088 methyl iodide, Geophysical Research Letters, 34(17), doi:10.1029/2007GL030528, 2007.

1089 Stephens, B.: ORCAS Merge Products. Version 1.0, [online] Available from:  
1090 <https://data.eol.ucar.edu/dataset/490.024> (Accessed 31 December 2018), 2017.

1091 Stephens, B. B., Keeling, R. F., Heimann, M., Six, K. D., Murnane, R. and Caldeira, K.: Testing global ocean  
1092 carbon cycle models using measurements of atmospheric O<sub>2</sub> and CO<sub>2</sub> concentration, Global Biogeochemical  
1093 Cycles, 12(2), 213–230, doi:10.1029/97GB03500, 1998.

1094 Stephens, B. B., Keeling, R. F. and Paplawsky, W. J.: Shipboard measurements of atmospheric oxygen using a  
1095 vacuum-ultraviolet absorption technique, Tellus B, 55(4), 857–878, doi:10.1046/j.1435-6935.2003.00075.x, 2003.

1096 Stephens, B. B., Long, M. C., Keeling, R. F., Kort, E. A., Sweeney, C., Apel, E. C., Atlas, E. L., Beaton, S., Bent, J.  
1097 D., Blake, N. J., Bresch, J. F., Casey, J., Daube, B. C., Diao, M., Diaz, E., Dierssen, H., Donets, V., Gao, B.-C.,  
1098 Gierach, M., Green, R., Haag, J., Hayman, M., Hills, A. J., Hoecker-Martínez, M. S., Honomichl, S. B., Hornbrook,  
1099 R. S., Jensen, J. B., Li, R.-R., McCubbin, I., McKain, K., Morgan, E. J., Nolte, S., Powers, J. G., Rainwater, B.,  
1100 Randolph, K., Reeves, M., Schauffler, S. M., Smith, K., Smith, M., Stith, J., Stossmeister, G., Toohey, D. W. and  
1101 Watt, A. S.: The O<sub>2</sub>/N<sub>2</sub> Ratio and CO<sub>2</sub> Airborne Southern Ocean Study, Bulletin of the American Meteorological  
1102 Society, 99(2), 381–402, doi:10.1175/BAMS-D-16-0206.1, 2018.

1103 Sturges, W. T., Cota, G. F. and Buckley, P. T.: Bromoform emission from Arctic ice algae, Nature, 358, 660, 1992.

1104 Sturges, W. T., Cota, G. F. and Buckley, P. T.: Vertical profiles of bromoform in snow, sea ice, and seawater in the  
1105 Canadian Arctic, Journal of Geophysical Research: Oceans, 102(C11), 25073–25083, doi:10.1029/97JC01860,  
1106 1997.

1107 Tilmes, S., Lamarque, J.-F., Emmons, L. K., Kinnison, D. E., Marsh, D., Garcia, R. R., Smith, A. K., Neely, R. R.,  
1108 Conley, A., Vitt, F., Val Martin, M., Tanimoto, H., Simpson, I., Blake, D. R. and Blake, N.: Representation of the  
1109 Community Earth System Model (CESM1) CAM4-chem within the Chemistry-Climate Model Initiative (CCMI),  
1110 Geoscientific Model Development, 9(5), 1853–1890, doi:10.5194/gmd-9-1853-2016, 2016.

1111 Tohjima, Y.: Preparation of gravimetric standards for measurements of atmospheric oxygen and reevaluation of  
1112 atmospheric oxygen concentration, Journal of Geophysical Research, 110(D11), doi:10.1029/2004JD005595, 2005.

1113 Tokarczyk, R. and Moore, R. M.: Production of volatile organohalogen by phytoplankton cultures, Geophysical  
1114 Research Letters, 21(4), 285–288, doi:10.1029/94GL00009, 1994.

1115 Tortell, P. D. and Long, M. C.: Spatial and temporal variability of biogenic gases during the Southern Ocean spring  
1116 bloom, Geophysical Research Letters, 36(1), doi:10.1029/2008GL035819, 2009.

1117 Tortell, P. D., Asher, E. C., Ducklow, H. W., Goldman, J. A. L., Dacey, J. W. H., Grzyski, J. J., Young, J. N.,  
 1118 Kranz, S. A., Bernard, K. S. and Morel, F. M. M.: Metabolic balance of coastal Antarctic waters revealed by  
 1119 autonomous  $p\text{CO}_2$  and  $\Delta\text{O}_2/\text{Ar}$  measurements: metabolic balance of Antarctic waters, *Geophysical Research*  
 1120 *Letters*, 41(19), 6803–6810, doi:10.1002/2014GL061266, 2014.

1121 Williams, J., Gros, V., Atlas, E., Maciejczyk, K., Batsaikhan, A., Schöler, H. F., Forster, C., Quack, B., Yassaa, N.,  
 1122 Sander, R. and Van Dingenen, R.: Possible evidence for a connection between methyl iodide emissions and Saharan  
 1123 dust, *Journal of Geophysical Research*, 112(D7), doi:10.1029/2005JD006702, 2007.

1124 [Engel, A., and M. Rigby \(Lead Authors\), Burkholder, J. B., Fernandez, R. P., Froidevaux, L., Hall, B. D., Hossaini,](#)  
 1125 [R., Saito, T., Vollmer, M. K. and B. Yao. Update on Ozone-Depleting Substances \(ODSs\) and Other Gases of](#)  
 1126 [Interest to the Montreal Protocol. Chapter 1 in \*Scientific Assessment of Ozone Depletion: 2018, Global Ozone\*](#)  
 1127 [Research and Monitoring Project-Report No. 58, World Meteorological Organization, Geneva, Switzerland, 2018.](#)

1128 [Wofsy, S. C.: HIAPER Pole-to-Pole Observations \(HIPPO\): fine-grained, global-scale measurements of climatically](#)  
 1129 [important atmospheric gases and aerosols, \*Philosophical Transactions of the Royal Society A: Mathematical,\*](#)  
 1130 [Physical and Engineering Sciences](#), 369(1943), 2073–2086, doi:10.1098/rsta.2010.0313, 2011.

1131 Wofsy, S. C., Afshar, S., Allen, H. M., Apel, E., Asher, E. C., Barletta, B., Bent, J., Bian, H., Biggs, B. C., Blake, D.  
 1132 R., Blake, N., Bourgeois, I., Brock, C. A., Brune, W. H., Budney, J. W., Bui, T. P., Butler, A., Campuzano-Jost, P.,  
 1133 Chang, C. S., Chin, M., Commane, R., Correa, G., Crouse, J. D., Cullis, P. D., Daube, B. C., Day, D. A., Dean-  
 1134 Day, J. M., Dibb, J. E., Digangi, J. P., Diskin, G. S., Dollner, M., Elkins, J. W., Erdesz, F., Fiore, A. M., Flynn, C.  
 1135 M., Froyd, K., Gesler, D. W., Hall, S. R., Hanco, T. F., Hannun, R. A., Hills, A. J., Hints, E. J., Hoffmann, A.,  
 1136 Hornbrook, R. S., Huey, L. G., Hughes, S., Jimenez, J. L., Johnson, B. J., Katich, J. M., Keeling, R., Kim, M. J.,  
 1137 Kupc, A., Lait, L. R., Lamarque, J.-F., Liu, H. B., McKain, K., McLaughlin, R. J., Meinardi, S., Miller, D. O.,  
 1138 Montzka, S. A., Moore, F. L., Morgan, E. J., Murphy, D. M., Murray, L. T., Nault, B. A., Neuman, J. A., Newman,  
 1139 P. A., Nicely, J. M., Pan, X., Paplawsky, W., Peischl, J., Prather, M. J., Price, D. J., Ray, E., Reeves, J. M.,  
 1140 Richardson, M., Rollins, A. W., Rosenlof, K. H., Ryerson, T. B., Scheuer, E., Schill, G. P., Schroder, J. C., Schwarz,  
 1141 J. P., St.Clair, J. M., Steenrod, S. D., Stephens, B. B., Strode, S. A., Sweeney, C., Tanner, D., Teng, A. P., Thames,  
 1142 A. B., Thompson, C. R., Ullmann, K., Veres, P. R., Vizenor, N., Wagner, N. L., Watt, A., Weber, R., Weinzierl, B.,  
 1143 et al.: ATom: Merged Atmospheric Chemistry, Trace Gases, and Aerosols, [online] Available from:  
 1144 [https://daac.ornl.gov/cgi-bin/dsviewer.pl?ds\\_id=1581](https://daac.ornl.gov/cgi-bin/dsviewer.pl?ds_id=1581) (Accessed 31 December 2018), 2018.

1145 Xiang, B., Miller, S. M., Kort, E. A., Santoni, G. W., Daube, B. C., Commane, R., Angevine, W. M., Ryerson, T. B.,  
 1146 Trainer, M. K., Andrews, A. E., Nehrkom, T., Tian, H. and Wofsy, S. C.: Nitrous oxide ( $\text{N}_2\text{O}$ ) emissions from  
 1147 California based on 2010 CalNex airborne measurements: California  $\text{N}_2\text{O}$  emissions, *Journal of Geophysical*  
 1148 *Research: Atmospheres*, 118(7), 2809–2820, doi:10.1002/jgrd.50189, 2013.

1149 Yang, B., Yang, G.-P., Lu, X.-L., Li, L. and He, Z.: Distributions and sources of volatile chlorocarbons and  
 1150 bromocarbons in the Yellow Sea and East China Sea, *Marine Pollution Bulletin*, 95(1), 491–502,  
 1151 doi:10.1016/j.marpolbul.2015.03.009, 2015.

1152 Yokouchi, Y., Nojiri, Y., Barrie, L. A., Toom-Saunty, D. and Fujinuma, Y.: Atmospheric methyl iodide: High  
 1153 correlation with surface seawater temperature and its implications on the sea-to-air flux, *Journal of Geophysical*  
 1154 *Research: Atmospheres*, 106(D12), 12661–12668, doi:10.1029/2001JD900083, 2001.

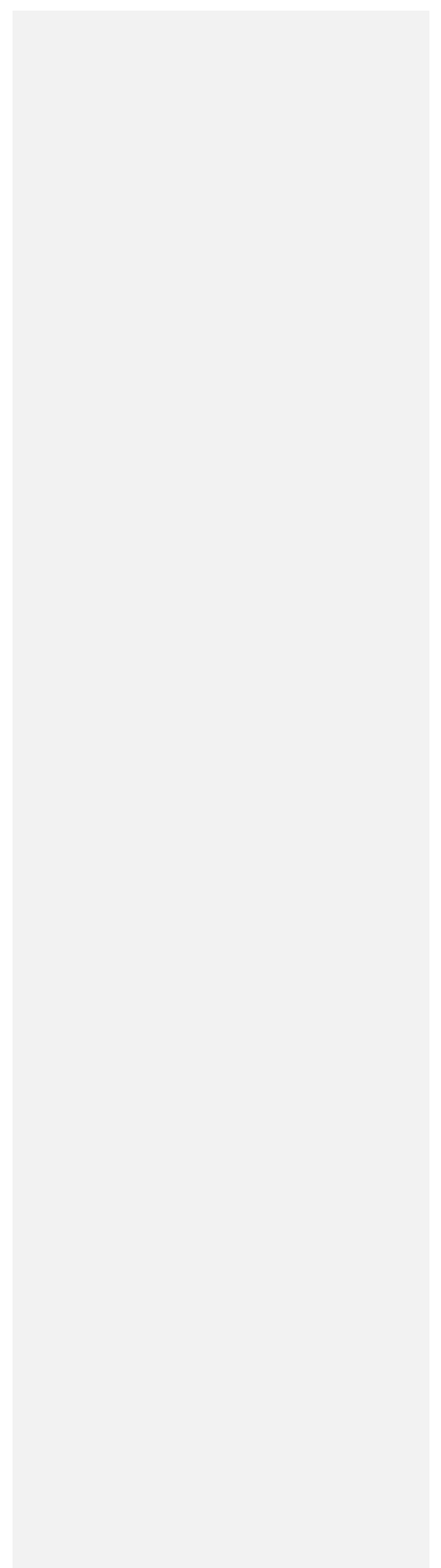
1155 Yokouchi, Y., Hasebe, F., Fujiwara, M., Takashima, H., Shiotani, M., Nishi, N., Kanaya, Y., Hashimoto, S., Fraser,  
 1156 P., Toom-Saunty, D., Mukai, H. and Nojiri, Y.: Correlations and emission ratios among bromoform,  
 1157 dibromochloromethane, and dibromomethane in the atmosphere, *Journal of Geophysical Research*, 110(D23),  
 1158 doi:10.1029/2005JD006303, 2005.

1159 Ziska, F., Quack, B., Abrahamsson, K., Archer, S. D., Atlas, E., Bell, T., Butler, J. H., Carpenter, L. J., Jones, C. E.,  
 1160 Harris, N. R. P., Hepach, H., Heumann, K. G., Hughes, C., Kuss, J., Krüger, K., Liss, P., Moore, R. M., Orlikowska,  
 1161 A., Raimund, S., Reeves, C. E., Reifenhäuser, W., Robinson, A. D., Schall, C., Tanhua, T., Tegtmeier, S., Turner,  
 1162 S., Wang, L., Wallace, D., Williams, J., Yamamoto, H., Yvon-Lewis, S. and Yokouchi, Y.: Global sea-to-air flux  
 1163 climatology for bromoform, dibromomethane and methyl iodide, *Atmospheric Chemistry and Physics*, 13(17),  
 1164 8915–8934, doi:10.5194/acp-13-8915-2013, 2013.

1165

Elizabeth Asher 9/3/2019 11:45 AM

**Deleted:** WMO (World Meteorological Organization): Scientific Assessment of Ozone Depletion: 2018, Global Ozone Research and Monitoring Project-Report, Geneva, Switzerland., 2018. -



1172 **Tables**

1173 Table 1. Mean ± uncertainty (see Sect. 3.4.1 and 3.4.2 for details) halogenated VOC emission  
 1174 estimates (pmol m<sup>-2</sup> hr<sup>-1</sup>) in Region 1 and Region 2 calculated in this study (with method  
 1175 indicated below each value), from CAM-Chem (Ordoñez et al., 2012) and from several other  
 1176 modeling and ship-based observational studies.

Elizabeth Asher 9/3/2019 11:17 AM  
 Deleted: H

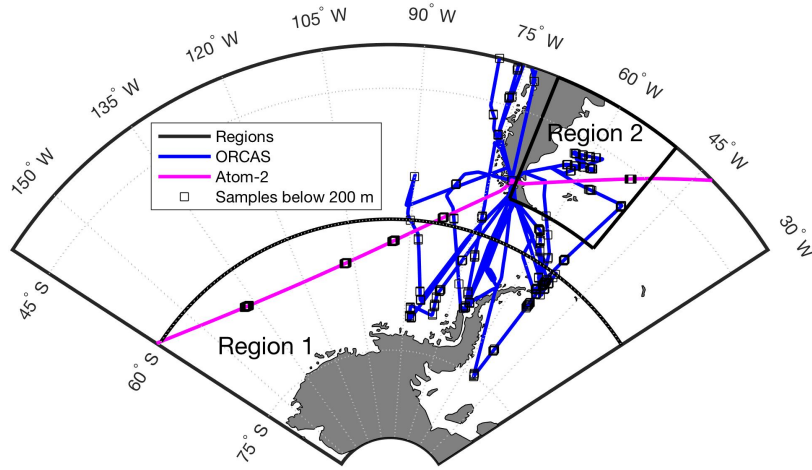
1177

| Region/Months                               | CHBr <sub>3</sub>                      | CH <sub>2</sub> Br <sub>2</sub>       | CH <sub>3</sub> I                      | CHClBr <sub>2</sub>                  | Reference                         |
|---|--|---------------------------------------|--|--------------------------------------|-----------------------------------|
| Region 1 (JF)<br>< 60° S                    | 91 ± 8<br><u>O<sub>2</sub> Regr.</u>   | 31 ± 18<br><u>O<sub>2</sub> Regr.</u> | 35 ± 29<br><u>MLR</u>                  | 11 ± 4<br><u>O<sub>2</sub> Regr.</u> | This Study                        |
| Region 2 (JF)<br>>55° S and<br><40° S       | 329 ± 23<br><u>O<sub>2</sub> Regr.</u> | 69 ± 5<br><u>O<sub>2</sub> Regr.</u>  | 392 ± 32<br><u>O<sub>2</sub> Regr.</u> | 25 ± 5<br><u>O<sub>2</sub> Regr.</u> | This Study                        |
| Region 1 (JF)                               | 10                                     | 1.9                                   | 120                                    | 0.38                                 | CAM-Chem                          |
| Region 2 (JF)                               | 360                                    | 44                                    | 800                                    | 8.7                                  | CAM-Chem                          |
| Southern Ocean<br>(≥50°S), (DJ)             | 200                                    | 200                                   | 200                                    | -----                                | Ziska et al.<br>2013 (model)      |
| Marguerite Bay<br>(DJF)                     | 3500                                   | 875                                   | -----                                  | -----                                | Hughes et al.<br>2009 (obs)       |
| 70°S-72°S<br>Antarctica                     | 1300                                   | -----                                 | -----                                  | -----                                | Carpenter et<br>al. 2007<br>(obs) |
| Southern Ocean<br>(≥50°S)<br>(Feb. - April) | 225                                    | 312                                   | 708                                    | -----                                | Butler et al.<br>2007 (obs)       |
| 40°S-52°S S.<br>Atlantic (Sept.-<br>Feb.)   | -1670                                  | -----                                 | 250                                    | -----                                | Chuck et al.<br>2005              |
| Southern Ocean<br>(≥50°S), (DJ)             | -330                                   | -----                                 | -----                                  | -----                                | Mattson et al.<br>2013 (model)    |

1178

1179

1180



1183

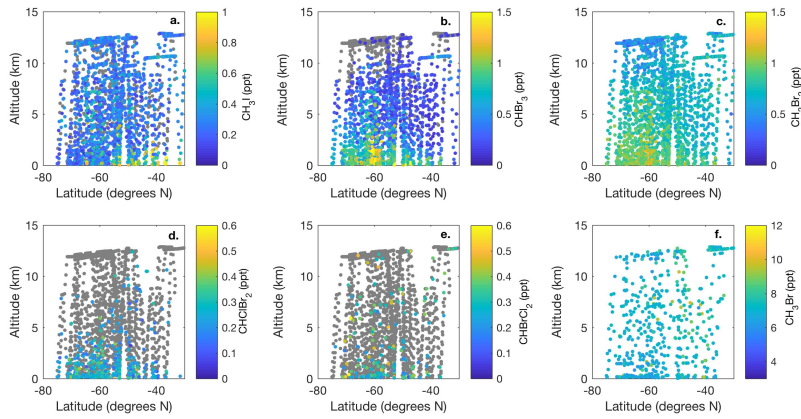
1184 **Figure 1.** Overview map ORCAS and ATom-2 flight tracks in the study regions: 1) high  
1185 latitudes in the Southern Hemisphere poleward 60° S and 2) the Patagonian Shelf. The ORCAS  
1186 and ATom-2 aircraft flights and dips below 200 m that took place within these regions are also  
1187 shown.

1188

1189

Unknown  
**Formatted:** Font:(Default) Times, 12 pt,  
**Bold**



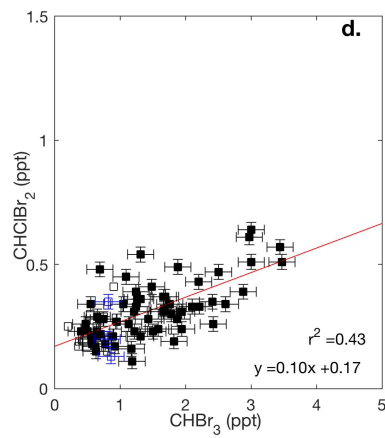
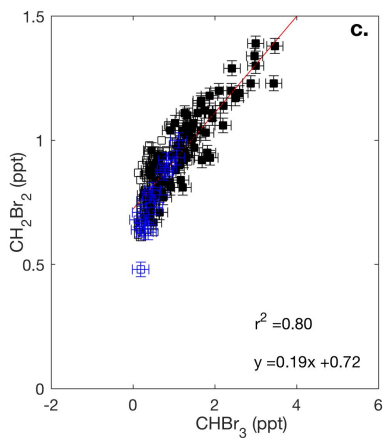
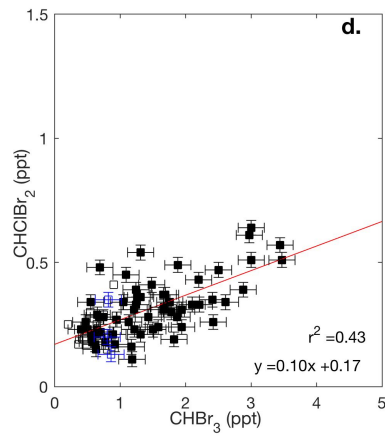
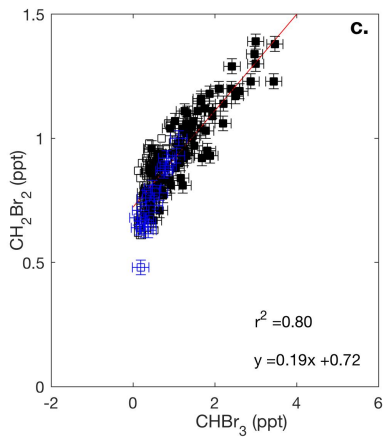


1190

1191 **Figure 2.** Meridional-altitudinal cross-sections of mixing ratios of a)  $\text{CH}_3\text{I}$ , b)  $\text{CHBr}_3$ , c)  
 1192  $\text{CH}_2\text{Br}_2$ , d)  $\text{CHClBr}_2$ , and e)  $\text{CHBrCl}_2$  from the TOGA and mixing ratios of f)  $\text{CH}_3\text{Br}$  from  
 1193 AWAS and WAS in 2016 and 2017, respectively, during the ORCAS and ATOm-2 campaigns  
 1194 over the Southern Ocean in the austral summer. Note the different color bar scales. Gray points  
 1195 denote measurements below the detection limit of each species ( $\text{CH}_3\text{I} - 0.03 \text{ ppt}$ ,  $\text{CHBr}_3 - 0.2$   
 1196  $\text{ppt}$ ,  $\text{CH}_2\text{Br}_2 - 0.03 \text{ ppt}$ ,  $\text{CHClBr}_2 - 0.03 \text{ ppt}$ ,  $\text{CHBrCl}_2 - 0.05 \text{ ppt}$ ,  $\text{CH}_3\text{Br} - 0.2 \text{ ppt}$ ).

1197

Unknown  
 Formatted: Font:(Default) Times, 12 pt,  
 Bold



1198

1199

1200

1201

1202 **Figure 3.** Mixing ratios of  $\text{CHBr}_3$  vs.  $\text{CH}_2\text{Br}_2$  and  $\text{CHClBr}_2$  across the ORCAS and ATom-2  
 1203 campaigns in Region 1 (Fig.3a,b) and in (Fig.3c,d), respectively. Type II major axis regression  
 1204 model (bivariate least squares regressions) are based on ORCAS data below 2 km and illustrate  
 1205 regional enhancement ratios. Error bars represent the uncertainty in halogenated VOC  
 1206 measurements.

1207

1208

1209

Unknown  
 Formatted: Font:(Default) Times, 12 pt,  
 Bold

Elizabeth Asher 9/3/2019 11:17 AM  
 Deleted: H

1211

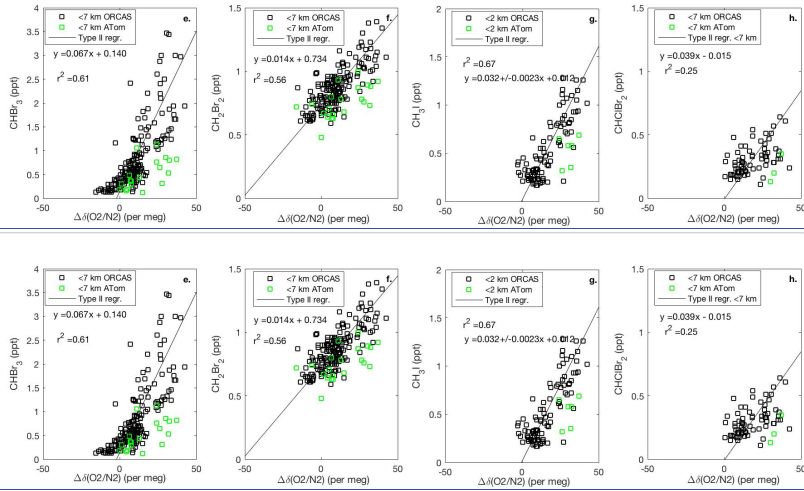
1212

1213

1214

1215 **Figure 4.** Mixing ratios of CHBr<sub>3</sub>, CH<sub>2</sub>Br<sub>2</sub>, and CH<sub>3</sub>I vs. O<sub>2</sub> on ORCAS and ATom-2 in Region  
 1216 | 1, poleward of 60° S (a-d) and Region 2 over the Patagonian Shelf (e-h). Slopes ± standard  
 1217 | errors from type II major axis regression model (bivariate least squares regression) fits of  
 1218 | ORCAS data for regressions with r<sup>2</sup> > 0.2 (fits were calculated on variables scaled to their full  
 1219 | range). The slopes reported in the figure are converted to pmol:mol ratios prior to estimating  
 1220 | biogenic halogenated VOC fluxes based on modeled CESM O<sub>2</sub> fluxes. Data from above 7 km  
 1221 | were excluded due to the influence of air masses transported from further north.

1222



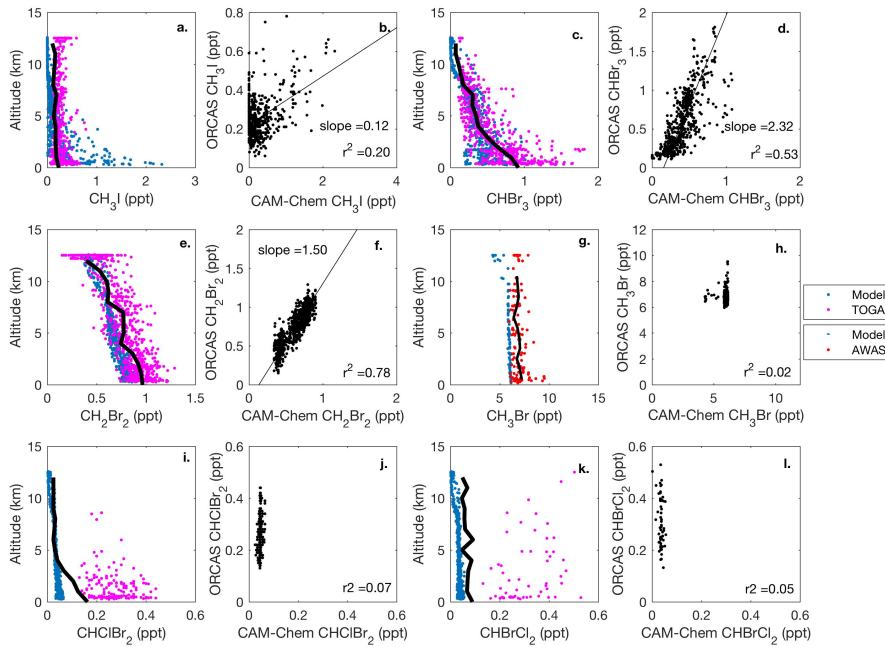
Unknown  
Formatted: Font:(Default) Times, 12 pt

Unknown  
Formatted: Font:(Default) Times, 12 pt

Elizabeth Asher 9/3/2019 11:17 AM  
Deleted: H

1224

1225

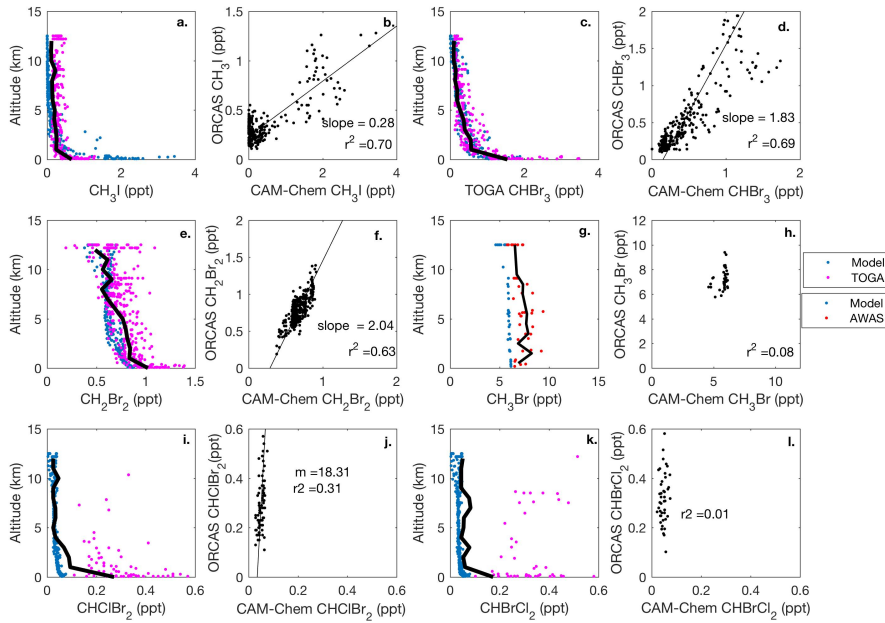


1226

1227 **Fig 5.** CAM-Chem1.2 model-aircraft measurement comparison during the ORCAS campaign  
 1228 between 1-12 km in Region 1, high latitudes in the Southern Hemisphere poleward 60° S. All  
 1229 regressions are type II major axis regression models bivariate least squares regressions (slopes  
 1230 are shown when the  $r^2 \geq 0.2$ ). The bold, black line in each vertical profile represents the binned  
 1231 (mean) mixing ratio of halogenated VOC measurements at that altitude. The binned mean  
 1232 includes measurements below the detection limit (DL), which for this calculation are assigned a  
 1233 value equal to the DL multiplied by the percentage of data below detection. Modeled values  
 1234 include locations where observations were below the DL.

Unknown  
 Formatted: Font:(Default) Times, 12 pt

Elizabeth Asher 9/3/2019 11:20 AM  
 Deleted: H



1236

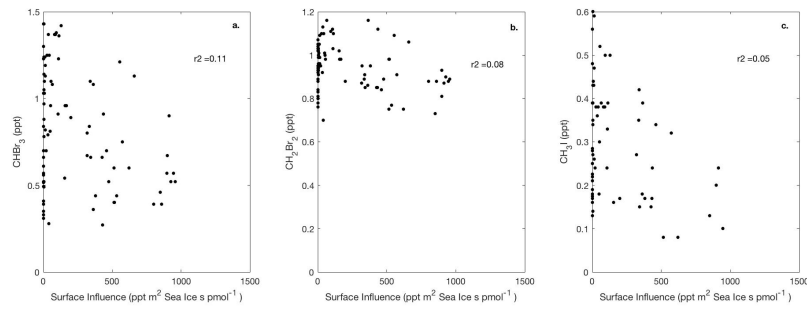
1237 **Figure 6.** CAM-Chem 1.2 model-aircraft measurement (TOGA and AWAS) comparison during  
 1238 ORCAS campaign between 1-12 km in Region 2, the Patagonian Shelf. All regressions are type  
 1239 II major axis regression between bivariate least squares regressions (slopes are shown when the  $r^2$   
 1240  $\geq 0.2$ ). The bold, black line in each vertical profile represents the binned (mean) mixing ratio of  
 1241 halogenated VOC measurements at that altitude. Again, the binned mean includes measurements  
 1242 below the detection limit (DL), which for this calculation are assigned a value equal to the DL  
 1243 multiplied by the percentage of data below detection. Modeled values include locations where  
 1244 observations were below the DL.

1245

1246

Unknown  
 Formatted: Font:(Default) Times, 12 pt

Elizabeth Asher 9/3/2019 11:20 AM  
 Deleted: H



1248

1249

1250

1251

1252

1253

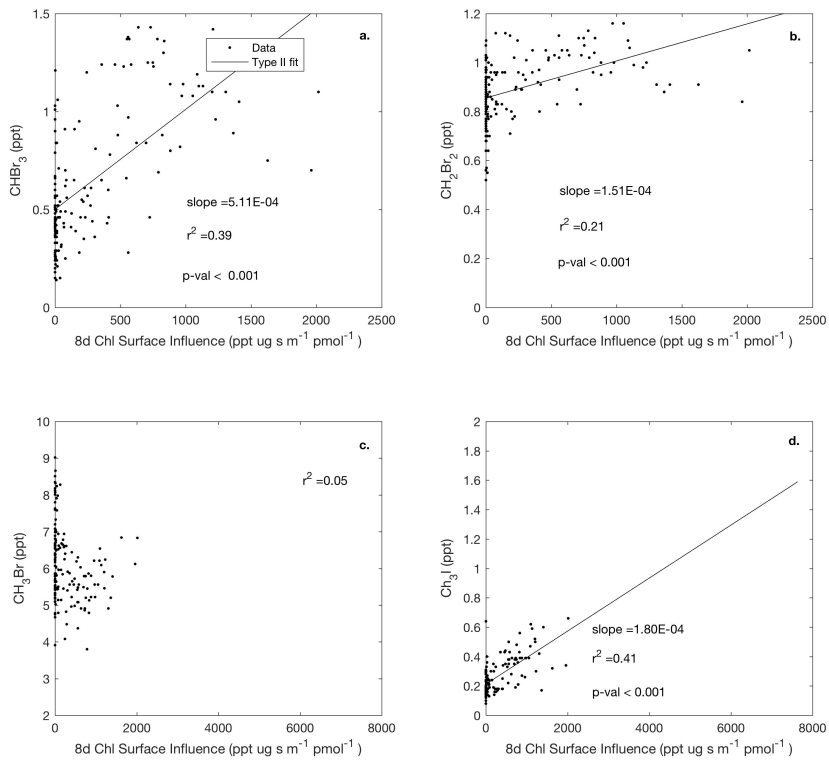
1254

1255

**Figure 7.** Linear type II regressions between influence functions convolved with sea ice distributions, which exclude land ice, and mixing ratios for  $\text{CHBr}_3$ ,  $\text{CH}_2\text{Br}_2$ , and  $\text{CH}_3\text{I}$  in Region 1, poleward of  $60^\circ \text{S}$ . Surface influence ( $\text{ppt m}^2 \text{ s pmol}^{-1}$ ) in each grid cell was multiplied by fractional sea ice concentration surface field, which is unit-less, yielding sea ice surface influence function units of  $\text{ppt m}^2 \text{ s pmol}^{-1}$ , as shown on the x-axis. Linear regression lines are not shown, as  $p \geq 0.001$ .

Unknown  
Formatted: Font:(Default) Times, 12 pt

Elizabeth Asher 7/6/2019 11:31 AM  
Deleted: predictor variable



1257

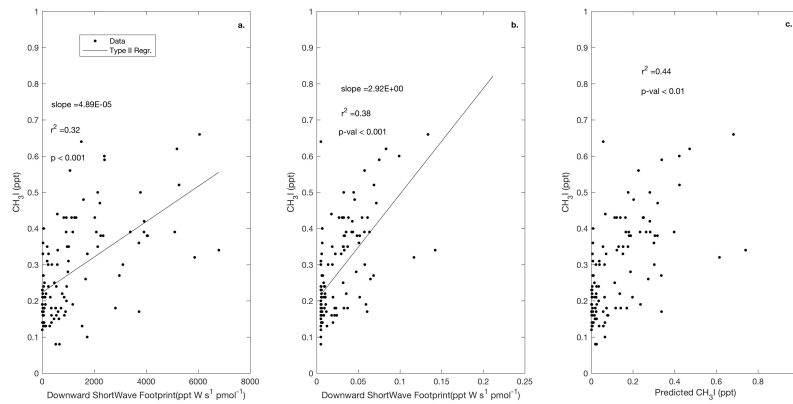
1258

1259 **Figure 8.** Linear type II regressions between influence functions of eight day composites of chl  
 1260 *a* and mixing ratios of halogenated VOCs (a-d) poleward of 60° S (Region 1). Surface influence  
 1261 (ppt m<sup>2</sup> s pmol<sup>-1</sup>) in each grid cell was multiplied by the chl *a* (μg m<sup>-3</sup>) surface field, resulting in  
 1262 surface influence function units of μg ppt s pmol<sup>-1</sup> m<sup>-1</sup>, shown on the x-axis. Linear regression  
 1263 lines are shown where when p < 0.001.

1264

Unknown  
 Formatted: Font:(Default) Times, 12 pt,  
 Bold

- Elizabeth Asher 9/3/2019 11:20 AM
- Deleted: H
- Elizabeth Asher 7/6/2019 11:31 AM
- Deleted: predictor variables
- Elizabeth Asher 7/6/2019 10:26 AM
- Deleted: .

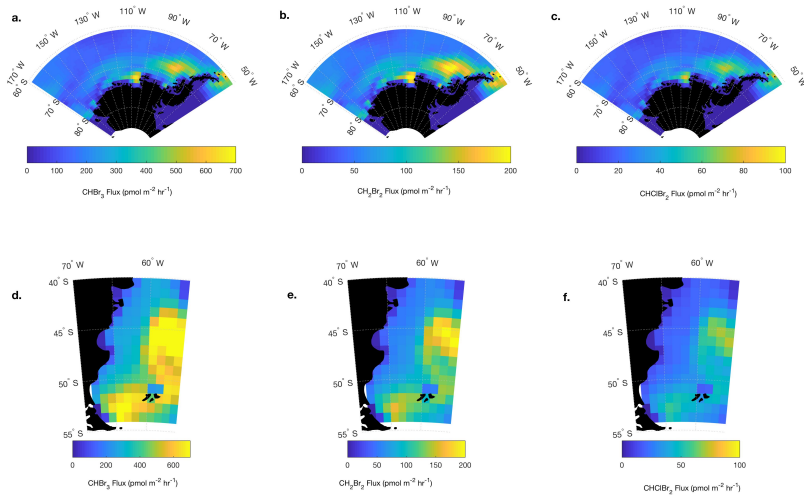


1269

1270 **Figure 9.** Observed  $\text{CH}_3\text{I}$  plotted against [the surface influence functions](#) of downward shortwave  
 1271 radiation (a) and absorption due to detritus (b). [Predicted mixing ratios of  \$\text{CH}\_3\text{I}\$  based on a](#)  
 1272 [multiple linear regressions \(MLR\) using these two predictors in Region 1 are shown in Fig. 9c](#)  
 1273 [according to Equation 3](#). Surface influence ( $\text{ppt m}^2 \text{ s pmol}^{-1}$ ) in each grid cell [was](#) multiplied by  
 1274 [the surface source field](#), such as shortwave radiation [at the surface](#) ( $\text{W m}^{-2}$ ), yielding units of  $\text{ppt}$   
 1275  $\text{Ws pmol}^{-1}$ , and [the surface ocean's](#) detrital absorption ( $\text{m}^{-1}$ ), yielding units of  $\text{ppt m s pmol}^{-1}$ ,  
 1276 shown on the x-axes.

1277





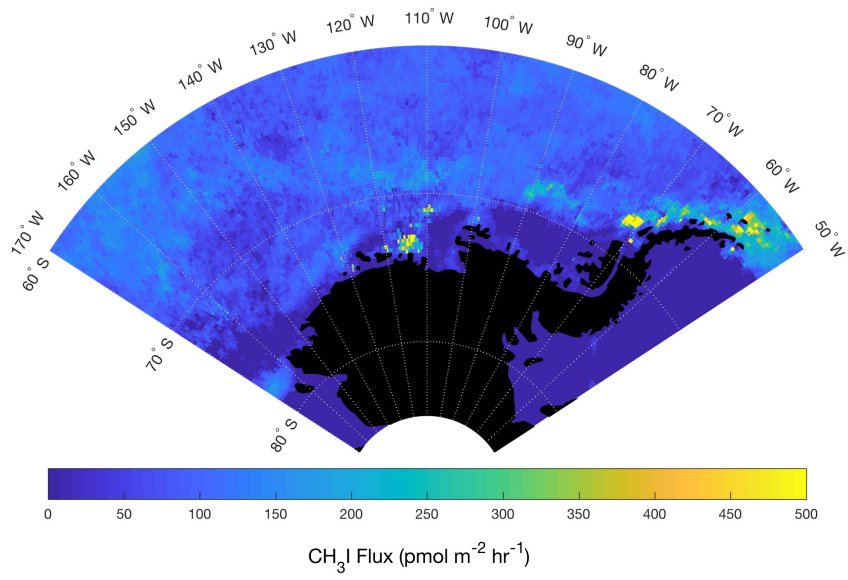
1278

1279 **Figure 10.** Resulting mean Jan. – Feb. 2016 O<sub>2</sub>-based (parameterized) CHBr<sub>3</sub> and CH<sub>2</sub>Br<sub>2</sub> and  
 1280 CHClBr<sub>2</sub> fluxes (pmol m<sup>-2</sup> s<sup>-1</sup>) in Region 1 (a-c) poleward of 60° S and Region 2 (d-f) over the  
 1281 Patagonian Shelf. CESM modeled O<sub>2</sub> fluxes are scaled by the slope between the oceanic  
 1282 contribution to δ(O<sub>2</sub>/N<sub>2</sub>) and CHBr<sub>3</sub>, and CH<sub>2</sub>Br<sub>2</sub>, and CHClBr<sub>2</sub> reported in Fig. 4. Note that these  
 1283 fluxes represent mean estimated biogenic fluxes in Jan. -Feb. 2016 (see Sect. 3.4.1 for details).

1284

Unknown

Formatted: Font:(Default) Times, 12 pt



1285

1286 | **Figure 11.** Mean estimated CH<sub>3</sub>I fluxes for Jan. – Feb. The multilinear regression in Fig. 9  
 1287 between CH<sub>3</sub>I mixing ratios and geophysical influence functions related to shortwave radiation  
 1288 and detrital material at the sea surface was used to derive a mean flux field in Jan.-Feb., 2016 for  
 1289 Region 1.

1290

1291 **Supplementary Text**

1292 Sea air exchange calculations

1293 To support the interpretation of our results, we calculate nominal equilibration times. For  
1294 estimates of bulk sea air equilibration times for halogenated VOCs, O<sub>2</sub>, and CO<sub>2</sub>, we assume a  
1295 mixed layer depth of 30 m, a temperature of 0° C, a salinity of 35 PSU, and carbonate buffering  
1296 according to eq. 8.3.10 in Sarmiento and Gruber (2006), and transfer velocities according to  
1297 Nightingale et al., (2000). The Schmidt number (i.e. the ratio of the kinematic viscosity of a gas,  
1298 divided by the molecular diffusivity) for O<sub>2</sub>, CO<sub>2</sub> and CH<sub>3</sub>Br were calculated according to  
1299 Wanninkof (2014), and the Schmidt numbers for CHBr<sub>3</sub> and CH<sub>3</sub>I were calculated according to  
1300 Quack and Wallace (2003), and Moore and Groszko (1999), respectively. The results are  
1301 provided in Sect. 3.1.2.

1302 Comparisons of TOGA, WAS and PFP

1303 Despite overall good agreement between co-located inflight AWAS, WAS, and PFP samples and  
1304 TOGA measurements, we observed notable discrepancies in several cases (e.g. Fig. S1b; Fig.  
1305 S2a-b). On ORCAS, we observed a non-linear relationship between inflight TOGA  
1306 measurements and co-located AWAS samples of CH<sub>3</sub>I (Fig. S1b), driven by a few samples with  
1307 high mixing ratios. Close inspection of upwind and downwind flights over Region 2 with the  
1308 campaign's high mixing ratios of CH<sub>3</sub>I indicated that TOGA measurements were consistent with  
1309 a modest flux of CH<sub>3</sub>I from the ocean to the atmosphere. On ATom-2, TOGA measurements  
1310 agreed better with co-located PFP samples than with co-located WAS samples; and differences  
1311 on the sixth and seventh research flights (i.e. the data used here) were relatively small.  
1312 Nevertheless these differences motivated an instrument inter-comparison following the ATom  
1313 campaign between these instruments. Thus far, results of this inter-comparison show that TOGA  
1314 and PFP measurements differ by < 25%.

1315

1316

1317 Supplementary Tables

1318 Table S1. The TOGA-PFP instrument comparison was done by sampling a 50L SS pontoon,  
1319 created at NCAR from a humidified dilution of the TOGA ATom standard. Data were analyzed  
1320 and reported by Rebecca Hornbrook (NCAR, TOGA) and Steve Montzka (NOAA, PFP).

| Pontoon Inter-comparison        | Concentration (dilution-based calc.) | TOGA (10/12/2018) | PFP (10/24/2018) |
|---------------------------------|--------------------------------------|-------------------|------------------|
| CHBr <sub>3</sub>               | 34                                   | 21.0 ± 0.1        | 26.6 ± 0.8       |
| CHClBr <sub>2</sub>             | 26                                   | 19.9 ± 1.0        | 22.9 ± 0.1       |
| CH <sub>2</sub> Br <sub>2</sub> | 52                                   | 47.7 ± 0.2        | 51.7 ± 2.0       |

1321

1322

Elizabeth Asher 7/8/2019 3:47 PM  
Deleted: -

Elizabeth Asher 7/8/2019 3:48 PM  
Deleted: -

Elizabeth Asher 9/3/2019 11:20 AM  
Deleted: H

Elizabeth Asher 7/7/2019 12:41 PM  
Deleted: ,

Elizabeth Asher 7/7/2019 12:41 PM  
Formatted: Subscript

Elizabeth Asher 7/7/2019 12:41 PM  
Formatted: Subscript

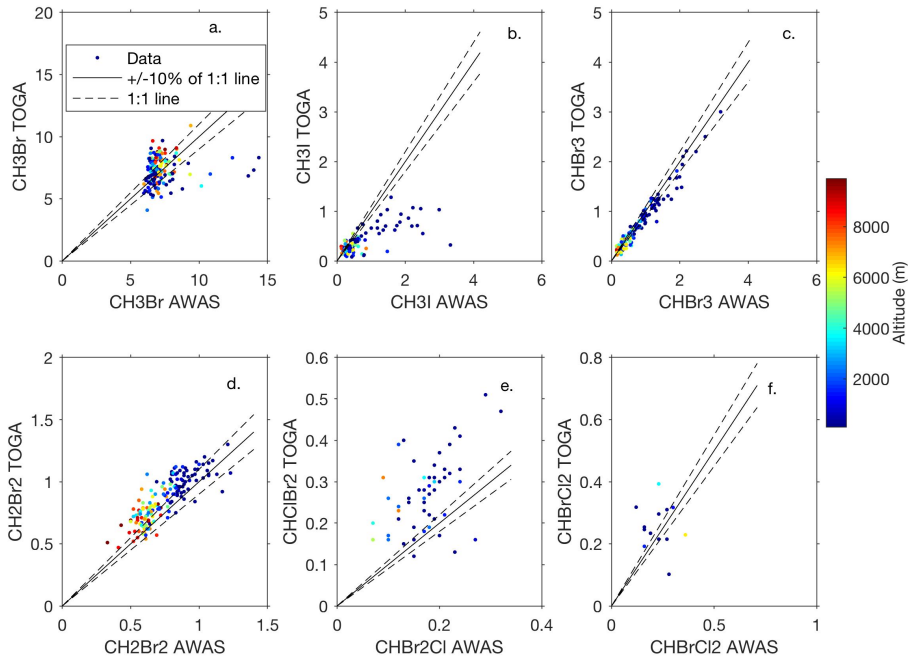
Elizabeth Asher 7/7/2019 12:41 PM  
Formatted: Subscript

Elizabeth Asher 7/7/2019 12:41 PM  
Formatted: Subscript

1327

1328 **Supplementary Figures**

1329



1330

1331

1332 **Figure S1.** Comparison between AWAS samples and TOGA measurements during ORCAS  
1333 below 10 km, when these two shared over half their sampling period. Points are colored by  
1334 altitude. Dashed lines represent  $\pm 10\%$  of the 1:1 line. Sample points below the DL are not  
1335 included in this quantitative comparison.

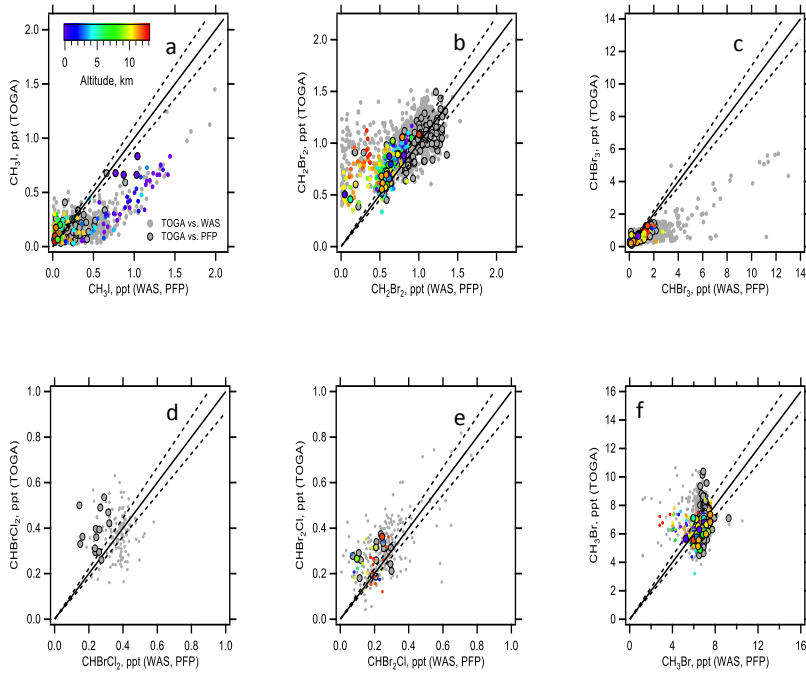
1336

1337

1338

1339

1340



1341

1342 **Figure S2.** Comparison between WAS, PFP and TOGA measurements during ATom-2 below 10

1343 km, when these instruments shared over half their sampling period. WAS measurements are

1344 shown in larger circles, PFP measurements in smaller circles, and measurements from the

1345 research flights six and seven used in this analysis are shown in color, while measurements on

1346 other research flights in ATom-2 are shown in gray. Dashed lines represent ± 10% of the 1:1

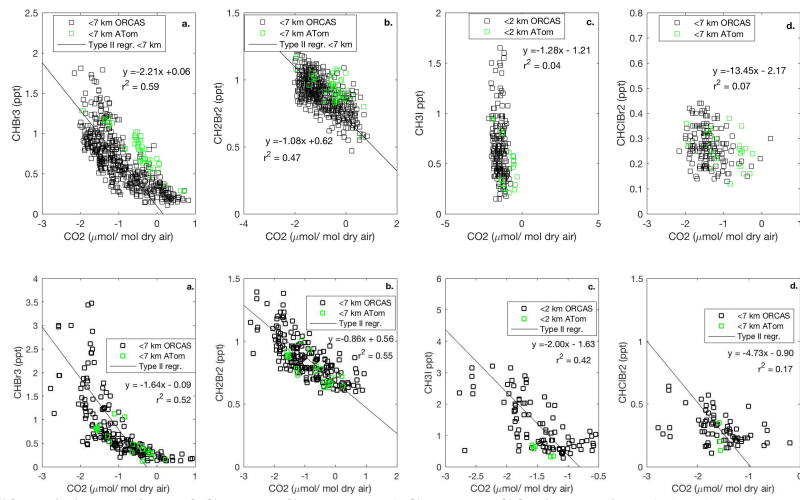
1347 line. Sample points below the DL are not shown.

1348

1349

1350

1351



1352

1353

1354

1355

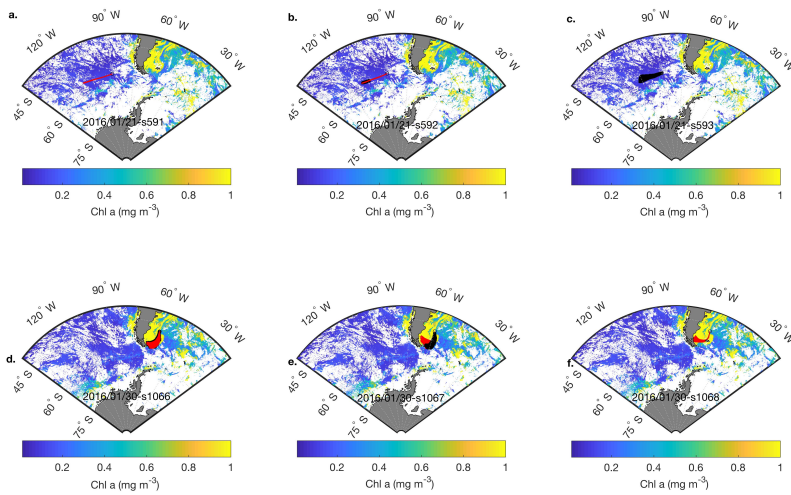
1356

**Figure S3.** Mixing ratios of CHBr<sub>3</sub>, CH<sub>2</sub>Br<sub>2</sub> and CH<sub>3</sub>I vs. CO<sub>2</sub> in Region 1 (a-c) and Region 2 (d-f). Type II major axis regression model (bivariate least squares regression) fits are shown for combined ORCAS and ATom-2 data, using data below 7 km for CHBr<sub>3</sub>, CH<sub>2</sub>Br<sub>2</sub>, and below 2 km for CH<sub>3</sub>I.

1357

1358

1359



1360  
 1361 | **Figure S4.** [Two sets of three](#) consecutive TOGA VOC sample locations, their back-trajectories  
 1362 and surface influences in the lower troposphere on two different flights (a-c; Jan. 21, 2016, and d-  
 1363 f; Jan. 30, 2016). For illustrative purposes, sampling locations are denoted by a black circle, 24-  
 1364 hour back trajectories are shown in red, and surface influences are shown with black squares in  
 1365 each subpanel, overlying weekly composites of remotely sensed chl *a*. Surface influence is  
 1366 multiplied by the underlying chl *a* (or other) [surface](#) field and averaged for each sample to yield  
 1367 a surface influence [function](#).

1368

1369